



Calhoun: The NPS Institutional Archive

[Theses and Dissertations](#)

[Thesis Collection](#)

1964

A simplified cell theory applied to the calculation of thermal neutron spectra in light water lattices.

MacVean, Charles Robert.

Cornell University

<http://hdl.handle.net/10945/13035>



Calhoun is a project of the Dudley Knox Library at NPS, furthering the precepts and goals of open government and government transparency. All information contained herein has been approved for release by the NPS Public Affairs Officer.

Dudley Knox Library / Naval Postgraduate School
411 Dyer Road / 1 University Circle
Monterey, California USA 93943

<http://www.nps.edu/library>

NPS ARCHIVE
1964
MACVEAN, C.

THESIS

A SIMPLIFIED CELL THEORY APPLIED TO
THE CALCULATION OF THERMAL
NEUTRON SPECTRA IN LIGHT
WATER LATTICES

CHARLES ROBERT MAC VEAN

1964

Library
U. S. Naval Postgraduate School
Monterey, California

A SIMPLIFIED CELL THEORY APPLIED TO THE CALCULATION OF
THERMAL NEUTRON SPECTRA IN LIGHT WATER LATTICES

A Thesis

Presented to the Faculty of the Graduate School
of Cornell University for the Degree of
Doctor of Philosophy

by

Charles Robert Mac Vean

September, 1964

Library
U. S. Naval Postgraduate School
Monterey, California

ABSTRACT

A simplified polyenergetic cell theory is formulated to determine spatially averaged energy dependent thermal fluxes in the moderator, cladding, and fuel regions within the unit cell of a reactor lattice. The derived spectra are then utilized in the calculations of the thermal integral parameters and average cross sections required for reactor computations.

The cell theory, as formulated, postulates an infinite moderator region with the absorption cross section of this region appropriately modified to account for the neutron leakage into and absorption by the fuel element. The modifications to the moderator absorption cross section are formulated both in terms of the net current at the fuel element-moderator interface and in terms of energy dependent moderator and fuel element escape probabilities, the latter approach offering physical transparency and ease of calculation.

Analytic expressions for the escape probabilities are presented, integral transport theory being applied to the fuel element region, while diffusion theory is utilized in the moderator region. Using these analytic expressions, the theory is applied to actual lattices in the form of the light water moderated and uranium dioxide fueled cores of the Cornell University Zero Power Reactor. Room temperature parameters and their temperature coefficients are determined using both the monatomic gas model and the Nelkin water kernel to describe the energy transfer process in the moderator. Calculations are made with PROGRAM COUTH, a Fortran-63 program written for use with the Control Data Corporation 1604 digital computer. A typical lattice calculation including the computation of the spatially averaged fuel, cladding, and moderator spectra and the thermal integral properties and average cross sections takes approximately thirty-five seconds of computer time. This figure is exclusive of the compiling time and the time required to calculate the moderator scattering kernel.

In an attempt to estimate the accuracy of the calculational results, the method is applied to the Brookhaven National Laboratory uranium dioxide cores and the results are then compared with those predicted by Honeck's THERMOS code. Disadvantage factors agree to within 1.0% while the thermal utilizations agree to within 0.5%. A study of the sensitivity of the calculated integral parameters to variations in the input data leads to the assignment of rather small uncertainties in the results calculated with the simplified cell theory.

NOTICE

Lieutenant C. R. Mac Vean, U. S. Navy, attended Cornell University under the provisions of the Junior Line Officers Advanced Scientific Educational Program which is sponsored by the U. S. Navy Bureau of Personnel and the U. S. Naval Postgraduate School, Monterey, California.

ACKNOWLEDGMENTS

The author wishes to gratefully acknowledge his association with Professor K. Bingham Cady. The initial impetus provided by his suggestion of this thesis topic and the continuing enthusiasm generated by him with regard to this topic have been the underlying factors contributing to the completion of this work. His guidance has proved invaluable. To Professor David D. Clark, the author's academic adviser, thanks are expressed for the support, direction, and assistance provided during the author's four years at Cornell. The helpful and constructively critical discussions with Professor Mark S. Nelkin led to the improvement of several facets of this work and they are acknowledged with gratitude.

The Commanding Officers of the U. S. Naval R.O.T.C. Unit at Cornell during the author's tour of duty there, Captains R. B. Bretland and C. V. Zalewski, who along with their staffs have provided a wealth of administrative and cooperative support, are wholeheartedly acknowledged. The author is privileged to have served under them.

The author is indebted to the U. S. Navy Bureau of Personnel and the U. S. Naval Postgraduate School in Monterey, California, who jointly sponsor the Junior Line Officers Advanced Scientific Educational Program. In particular, the author wishes to express his gratitude to Mrs. C. M. Gumz of the Bureau of Personnel for the courteous and meaningful liaison which she has provided.

The efforts and cooperation of the Cornell Computing Center are gratefully acknowledged, and the author wishes to thank Mrs. Betty Blake and Mrs. Barbara Boettcher for their skillful preparation of the final manuscript.

Several of the Cornell graduate students in the field of Nuclear Science and Engineering have provided assistance in this work and the discussions with Donald H. Bryce, Floyd E. Gelhaus, William E. Schilling, Robert A. Shaw, and Lt. Walter P. Wynn, Jr., U.S.N. are acknowledged with thanks.

Finally, the author wishes to thank his wife, Ellen, for the constant and continuing encouragement and motivation which she has contributed during this work.

TABLE OF CONTENTS

CHAPTER		PAGE
1	INTRODUCTION	1
2	A SIMPLIFIED CELL THEORY	6
	2.1 General Formulation	6
	2.2 A Practical Approximation of Heterogeneous Effects	12
	2.3 Formulation in Terms of Escape Probabilities	17
3	MODERATOR ESCAPE PROBABILITIES	21
	3.1 $P_s(E)$	21
	3.2 $P_m(E)$	24
4	THE FUEL ELEMENT ESCAPE PROBABILITY	27
	4.1 The Fuel Rod Escape Probability	27
	4.2 Void Considerations	31
	4.3 Cladding Effects	33
5	MODELS FOR THE SCATTERING KERNEL	41
	5.1 The Monatomic Gas Model	41
	5.2 The Nelkin Water Kernel	46
6	THERMAL LATTICE SPECTRA AND INTEGRAL PRO- ERTIES	61
7	APPLICATION OF THE METHOD TO ACTUAL LATTICES .	73
	7.1 Room Temperature Calculations	73
	7.2 Temperature Coefficients	94
8	ACCURACY OF THE RESULTS	102
9	SUMMARY AND CONCLUSIONS	113

Chapter	Page
APPENDIX A. LATTICE PARAMETERS FOR THE CORNELL UNIVERSITY ZERO POWER REACTOR	117
APPENDIX B. NUMERICAL RESULTS FOR THE CORNELL UNIVERSITY ZERO POWER REACTOR	121
APPENDIX C. NUMERICAL METHODS IN COUTH	150
APPENDIX D. INPUT-OUTPUT FOR COUTH	160
APPENDIX E. FORTRAN LISTING OF COUTH	170
APPENDIX F. NOTATION	189
WORKS CITED	196

LIST OF TABLES

TABLE	PAGE
8.1 Percentage Changes in Input Parameters Required to Change Integral Properties by +0.1 Percent . . .	109
A.1 Cornell University Zero Power Reactor Fuel Element Parameters	118
A.2 Cornell University Zero Power Reactor Lattice Parameters	119
A.3 Cornell University Zero Power Reactor Material Concentrations and Cross Sections	120
B.1 Energy, Velocity, and Lethargy Mesh Utilized by COUTH	122
B.2 Nelkin Water Model for the Scattering Matrix at 20°C	123
B.3 Nelkin Water Model for the Scattering Matrix at 40°C	129
B.4 Energy Dependent Cross Sections	134
B.5 Energy Dependent Cross Sections	135
B.6 Spatially Averaged Thermal Spectra for the Cornell ZPR 1:1 Core	136
B.7 Spatially Averaged Thermal Spectra for the Cornell ZPR 1.5:1 Core	137
B.8 Spatially Averaged Thermal Spectra for the Cornell ZPR 2:1 Core	138
B.9 Spatially Averaged Thermal Spectra for the Cornell ZPR 3:1 Core	139
B.10 Spatially Averaged Thermal Spectra for the Cornell ZPR 4:1 Core	140
B.11 Cornell University Zero Power Reactor Integral Properties	141
B.12 Cornell University Zero Power Reactor Integral Property Temperature Coefficients	143

Table		Page
B.13	Cornell University Zero Power Reactor Effective Cross Sections	144
B.14	Cornell University Zero Power Reactor Effective Cross Section Temperature Coefficients . . .	145
B.15	Cornell University Zero Power Reactor Mean Cross Sections	147
B.16	Cornell University Zero Power Reactor Mean Cross Section Temperature Coefficients . . .	148

LIST OF ILLUSTRATIONS

FIGURE		PAGE
2.1	The Fuel Element and Moderator Escape Probabilities	18
3.1	The Moderator Escape Probability, $P_s(E)$. . .	23
3.2	The Moderator Escape Probability, $P_m(E)$. . .	25
4.1	The Fuel Rod Escape Probability, $P_r(E)$. . .	32
4.2	The Fuel Element Escape Probability, $P_e(E)$. . .	38
4.3	The Ratio of the Fuel Rod Absorption Rate to the Fuel Element Absorption Rate	40
5.1	Approximations Used in the Calculation of the Nelkin Water Kernel	53
5.2	The Average Cosine of the Scattering Angle and the Transport Cross Section for Water	57
7.1	Apparent Lattice Absorption Cross Section	79
7.2	Spatially Averaged Moderator Thermal Spectra	80
7.3	Comparison of the Moderator Spectra Predicted with the Nelkin Water and Monatomic Gas Models	81
7.4	Spatially Averaged Cell Spectra	83
7.5	Average Neutron Velocities	84
7.6	Average Neutron Velocity for the Homogenized Cell	86
7.7	Neutron Density Disadvantage Factors	86a
7.8	Thermal Utilization	88
7.9	Integral Properties, η and η_f	89
7.10	Thermal Lifetime	90
7.11	Effective and Mean Absorption Cross Sections for the Homogenized Cell	92

Figure		Page
7.12	Thermal Diffusion Coefficient and Length for the Homogenized Cell	93
7.13	Temperature Coefficient of the Average Neutron Velocity for the Homogenized Cell	96
7.14	Temperature Coefficients of the Neutron Density Disadvantage Factors	97
7.15	Temperature Coefficients of the Integral Properties, f and ηf	99
7.16	Temperature Coefficients of the Thermal Diffusion Coefficient and Length for the Homogenized Cell	100
8.1	Thermal Utilization	104
8.2	Integral Property, η	105
8.3	Neutron Density Moderator Disadvantage Factor	107

CHAPTER 1

INTRODUCTION

The analysis and design of any thermal reactor requires an accurate knowledge of the various and competing neutron reaction rates within the reactor assembly. This, in turn, implies a knowledge of the distribution of thermal neutrons in space and energy. In the calculation of the thermal neutron spectra one must consider the two processes which affect these distributions in a heterogeneous reactor lattice. The first of these is the moderation process wherein a neutron is scattered by a moderator atom or molecule with a subsequent change in energy. The second process is the transport or diffusion mechanism whereby the neutrons are carried into regions of relatively different absorption characteristics. Although the time independent Boltzmann's equation or the integral transport equation^{1/} correctly describes both the moderation and transport phenomena, the difficulty in obtaining solutions to these equations have led previous investigators to develop their work along one of two lines. Initial attempts to characterize the distribution of thermal neutrons were done for infinite homogeneous media^{2,3/} where

^{1/} A. M. Weinberg and E. P. Wigner, The Physical Theory of Neutron Chain Reactors, pp. 221-234, The University of Chicago Press, Chicago, 1958.

^{2/} M. J. Poole, M. S. Nelkin, and R. S. Stone, "The Measurement and Theory of Reactor Spectra," Progress in Nuclear Energy, Series I, Vol. 2, pp. 91-164, Pergamon Press, New York, London, Paris, and Los Angeles, 1958.

there is no net transport or diffusion and the spatial variable is of no consequence. This approach allows concentration on the moderation or energy transfer process and sophisticated mathematical models may be incorporated into the calculation.

The other approach, as exemplified by multigroup diffusion calculations,^{4/} attempts to consider spatial effects at the expense of the details of the moderation process. In these calculations, the scattering kernel is often characterized by a simple model which allows ease of mathematical description but which may lack accuracy in its approximation of the energy transfer process.

More recently, interest has been focused on the use of transport theory^{5/} for dealing with the heterogeneities present in a reactor lattice. This approach is embodied in the work of Honeck^{6,7/} where both the spatial and

^{3/} Neutron Spectra in Lattices and Infinite Media, Proceedings of the Brookhaven Conference on Neutron Thermalization, BNL 719, Vol. II, Brookhaven National Laboratory (1962).

^{4/} A. Hassitt, "Methods of Calculation for Heterogeneous Reactors," Progress in Nuclear Energy, Series I, Vol. 2, pp. 271-313, Pergamon Press, New York, London, Paris, and Los Angeles, 1958.

^{5/} Neutron Spectra in Lattices and Infinite Media, see Footnote 3.

^{6/} H. C. Honeck, "THERMOS -- A Thermalization Transport Theory Code for Reactor Lattice Calculations" BNL 5826, Brookhaven National Laboratory (1961).

moderation effects on the spectra are considered through a space and energy calculation utilizing integral transport theory with only slight restrictions on the complexity of the scattering model used.

Still another approach is that found in the work of Leslie.^{8,9/} In this formulation the effect of moderation and heterogeneity are both considered, but the spatial effects are mathematically subordinated by consideration of only the spatially averaged fluxes in the moderator and the fuel. This method of attack leads to physical transparency while allowing one to maintain and concentrate on the importance of the moderator scattering model.

This work is an extension of Leslie's ideas, culminating in a computer code which provides for the rapid calculation of the spatially averaged thermal neutron spectra in the moderator, fuel, and cladding regions of a reactor lattice. The simplified cell theory utilized in these calculations is formulated in Chap. 2. A general formulation is presented as well as a formulation in terms of escape probabilities defined for the fuel element and the moderator regions. The escape probabilities utilized are a polyenergetic generalization of those defined by Amouyal,

^{7/} H. C. Honeck, "The Calculation of the Thermal Utilization and Disadvantage Factor in Uranium/Water Lattices," Nucl. Sci. Eng. 18, 49-68 (1964).

^{8/} D. C. Leslie, "The Spectrox Method for Thermal Spectra in Lattice Cells," AEEW-M211, United Kingdom Atomic Energy Authority (1962).

Benoist, and Horowitz^{10/} in their one velocity thermal utilization theory. Chapter 3 deals with the escape probabilities defined for the moderator region, while Chap. 4 details the calculational methods available for the determination of the fuel element escape probability. Mathematical models for the energy transfer or scattering kernel are discussed in Chap. 5. Emphasis is placed on the models actually used for calculational purposes; the monatomic gas kernel^{11,12/} and the Nelkin water kernel.^{13/} Chapter 6 defines the calculations necessary in the determination of spatially averaged, energy dependent thermal fluxes for the moderator, cladding, and fuel regions in a lattice utilizing the simplified cell theory. Integral thermal properties are defined as are the averaged cross sections necessary for the accurate calculation of reaction rates. In Chap. 7 the formulated theory is applied to actual lattices. A study is made of the low enrichment, high density, uranium dioxide fueled and light water moderated Cornell University Zero

^{9/} D. C. Leslie, "The Calculation of Thermal Spectra in Lattices," Proceedings of the Brookhaven Conference on Neutron Thermalization, BNL 719, Vol. II, pp. 592-609, Brookhaven National Laboratory (1962).

^{10/} A. Amouyal, P. Benoist, and J. Horowitz, "Nouvelle Méthode de Determination du Facteur d'Utilization Thermique d'une Cellule," J. Nucl. Energy 6, 79 (1957).

^{11/} E. P. Wigner and J. E. Wilkins, Jr., "Effect of the Temperature of the Moderator on the Velocity Distribution of Neutrons with Numerical Calculations for H as the Moderator," AECD-2275 (1944).

Power Reactor cores.^{14/} Temperature effects are predicted through the use of temperature dependent models for the scattering kernel. The accuracy of these results are discussed in Chap. 8. This chapter also includes a comparison of the results predicted with the simplified cell theory to those calculated by Honeck with THERMOS^{15/} for the Brookhaven light water moderated, and uranium dioxide fueled lattices. Chapter 9 contains a summary of the work undertaken as well as the conclusions which may be drawn from it.

-
- ^{12/} J. E. Wilkins, Jr., "Effect of Temperature of the Moderator on the Velocity Distribution of Neutrons for a Heavy Moderator," CP-2481 (1944).
 - ^{13/} M. S. Nelkin, "Scattering of Slow Neutrons by Water," Phys. Rev. 119, 741-746 (1960).
 - ^{14/} D. D. Clark, "The Cornell University Nuclear Reactor Laboratory," CURL-1, Cornell University (1961).
 - ^{15/} H. C. Honeck, see Footnote 7.

CHAPTER 2

A SIMPLIFIED CELL THEORY

2.1 General Formulation

Recognizing that the neglect or oversimplification of the spatial effects in a heterogeneous lattice leads to answers which have little relationship to the physical processes taking place, one is prompted to overemphasize the spatial variations by resorting to multigroup diffusion^{16/} or transport^{17/} codes. However, these codes consume a considerable amount of computer time, particularly if the more complex models of the scattering kernel are used.

Thus, there is a need for a simple polyenergetic formulation for determining the thermal distribution of neutrons in the various regions of a heterogeneous lattice. Hopefully one could retain the calculational ease of the homogeneous, infinite medium thermal spectrum computation, thereby offering only slight limitations on the complexity of the scattering model used, while still accounting for the heterogeneities of the lattice in a meaningful way.

This section formulates a simplified cell theory for use in the calculation of thermal spectra and parameters in a lattice composed of uniformly arrayed unit cells. The

^{16/} R. S. Varga, "Numerical Methods for Solving Multi-Dimensional Multigroup Diffusion Equations," Proceedings of Symposia in Applied Mathematics, Vol. XI, pp. 164-189, Nuclear Reactor Theory, American Mathematical Society, Providence (1961).

heterogeneous effects due to neutron transport within the cell are formulated in a physically transparent manner, thereby allowing sufficient emphasis to be placed on the moderation process in any calculation.

Consider first the neutron balance equation to be solved in the case of an infinite, homogeneous, moderating medium:^{18/}

$$\left[\Sigma_a^m(E) + \Sigma_s^m(E) \right] \phi^m(E) = S(E) + \int_0^{E_c} \Sigma(E' \rightarrow E) \phi^m(E') dE'. \quad (2.1)$$

E_c is the thermal cutoff energy above which the moderator flux per unit energy, $\phi^m(E)$, is assumed to be $1/E$, while $\Sigma(E' \rightarrow E)$ is the energy transfer or scattering kernel expressed in $(\text{cm-eV})^{-1}$. $\Sigma_a^m(E)$ and $\Sigma_s^m(E)$ are the macroscopic absorption and scattering cross sections respectively of the moderator, $\Sigma_s^m(E)$ being defined by

$$\Sigma_s^m(E) = \int_0^{E_c} \Sigma(E \rightarrow E') dE'. \quad (2.2)$$

^{17/} H. C. Honeck, "THERMOS -- A Thermalization Transport Theory Code for Reactor Lattice Calculations," BNL-5826, Brookhaven National Laboratory (1961).

^{18/} M. J. Poole, M. S. Nelkin, and R. S. Stone, "The Measurement and Theory of Reactor Spectra," Progress in Nuclear Energy, Series I, Vol. 2, pp. 91-164, Pergamon Press, New York, London, Paris, and Los Angeles, 1958.

The source of thermal neutrons, $S(E)$, due to down scattering from energies above E_c is given by

$$S(E) = \int_{E_c}^{\infty} \Sigma(E' \rightarrow E) \varphi_c^m(E') dE' , \quad (2.3)$$

where $\varphi_c^m(E)$ is proportional to $1/E$.

Neutron conservation requires that

$$\int_0^{E_c} S(E) dE = \int_0^{E_c} \Sigma_a^m(E) \varphi^m(E) dE , \quad (2.4)$$

which is obtained by integrating Eq. (2.1) over energy from 0 to E_c .

The problem as stated places no restrictions on the form of the scattering kernel, $\Sigma(E' \rightarrow E)$, however, we require that it satisfy detailed balance:

$$\Sigma(E' \rightarrow E) M(E') = \Sigma(E \rightarrow E') M(E) , \quad (2.5)$$

where the Maxwellian distribution, $M(E)$, is given by

$$M(E) = E/(kT)^2 \exp(-E/kT) . \quad (2.6)$$

The moderator temperature in electron volts is equal to kT , T being the moderator physical temperature while k is Boltzmann's constant.

There are of course practical limitations which restrict the complexity of the kernel and the number of energy points to be utilized in the computer solution of Eq. (2.1).

The infinite medium calculation is now extended to the heterogeneous lattice utilizing the ideas embodied in Leslie's SPECTROX method.^{19/} Since the only effect which the fuel element has upon the spectrum in the moderator of a lattice cell is to modify the transport process in the vicinity of the fuel element, while contributing very little to the moderation process itself, one may postulate an infinite moderator region with a contrived energy dependent absorption cross section which includes the heterogeneous properties of the lattice. In other words, if the absorption cross section of the moderator can be appropriately modified to account for the neutron leakage into and absorption by the fuel element, one can then turn his attention to the choice of a proper scattering kernel. The calculational ease of Eq. (2.1) is still available along with the fact that the non moderating part of the reactor lattice has been accounted for.

Considering the energy dependent absorption rates, one defines

$$f(E) = \frac{\text{absorption rate in the fuel element at energy } E, \text{ per eV}}{\text{absorption rate in the lattice cell at energy } E, \text{ per eV}}. \quad (2.7)$$

The "fuel element" includes the fuel rod and its cladding, and in the case where there is no neutron absorption in the cladding, $f(E)$ can be considered to be the energy dependent thermal utilization. In terms of $f(E)$ the neutron

^{19/} D. C. Leslie, "The SPECTROX Method for Thermal Spectra in Lattice Cells," AEEW-M211, United Kingdom Atomic Energy Authority (1962).

loss rate per unit volume of the moderator due to leakage into and absorption by the fuel element may be expressed as $\Sigma_a^m(E)\bar{\phi}^m(E)f(E)/[1-f(E)]$, where $\bar{\phi}^m(E)$ is the spatially averaged flux in the moderator region having a volume of V^m :

$$\bar{\phi}^m(E) = \frac{1}{V^m} \int \phi^m(\vec{r}, E) dV . \quad (2.8)$$

Equation (2.1) may now be rewritten for the cell in a heterogeneous lattice as

$$\left(\Sigma_s^m(E) + \Sigma_a^m(E) \left[1 + \frac{f(E)}{1-f(E)} \right] \right) \bar{\phi}^m(E) = \bar{S}(E) + \int_0^{E_c} \Sigma(E' \rightarrow E) \bar{\phi}^m(E') dE' . \quad (2.9)$$

$\bar{S}(E)$ is now the spatially averaged slowing source of neutrons which appear in dE at E due to scattering collisions at energies greater than E_c .

$$\bar{S}(E) = \frac{1}{V^m} \int S(\vec{r}, E) dV . \quad (2.10)$$

As it stands, Eq. (2.9) is correct for an infinite reactor lattice and it could be modified to include the effects of thermal leakage out of the reactor assembly. However, since one is usually interested in the intensive properties of the lattice, conventional approaches neglect

this thermal leakage calculation. In addition, Eq. (2.9) becomes approximate as soon as one postulates appropriate mathematical models for the scattering kernel, $\Sigma(E' \rightarrow E)$, and for the relative fuel element absorption, $f(E)/[1-f(E)]$, in the quest for a practical and economic computer solution.

The most general formulation for the relative fuel element absorption may be obtained by considering a unit cell in an infinite reactor lattice. Assume a source of neutrons in dE at energy E and position \vec{r} , $N(\vec{r}, E)$, so that the spatially average source of neutrons, $N(E)$, per unit volume, V , is expressed by:

$$N(E) = \frac{1}{V} \int N(\vec{r}, E) dV . \quad (2.11)$$

Given $N(\vec{r}, E)$, one can in principle calculate the net current into the fuel element, $J_n(E)$, at each energy. The total number of neutrons absorbed by the fuel element at energy E is then $AJ_n(E)$, where A is the surface area of the fuel element. Since the total number of neutrons produced at E must equal the total number absorbed, the number of neutrons absorbed by the moderator is $VN(E) - AJ_n(E)$. The relative fuel element absorption is then expressed as:

$$\frac{f(E)}{1-f(E)} = \frac{AJ_n(E)}{VN(E) - AJ_n(E)} . \quad (2.12)$$

In the assumption of a spatially dependent neutron source, $N(\vec{r}, E)$, and the subsequent calculation of the net

current into the fuel element, any of several means may be utilized including the use of multigroup transport codes, integral transport theory, or energy dependent diffusion theory. The accuracy of the results is directly related to the effort expended on these calculations, and this fact must be reconciled with the desire to produce economy in the use of the computer along with the knowledge that certain errors will be introduced with the use of mathematical models for the scattering kernel.

It is to be noted that by incorporating and concentrating all of the heterogeneous effects into the function $f(E)$, the calculational simplicity of the infinite, homogeneous case has been retained as is seen in Eq. (2.9). A discussion of practical approximations for $f(E)$ is found in Secs. (2.2) and (2.3).

2.2 A Practical Approximation of Heterogeneous Effects

In formulating an analytic approximation for $f(E)$, the function which takes into account all of the heterogeneous effects in the lattice cell, one is forced to compromise between accuracy and computational ease. As an initial approach, the following simple model is postulated in an attempt to investigate the feasibility of this method in determining the thermal spectra within a lattice cell. In this work we have restricted ourselves to systems with cylindrical symmetry, recognizing that analogous results for spheres and slabs are obtainable.

Consider a cylindrical unit cell situated in the regular, rectangular or hexagonal, array of a lattice. It is characterized by the fuel element radius, r_o , and the moderator radius, r_1 . In determining r_1 from the actual lattice parameters, the Wigner-Seitz criterion^{20/} is applied. A spatially flat source of neutrons in the moderator, $N(E)$, is assumed. The validity of this assumption for the calculation of integral properties has been discussed by Pomraning.^{21/} Leslie^{22/} has indicated that multigroup transport calculations yield moderator flux shapes which compare favorably with those predicted by one group diffusion theory. In light of this it is proposed to calculate the net current into the fuel element, $J_n(E)$, through the extension of monoenergetic diffusion theory to the polyenergetic case. The flux shape in the cell moderator at any energy E is assumed to be spatially distributed in a manner given by solution of the constant cross section diffusion theory approximation, using cross sections evaluated at the energy E :

$$D_m(E) \nabla^2 \phi^m(r, E) - \sum_a^m(E) \phi^m(r, E) + N(E) = 0 . \quad (2.13)$$

^{20/} S. Glasstone and M. C. Edlund, The Elements of Nuclear Reactor Theory, p. 265, D. Van Nostrand Company, Inc., Princeton, Toronto, London, and New York, 1952.

^{21/} G. C. Pomraning, "On the Validity of the Constant Source Assumption for the Cell Problem," Nucl. Sci. Eng. 18, 400-403 (1964).

^{22/} D. C. Leslie, see Footnote 19.

The boundary conditions applied are

$$\nabla \varphi^m(r_1, E) = 0 , \quad (2.14)$$

and

$$\frac{\varphi^m(r_o, E)}{\nabla \varphi^m(r_o, E)} = d(E) . \quad (2.15)$$

$D_m(E) = 1/3 \Sigma_{tr}^m(E)$ is the moderator diffusion coefficient, $\Sigma_a^m(E)$ is the moderator macroscopic absorption cross section, and $d(E)$ is the energy dependent linear extrapolation length. The linear extrapolation length may be determined from $d_o(E)$, the linear extrapolation length into a black cylindrical hole,^{23/} by characterizing the fuel element with its escape probability, $P_e(E)$. This has the added advantage of eliminating the need to state anything explicit about the shape of the flux within the fuel element. The fuel element spatial flux is implied in any calculation of the escape probability, but by dealing strictly with $P_e(E)$ one can extract and utilize in a simple manner the accuracy of transport theory calculations.^{24/}

Considering the escape probability of the fuel element as its albedo,^{25/} and including the term in $\nabla^2 \varphi$ which can

^{23/} A. M. Weinberg and E. P. Wigner, The Physical Theory of Neutron Chain Reactors, p. 765, The University of Chicago Press, Chicago, 1958.

^{24/} K. B. Cady and M. Clark, Jr., "Neutron Transport in Cylindrical Rods," Nucl. Sci. Eng., 18, 491-507 (1964).

^{25/} S. Glasstone and M. C. Edlund, p. 129, see Footnote 20.

be obtained in the derivation of Fick's Law,^{26/} one can write

$$P_e(E) = \frac{\phi^m(r_o, E) - 2D_m(E)\nabla\phi^m(r_o, E) + G(E)\nabla^2\phi^m(r_o, E)}{\phi^m(r_o, E) + 2D_m(E)\nabla\phi^m(r_o, E) + G(E)\nabla^2\phi^m(r_o, E)} . \quad (2.16)$$

For a black cylindrical hole, $P_e(E)$ is by definition zero so that $G(E)$ is given by

$$G(E) = \frac{\nabla\phi^m(r_o, E)}{\nabla^2\phi^m(r_o, E)} \left[2D_m(E) - d_o(E) \right] . \quad (2.17)$$

In the actual cell, where $P_e(E)$ is known from transport theory calculations, substitution of Eq. (2.17) into Eq. (2.16) yields with rearrangement

$$d(E) = \frac{\phi^m(r_o, E)}{\nabla\phi^m(r_o, E)} = \frac{4D_m(E)P_e(E)}{1-P_e(E)} + d_o(E) . \quad (2.18)$$

An approximate expression for $d_o(E)$ is given in Appendix C while the calculation of the fuel element escape probability is discussed in Chap. 4.

The relative fuel absorption, $f(E)/[1-f(E)]$, may now be found from the solution of Eq. (2.13) utilizing the boundary conditions in Eqs. (2.14), (2.15), and (2.18). For a cylindrical cell, Eq. (2.12) may be expressed as

$$\frac{1-f(E)}{f(E)} = \frac{N(E)r_o(y^2-1)}{2D_m(E)\nabla\phi^m(r_o, E)} - 1 , \quad (2.19)$$

where $y = r_1/r_o$. Denoting $\Sigma_a^m(E)/D_m(E)$ by κ^2 , it follows that

^{26/} A. M. Weinberg and E. P. Wigner, pp. 192-194, see Footnote 23.

$$\nabla \phi^m(r_o, E) = \frac{N(E)/\Sigma_a^m(E)}{\chi(E)/\kappa + d_o(E) + \frac{4D_m(E)P_e(E)}{1-P_e(E)}} , \quad (2.20)$$

where

$$\chi(E) = \frac{K_1(\kappa r_1)I_0(\kappa r_o) + I_1(\kappa r_1)K_0(\kappa r_o)}{K_1(\kappa r_1)I_0(\kappa r_o) - I_1(\kappa r_1)K_0(\kappa r_o)} . \quad (2.21)$$

I_o , I_1 , K_o , and K_1 are the modified Bessel functions of the first and second kind, respectively. Substitution into Eq. (2.19) yields

$$\begin{aligned} \frac{1-f(E)}{f(E)} &= \frac{2r_o(y^2-1)\Sigma_a^m(E)P_e(E)}{1-P_e(E)} + \frac{r_o(y^2-1)\kappa\chi(E)}{2} \\ &\quad + \frac{r_o(y^2-1)\Sigma_a^m(E)d_o(E)}{2D_m(E)} - 1 . \end{aligned} \quad (2.22)$$

Insertion of Eq. (2.22) into Eq. (2.9) thus attempts to account for the heterogeneous effects in the lattice through use of diffusion theory in the moderator and transport theory in the fuel element. The formulation is not restricted to the use of diffusion theory in the moderator region but it is utilized because of its calculational ease and good approximation to one velocity transport theory.

2.3 Formulation In Terms of Escape Probabilities

The expression, Eq. (2.22), which approximates the relative fuel absorption, and hence, the heterogeneous effects in the cell may also be arrived at by the formulation of the energy dependent absorption rates in terms of moderator and fuel element escape probabilities. This approach is an extension of Amouyal, Benoist, and Horowitz's one velocity thermal utilization theory^{27/} to the polyenergetic case.

One begins by defining the following energy dependent escape probabilities, all of which are calculated assuming the adjacent region is black:

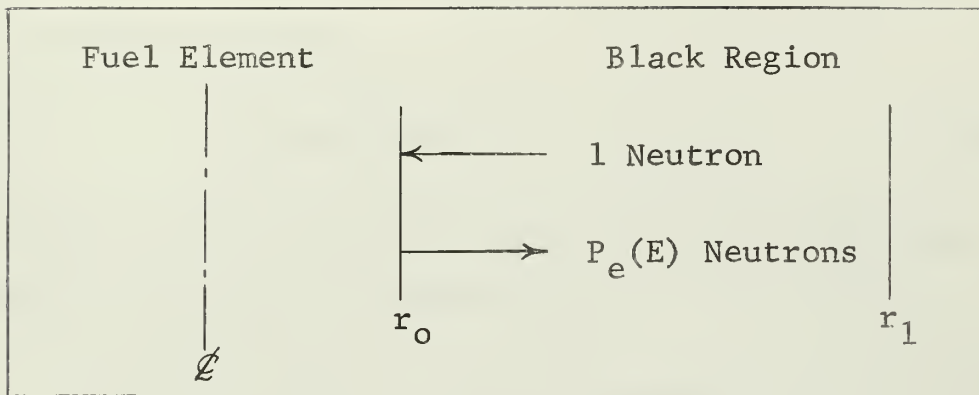
$P_e(E)$ is the escape probability of neutrons incident on the fuel element in the actual lattice directional distribution,

$P_s(E)$ is the escape probability of neutrons in the moderator at energy E due to collisions at other energies, and,

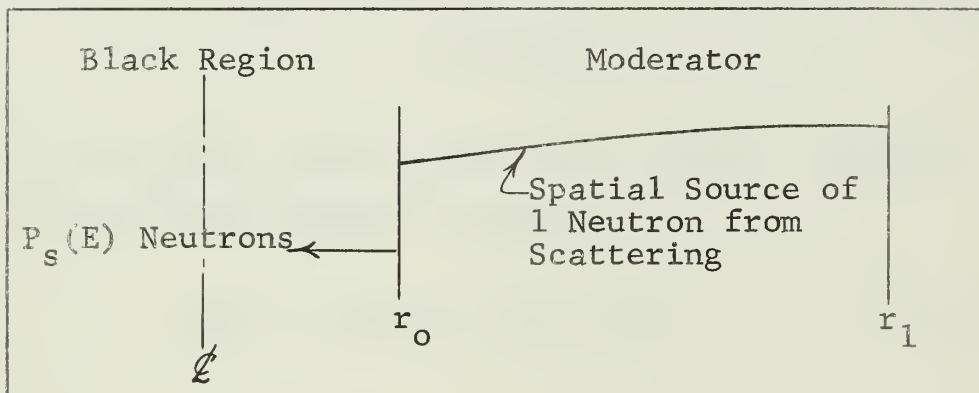
$P_m(E)$ is the escape probability of neutrons incident on the moderator from the fuel element.

These escape probabilities are schematically depicted in Fig. 2.1 for a Wigner-Seitz cylindrical cell. If one

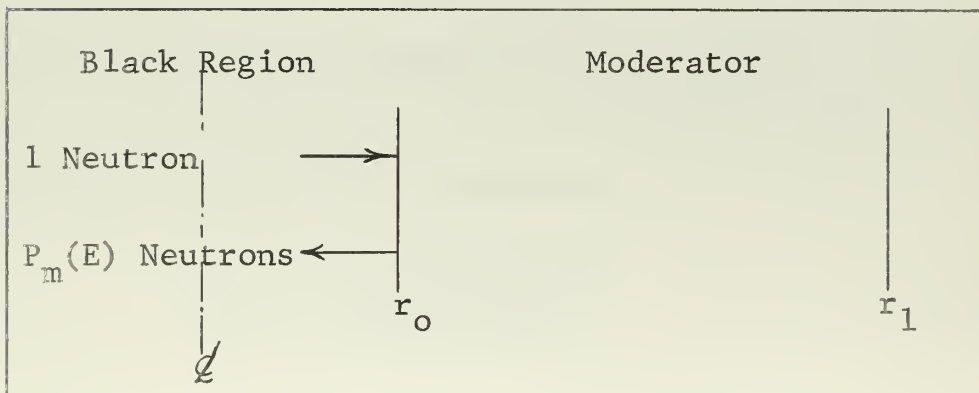
^{27/} A. Amouyal, P. Benoist, and J. Horowitz, "Nouvelle Méthode de Determination du Facteur d'Utilization Thermique d'une Cellule," J. Nucl. Energy 6, 79 (1957).



Fuel Element Escape Probability, $P_e(E)$



Moderator Escape Probability, $P_s(E)$



Moderator Escape Probability, $P_m(E)$

Figure 2.1 The Fuel Element and Moderator Escape Probabilities

considers a spatial source of neutrons from scattering which has been normalized to one:

$$\int N(\vec{r}, E) dV = 1 , \quad (2.23)$$

then reference to Fig. 2.1 shows that the current into the fuel element, $J_n(E)$, may be expressed as

$$AJ_n(E) = P_s(E) + P_e(E)P_m(E)AJ_n(E) , \quad (2.24)$$

or,

$$AJ_n(E) = \frac{P_s(E)}{1 - P_e(E)P_m(E)} , \quad (2.25)$$

where A is the surface area of the fuel element. The net current into the fuel element is given by

$$J_n(E) = J_n(E) - P_e(E)J_n(E) , \quad (2.26)$$

so that

$$AJ_n(E) = \frac{[1 - P_e(E)]P_s(E)}{1 - P_e(E)P_m(E)} . \quad (2.27)$$

Since the source has been normalized to one neutron, Eq. (2.27) is the ratio of the absorption rate in the fuel element to the absorption rate in the cell. Therefore,

$$f(E) = \frac{[1 - P_e(E)]P_s(E)}{1 - P_e(E)P_m(E)} . \quad (2.28)$$

Rearranging Eq. (2.28) or substituting Eq. (2.27) into Eq. (2.12) yields:

$$\frac{1-f(E)}{f(E)} = \frac{P_e(E)}{1-P_e(E)} \left[\frac{1-P_m(E)}{P_s(E)} \right] + \frac{1-P_s(E)}{P_s(E)} . \quad (2.29)$$

Writing the heterogeneous effects in terms of these escape probabilities has several advantages. In the first place a certain amount of physical transparency is gained by separating the contributions of the fuel and moderator into easily defined quantities. Secondly, $P_e(E)$ is a functional of the fuel element properties and its calculation depends only slightly on the moderator through the directional distribution of the current entering the fuel elements. $P_s(E)$ and $P_m(E)$ are functionals of the moderator and are very nearly independent of the fuel element properties. In addition, there are no restrictions on this simple model and the escape probabilities may be calculated with as much sophistication as is desirable. Calculational techniques for determining the moderator escape probabilities, $P_s(E)$ and $P_m(E)$, are discussed in Chap. 3, while the fuel element escape probability, $P_e(E)$, is discussed in Chap. 4.

CHAPTER 3

MODERATOR ESCAPE PROBABILITIES

3.1 $P_s(E)$

In this chapter the moderator escape probabilities, $P_s(E)$ and $P_m(E)$, as defined in Sec. 2.3 are discussed. It will be shown that by making appropriate assumptions, the formulation of the heterogeneous effects in terms of escape probabilities, Eq. (2.29), is identical to the expression derived utilizing diffusion theory in the moderator and characterizing the fuel element with its escape probability, $P_e(E)$, as given in Eq. (2.22).

The simplest model for $P_s(E)$ in cylindrical geometry is obtained by assuming, as in Sec. 2.2, a spatially flat source of neutrons in the moderator. Again as an expediency it is assumed that the flux shape in the moderator is given by one velocity diffusion theory applied at each energy. One finds $P_s(E)$ by calculating the net current into a black cylindrical hole of radius r_o . For a spatial source normalized to one neutron, $P_s(E)$ is given by

$$P_s(E) = AD_m(E)\nabla\phi^m(r_o, E) . \quad (3.1)$$

Solving the diffusion equation, Eq. (2.13), with the boundary conditions given by

$$\nabla\phi^m(r_1, E) = 0 , \quad (3.2)$$

and,

$$\frac{\varphi^m(r_o, E)}{\nabla\varphi^m(r_o, E)} = d_o(E) ,$$

yields

$$\nabla\varphi^m(r_o, E) = \frac{1/[V^m \sum_a^m(E)]}{\chi(E)/\kappa + d_o(E)} . \quad (3.3)$$

V^m is the moderator volume, $\kappa^2 = \sum_a^m(E)/D_m(E)$, and $\chi(E)$ is given by Eq. (2.21). In accordance with Eq. (3.1), $P_s(E)$ is then given by

$$P_s(E) = \frac{2}{r_o(y^2-1)\kappa} \cdot \frac{1}{\chi(E) + \kappa d_o(E)} , \quad (3.4)$$

or rearranging,

$$\frac{1-P_s(E)}{P_s(E)} = \frac{r_o}{2} (y^2-1)\kappa^2 d_o(E) + \frac{r_o}{2} (y^2-1)\kappa \chi(E) - 1 . \quad (3.5)$$

As before, $y = r_1/r_o$. Figure 3.1 shows $P_s(E)$ as calculated for the Cornell University Zero Power Reactor cores. The effect of various water to uranium dioxide volume ratios is shown as well as the energy dependence. The parameters for the cores utilized in these calculations are given in Appendix A, while the cross section data incorporated in these computations are discussed in Chap. 7.

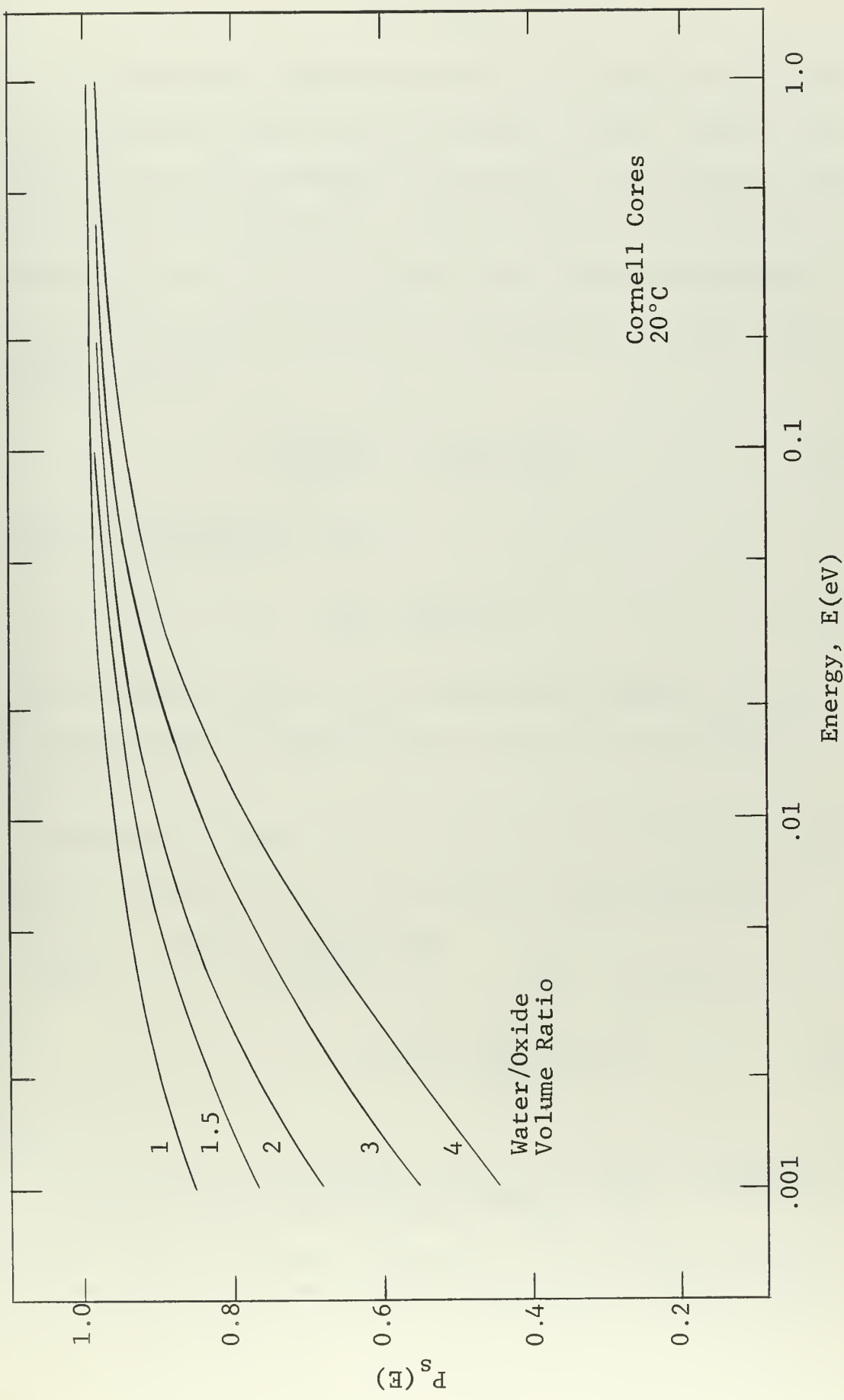


Figure 3.1 The Moderator Escape Probability, $P_s(E)$

3.2 $P_m(E)$

The moderator escape probability for neutrons incident on the moderator from the fuel element, $P_m(E)$, may be calculated from $P_s(E)$ through a reciprocity relationship under the following assumptions. If the flux in the moderator is isotropic, and if $P_s(E)$ is calculated using a spatially uniform source, as it has been, then $P_s(E)$ and $P_m(E)$ are related by^{28,29/}

$$\frac{1-P_m(E)}{P_s(E)} = 4 \sum_a^m(E) \frac{V^m}{A} , \quad (3.6)$$

where for cylindrical cells

$$\frac{V^m}{A} = \frac{r_o}{2}(y^2 - 1) . \quad (3.7)$$

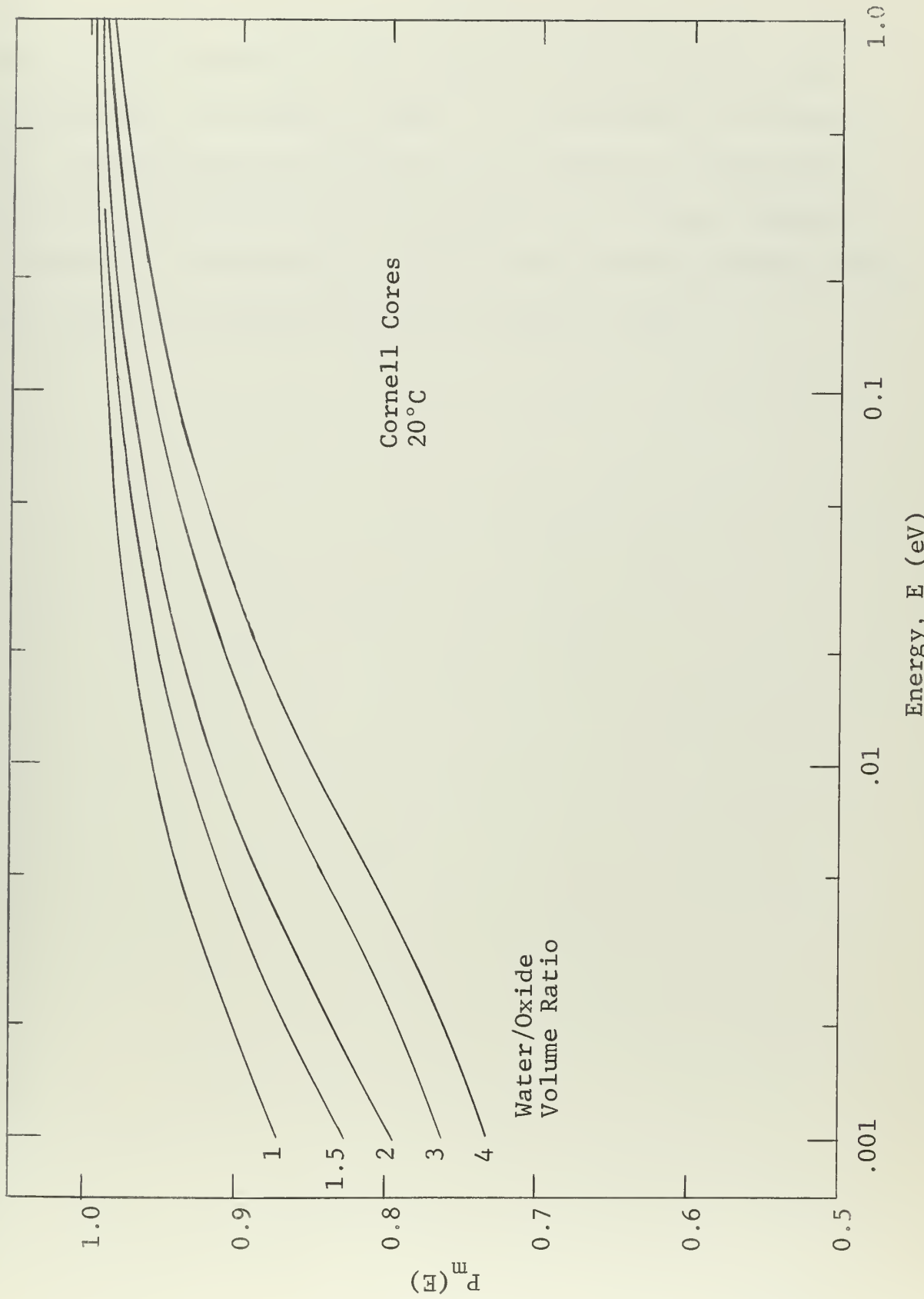
$P_m(E)$ is shown in Fig. 3.2 as calculated from Eq. (3.6) utilizing $P_s(E)$ as defined by Eq. (3.6) and depicted in Fig. 3.1.

Insertion of Eqs. (3.5), (3.6), (3.7) into Eq. (2.29) yields an expression for the relative fuel absorption:

$$\begin{aligned} \frac{1-f(E)}{f(E)} &= \frac{2r_o(y^2-1)\sum_a^m(E)P_e(E)}{1-P_e(E)} + \frac{r_o}{2}(y^2-1)\kappa\chi(E) \\ &\quad + \frac{r_o(y^2-1)\sum_a^m(E)d_o(E)}{2D_m(E)} - 1 , \end{aligned} \quad (3.8)$$

^{28/} K. M. Case, F. de Hoffmann, and G. Placzek, Introduction to the Theory of Neutron Diffusion, Vol. I, United States Government Printing Office, 1953.

^{29/} K. B. Cady, "Neutron Transport in Cylindrical Rods," Massachusetts Institute of Technology Thesis, 1962.

Figure 3.2 The Moderator Escape Probability, $P_m(E)$

which is identical with Eq. (2.22) as derived in Sec. 2.2. This is the expression which will be incorporated in the calculations discussed in Chap. 7 in an attempt to account for the heterogeneous effects of the lattice. Due to the physical transparency and separability of effects achieved through the consideration of the various escape probabilities, all future discussion will be in terms of them.

CHAPTER 4

THE FUEL ELEMENT ESCAPE PROBABILITY

4.1 The Fuel Rod Escape Probability

As was noted in Sec. 2.2, it is in many respects desirable to characterize the fuel element in terms of its escape probability, $P_e(E)$, thereby eliminating the need to explicitly define the flux in the various regions of the element. In addition, computation of $P_e(E)$ allows one to complete the calculation of the relative fuel absorption as defined in Eq. (3.8).

In the most general case, the fuel element is composed of a cladding region, a void region, and a fuel rod or fuel meat region. In the determination of $P_e(E)$, the fuel rod may be characterized by its escape probability, $P_r(E)$. The effect of the void may be accounted for by strictly geometric factors, while the cladding effects may be expressed in terms of several transmission factors. The results derived from the calculation of any of the above factors are of course dependent upon the assumption of an angular distribution of the current entering each respective region.

The fuel rod escape probability depends on the fuel rod radius, $a = \sum_t^f(E)r_f$, measured in mean free paths (mfp's) and the ratio, $c = \sum_s^f(E)/\sum_t^f(E)$ of the fuel scattering cross section to total cross section. The simplest expression for $P_r(E)$ is derived from diffusion theory and it is just the albedo of the rod:

$$P_r(E) = \frac{1-2D_f(E)\beta(E)}{1+2D_f(E)\beta(E)} , \quad (4.1)$$

where

$$\beta(E) = \kappa_f \frac{I_1(\kappa_f r_f)}{I_0(\kappa_f r_f)} . \quad (4.2)$$

I_0 and I_1 are the modified Bessel functions of the first kind, while $\kappa_f^2 = \Sigma_a^f(E)/D_f(E)$, $D_f(E)$ being the diffusion coefficient of the fuel. The quantity κ_f may be obtained either from P-1 theory^{30/}

$$\kappa_f/\Sigma_t^f(E) = \sqrt{3(1-c)} , \quad (4.3)$$

or from Wigner's "elementary theory,"

$$c \tanh^{-1}(\kappa_f/\Sigma_t^f(E)) = \kappa_f/\Sigma_t^f(E) . \quad (4.4)$$

Transport theory expressions for the fuel rod escape probability have also been developed from Boltzmann's one velocity transport equation under the assumption of isotropic scattering in the laboratory system. This results in the integral transport or Peierls' equation:

$$\phi(\vec{r}) = \phi_u(\vec{r}) + c \sum_t \int \frac{d\vec{r}'}{4\pi |\vec{r}-\vec{r}'|^2} e^{-\Sigma_t |\vec{r}-\vec{r}'|} \phi(\vec{r}') , \quad (4.5)$$

^{30/} A. M. Weinberg and E. P. Wigner, The Physical Theory of Neutron Chain Reactors, The University of Chicago Press, Chicago, 1958.

where $\phi_u(\vec{r})$ is the uncollided flux due to incident surface sources. Escape probabilities in terms of the solution of Eq. (4.5) have been considered by several authors.^{31, 32, 33/} This work utilizes the treatment by Cady for an isotropic flux incident upon the fuel rod. The calculational techniques utilized in the computation of $P_r(E)$ are quoted below.^{34/}

For thin rods of less than 0.5 mfp's a very accurate expression results from the uniform flux approximation. In terms of Placzek's collision probability,^{35/} M_{OO} , this yields the following expression for $P_r(E)$:

$$P_r(E) = 1 - 2a(1-c) \left[\frac{1-M_{OO}}{1-cM_{OO}} \right]. \quad (4.6)$$

M_{OO} is calculated in terms of the modified Bessel functions of the first and second kind with an argument of a :

$$M_{OO} = 1 - \frac{2}{3} \left(I_1 K_1 + 1 - 2a[I_1 K_0 + 1 - a(I_1 K_1 + I_0 K_0)] \right). \quad (4.7)$$

For rods which have radii, a , greater than 0.5 mfp's, the parabolic flux approximation yields more accurate results.

In this case

$$P_r(E) = 1 - 2a(1-c) \left\{ 1 - (1-c) \left[\frac{M_{OO} - c(M_{OO} M_{22} - 3M_{O2}^2)}{1 - c(4M_{OO} + 4M_{22} - 6M_{O2}) + c^2(4M_{OO} M_{22} - 2M_{O2}^2)} \right] \right\}, \quad (4.8)$$

where the following quantities are calculated in order:

^{31/} K. B. Cady, "Neutron Transport in Cylindrical Rods," Massachusetts Institute of Technology Thesis, 1962.

^{32/} K. B. Cady and M. Clark, Jr., "Neutron Transport in Cylindrical Rods," Nucl. Sci. Eng. 18, 491-507 (1964).

$$A = a[I_1(a)K_1(a) + I_0(a)K_0(a)] , \quad (4.9)$$

$$B = 2a(I_1 K_0 + 1 - A) , \quad (4.10)$$

$$C = \frac{2}{3}(I_1 K_1 + 1 - B) , \quad (4.11)$$

$$D = \frac{2}{3}(I_2 K_0 - 1 + B + C) , \quad (4.12)$$

$$E = \frac{4}{5}(\frac{2I_2 K_1}{a} + C - D) , \quad (4.13)$$

$$F = \frac{6}{7}(\frac{1}{a^2} - \frac{4I_2 K_2}{a^2} + E) , \quad (4.14)$$

$$M_{00} = 1 - C , \quad (4.15)$$

$$M_{02} = 1 - 2C + E , \quad (4.16)$$

and,

$$M_{22} = 1 - 3C + 3E - F .$$

Consideration of the asymptotic expansions for the moments, M_{00} , M_{02} , and M_{22} , yields the following approximations for the fuel rod escape probability. For the uniform flux approximation,

$$P_r(E) \approx \frac{1}{1 + 2a(1-c)} = \frac{1}{1 + 2\sum_f(E)r_f} , \quad (4.17)$$

and for the parabolic flux approximation,

$$P_r(E) \approx \frac{1 + 2a(1-c)}{1+4a(1-c) + \frac{16}{3} a^2(1-c)^2 + \frac{32}{3} a^3(1-c)^4} . \quad (4.18)$$

33/ G. W. Stuart and R. W. Woodruff, "Method of Successive Generations," Nucl. Sci. Eng. 10, 388 (1961).

Figure 4.1 shows the fuel rod escape probability as calculated utilizing the expressions stated above. The effect of the 0.27 U^{235} resonance is plainly evident. The parameters used in the computations are those of the low enrichment, high density uranium dioxide fuel of the Cornell University Zero Power Reactor. These parameters are listed in Appendix A, while cross section data are discussed in Chap. 7. The numerical methods needed for calculation of the modified Bessel functions are outlined in Appendix C.

4.2 Void Considerations

Any void space which is present between the fuel rod and the cladding is accounted for by considering the fraction of neutrons entering the void space from the cladding which are heading toward the fuel rod. The escape probability for the fuel rod and the void, $P_{rv}(E)$, may then be expressed as

$$P_{rv}(E) = (1 - \zeta) + \zeta P_r(E), \quad (4.19)$$

where ζ is the fraction of the neutrons headed toward the fuel rod. For an assumed isotropic flux emergent from the cladding,^{36/}

$$\zeta = r_f/r_c \quad (4.20)$$

^{34/} K. B. Cady, see Footnote 31.

^{35/} K. M. Case, F. de Hoffman, and G. Placzek, Introduction to the Theory of Neutron Diffusion, Vol. I, United States Government Printing Office, 1953.

^{36/} K. B. Cady, p. 161, see Footnote 31.

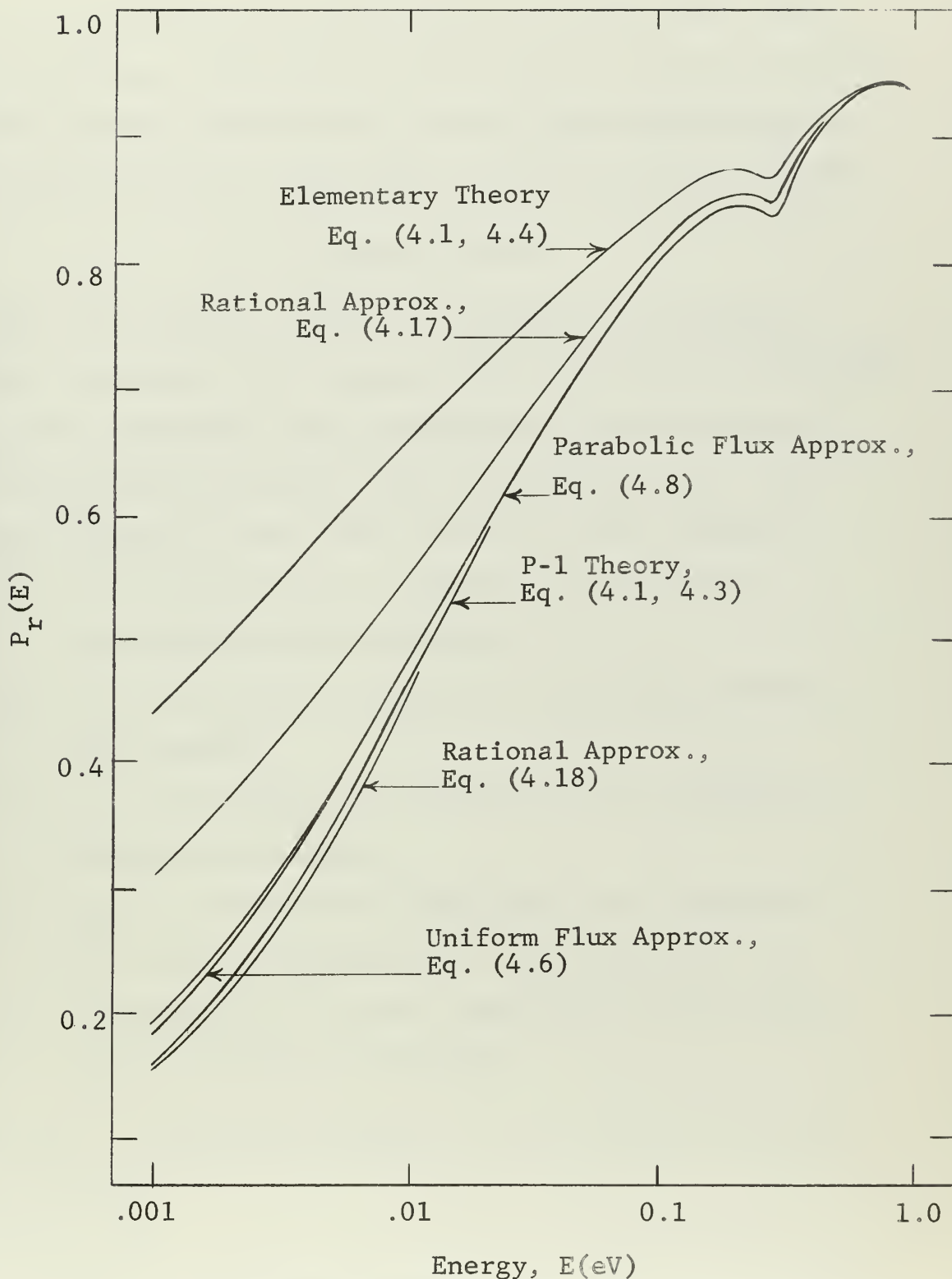


Figure 4.1 The Fuel Rod Escape Probability, $P_r(E)$

where r_f is the fuel rod radius and r_c is the inner radius of the cladding. Examination of Eqs. (4.19) and (4.20) shows that the correct limits exist in that $P_{rv}(E)$ goes to $P_r(E)$ as r_c goes to r_f , and $P_{rv}(E)$ goes to one as r_f goes to zero.

4.3 Cladding Effects

The fuel element cladding is treated in accordance with the cylindrical thin region theory developed by Cady.^{37/} The neutron reflection and transmission characteristics of the cladding can be divided into several fractions. For neutrons incident on the outer surface of the cladding,

1. g is the fraction of neutrons, which return uncollided to the moderator,
2. T is the fraction transmitted uncollided through the cladding,
3. r_{in} is the fraction scattered in and transmitted through the cladding,
4. r_{out} is the fraction scattered in and reflected out of the cladding back to the moderator, and
5. $1-(g+T+r_{in}+r_{out})$ is the remaining fraction which is absorbed in the cladding.

Similarly, for neutrons incident on the cladding from the fuel rod region,

^{37/} K. B. Cady, p. 63, see Footnote 31.

1. τ is the fraction transmitted uncollided through the cladding into the moderator,
2. ρ_{in} is the fraction scattered in the cladding and reflected back into the fuel rod and void region,
3. ρ_{out} is the fraction scattered in and transmitted through the cladding, and,
4. $1-(\tau+\rho_{in}+\rho_{out})$ is the remaining fraction which is absorbed in the cladding.

In terms of these energy dependent fractions, the escape probability for the entire fuel element may be expressed as

$$P_e(E) = g + r_{out} + (\tau + \rho_{out}) J_o(E) . \quad (4.21)$$

$J_o(E)$ is the net current entering the inner surface of the cladding from the fuel rod and is a function of $P_{rv}(E)$, the escape probability of the void and fuel rod region:

$$J_o(E) = \frac{(\tau + r_{in}) P_{rv}(E)}{1 - \rho_{in} P_{rv}(E)} . \quad (4.22)$$

The computational receipes used for the calculation of the various fractions mentioned above are stated below. These schemes assume isotropic fluxes on both sides of the cladding and they are performed at each energy where applicable. The outer radius of the cladding is denoted by r_o , the inner cladding radius is r_c . Macroscopic cross sections refer to the cladding material.

$$\xi = r_c/r_o , \quad (4.23)$$

$$t = r_o - r_c , \quad (4.24)$$

$$\Theta = 1 - \xi^2 , \quad (4.25)$$

$$F_o = \frac{2}{\pi} \sin^{-1} \xi , \quad (4.26)$$

$$F_1 = \xi , \quad (4.27)$$

$$F_2 = F_o + \frac{2}{\pi} \xi \sqrt{\Theta} , \quad (4.28)$$

$$F_3 = \frac{3}{2} \xi (1 - \xi^2/3) , \quad (4.29)$$

$$D_1 = \frac{\pi}{4} \xi^2 , \quad (4.30)$$

$$\Lambda = \ln(4/\sqrt{\Theta}) , \quad (4.31)$$

$$D_2 = \frac{2}{3} \left[1 - \frac{3}{4}\Theta - \frac{3}{16}(\Lambda - \frac{1}{4})\Theta^2 - \frac{3}{64}(\Lambda - \frac{11}{12})\Theta^3 \right] , \quad (4.32)$$

$$\bar{L}_1^1 = (F_2 - \frac{4}{\pi} D_1)/F_1 , \quad (4.33)$$

$$\bar{L}_1^2 = (\frac{8}{3} F_3 - 2\Theta F_1 - 4D_2)/F_1 , \quad (4.34)$$

$$T = F_1 - \Sigma_t^c(E)r_o F_1 \bar{L}_1^1 + \frac{1}{2}(\Sigma_t^c(E)r_o)^2 F_1 \bar{L}_1^2 , \quad (4.35)$$

$$C_1 = (\frac{1}{2\xi})(\frac{\pi}{2} F_o + \xi \sqrt{\Theta}) , \quad (4.36)$$

$$C_2 = D_2 / \xi^2 , \quad (4.37)$$

$$\bar{Z}_1^1 = \frac{4}{\pi} C_1 - \xi , \quad (4.38)$$

$$\bar{Z}_1^2 = 2\Theta - \frac{8}{3} \xi - 4\xi C_2 , \quad (4.39)$$

$$\tau = 1 - \Sigma_t^c(E) r_o \bar{x}_1^1 + \frac{1}{2} (\Sigma_t^c(E) r_o)^2 \bar{x}_1^2 , \quad (4.40)$$

$$\gamma = 0.577215 \dots, \text{ Euler's Constant}, \quad (4.41)$$

$$x = \Sigma_t^c(E) t , \quad (4.42)$$

$$\begin{aligned} P_u &= \frac{x}{2} [\gamma + \ln(x) - \frac{3}{2}] + 1 - \frac{x^2}{6} \\ &\quad + \frac{x^3}{48} - \frac{x^4}{360} + \frac{x^5}{2880} , \end{aligned} \quad (4.43)$$

and,

$$P_{\text{unif}} = \frac{P_u}{1 - \frac{\Sigma_s^c(E)}{\Sigma_t^c(E)} (1 - P_u)} . \quad (4.44)$$

For $x \leq .05$,

$$g = (1 - F_1) - 2 \Sigma_t^c(E) r_o (1 - F_2) + \frac{1}{2} (\Sigma_t^c(E) r_o)^2 \cdot \frac{16}{3} (1 - F_3) , \quad (4.45)$$

while for $.05 < x \leq 0.2$,

$$g = -.0212 - .0266 \ln(x) / \xi^2 \cdot 2 . \quad (4.45)$$

$$r_{\text{in}} + r_{\text{out}} = \frac{\Sigma_s^c(E)}{\Sigma_t^c(E)} (1 - g - T) P_{\text{unif}} , \quad (4.46)$$

$$\rho_{\text{in}} + \rho_{\text{out}} = \frac{\Sigma_s^c(E)}{\Sigma_t^c(E)} (1 - \tau) P_{\text{unif}} , \quad (4.47)$$

$$f_{\text{in}} = \frac{1}{\pi} \sin^{-1} \left(\frac{2\xi}{1+\xi} \right) , \quad (4.48)$$

$$r_{in} = f_{in}(r_{in} + r_{out}) , \quad (4.49)$$

$$r_{out} = (r_{in} + r_{out}) - r_{in} , \quad (4.50)$$

$$\rho_{in} = f_{in} (\rho_{in} + \rho_{out}) , \quad (4.51)$$

and,

$$\rho_{out} = (\rho_{in} + \rho_{out}) - \rho_{in} . \quad (4.52)$$

Calculations have been made using the above techniques for the fuel elements of the Cornell University Zero Power Reactor, the specifications of which are given in Appendix A. The results of these computations in the form of the fuel element escape probability are shown in Fig. 4.2. In these calculations, the parabolic flux approximation, Eq. (4.8), was used for the calculation of $P_r(E)$. Again the effect of the U^{235} resonances can be seen.

In terms of previously defined quantities, the ratio of the number of neutrons absorbed in the fuel rod to the number absorbed in the fuel element is given by

$$\frac{\text{rod abs. rate}}{\text{element abs. rate}} = \frac{J_o(E)[1-P_{rv}(E)]}{P_{rv}(E)[1-P_e(E)]} . \quad (4.53)$$

Similarly the ratio of the number of neutrons absorbed in the cladding to the number absorbed in the fuel element can be defined by

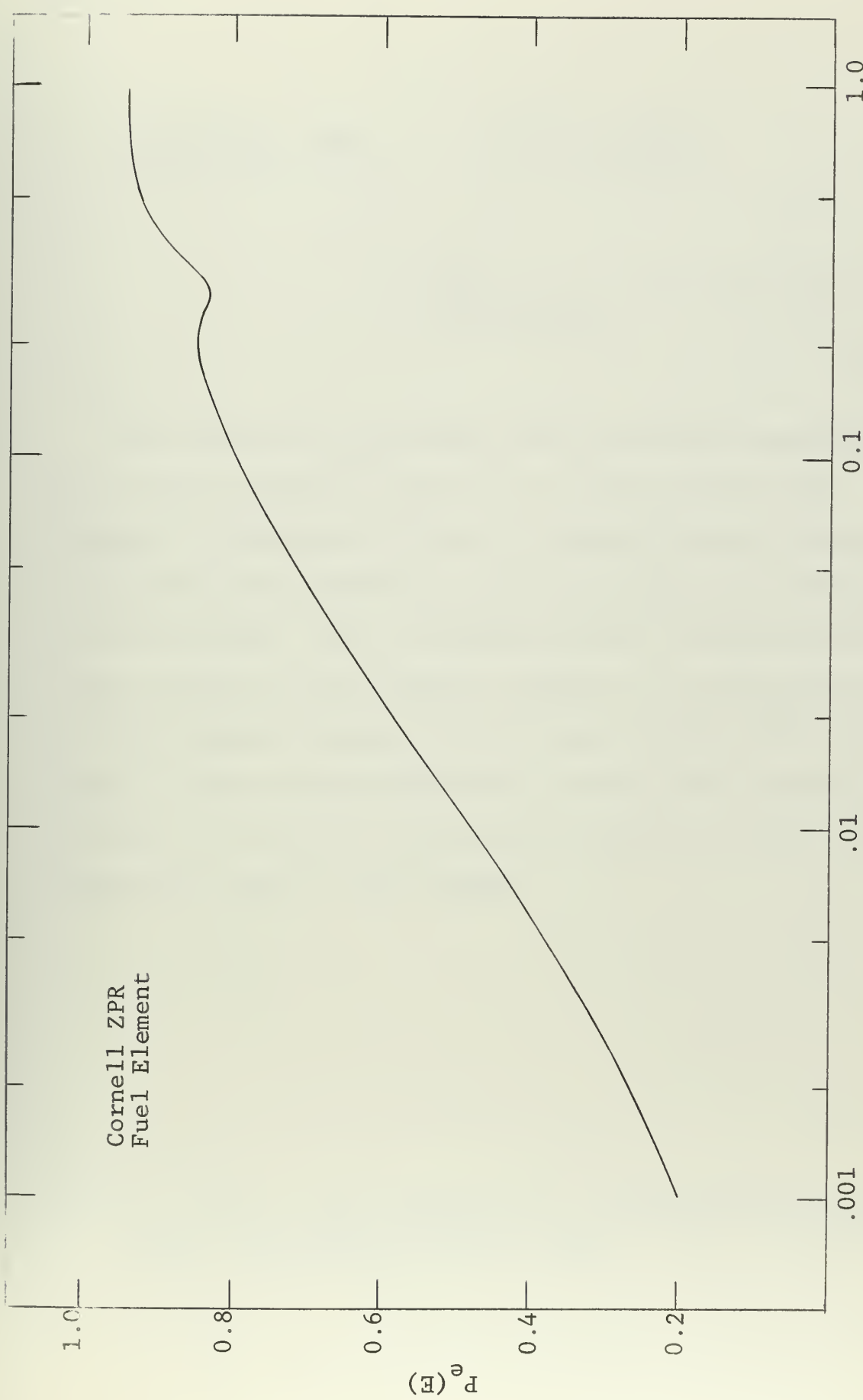


Figure 4.2 The Fuel Element Escape Probability, $P_e(E)$

$$\frac{\text{clad abs. rate}}{\text{element abs. rate}} = 1 - \frac{J_o(E)[1-P_{rv}(E)]}{P_{rv}(E)[1-P_e(E)]}, \quad (4.54)$$

$$= \frac{\Sigma_a^c(E)}{\Sigma_a^c(E) + \Sigma_s^c(E)P_u} [(1-g-T) + J_o(E)(1-\tau)]. \quad (4.55)$$

The results of performing the calculation expressed by Eq. (4.53) are shown in Fig. 4.3 for the Cornell fuel elements. Inspection of Fig. 4.3 shows that only about 1% of the neutrons absorbed by the fuel element are absorbed in the cladding. This is because of the low absorption cross section of the aluminum cladding. On the other hand, in the Brookhaven uranium dioxide fuel elements,^{38/} (see Chap. 8), where stainless steel is used as the cladding material, about 12% of the neutrons absorbed in the fuel element are lost to the cladding.

^{38/} H. C. Honeck, "The Calculation of Thermal Utilization and Disadvantage Factor in Uranium Water Lattices," Nucl. Sci. Eng. 18, 49-68 (1964).

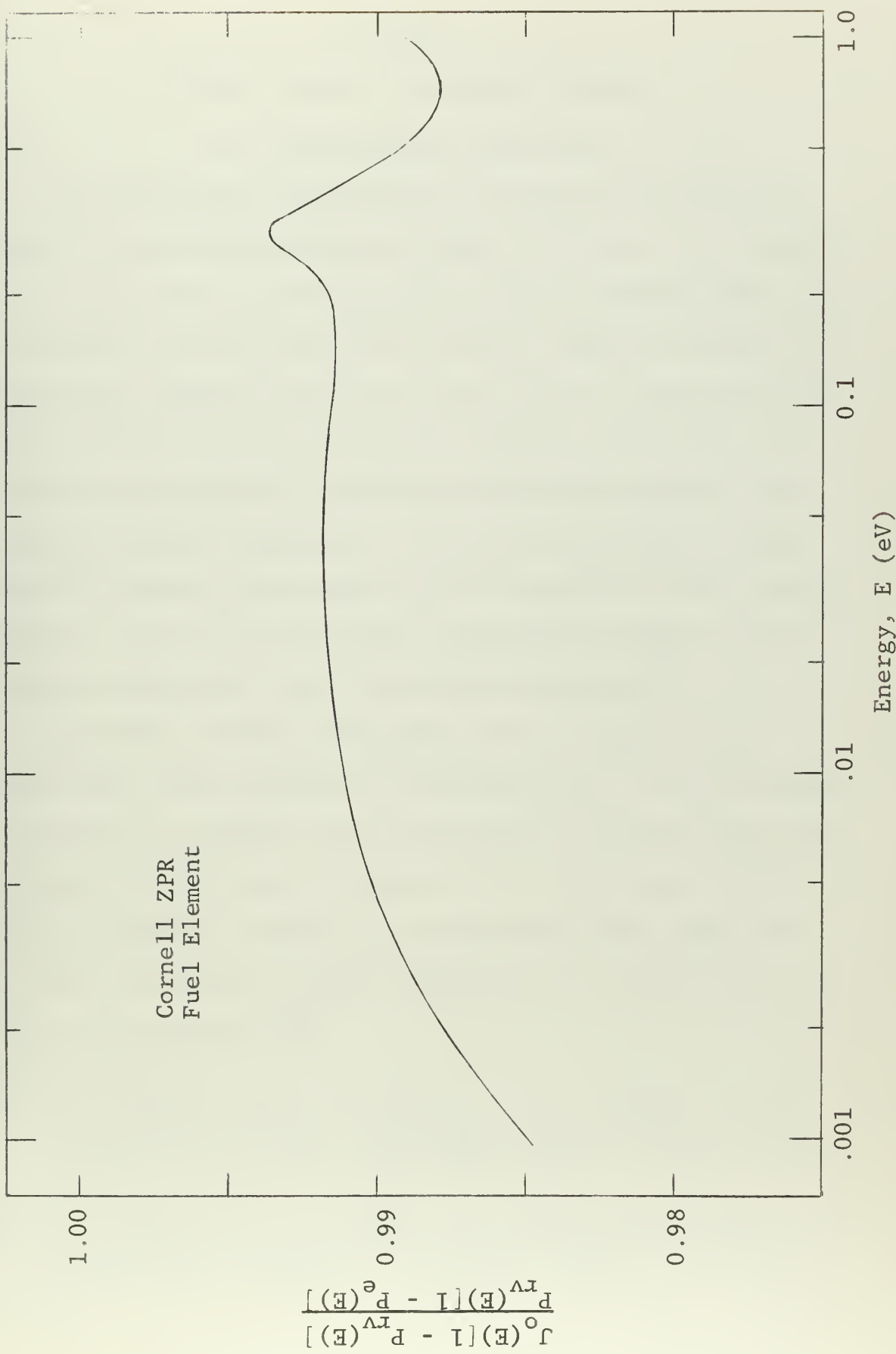


Figure 4.3 The Ratio of the Fuel Rod Absorption Rate to the Fuel Element Absorption Rate

CHAPTER 5

MODELS FOR THE SCATTERING KERNEL

5.1 The Monatomic Gas Model

By formulating the lattice heterogeneous effects in terms of contrived absorption rates as in Secs. 2.1 and 2.3, one is left free to incorporate as much sophistication as is desired into the calculation of the energy transfer or scattering kernel to be used in Eq. (2.9). With this type of an approach one can determine directly the effect of different mathematical models on the neutron spectra and lattice integral properties. One can then decide on the basis of computer time used and the accuracy of the results whether or not use of the more complicated models for the kernel is desirable for a particular computation.

Numerous mathematical models for the scattering kernel have been proposed.^{39,40,41,42,43,44/} In an attempt to bracket the degrees of computational difficulty and the accuracy of the results predicted with these many models, we have limited ourselves to calculations with only two of them; the Wigner-Wilkins monatomic gas model^{45/} and the Nelkin water kernel.^{46/}

^{39/} E. P. Wigner and J. E. Wilkins, Jr., "Effect of the Temperature of the Moderator on the Velocity Distribution of Neutrons with Numerical Calculations for H as the Moderator," AECD-2275 (1944).

^{40/} J. E. Wilkins, Jr., "Effect of Temperature of the Moderator on the Velocity Distribution of Neutrons for a Heavy Moderator," CP-2481 (1944).

The choice of the monatomic gas model is mainly dictated by its ease of calculation. This model treats the moderator as a free gas in thermal equilibrium at the temperature of the moderator. Although crystalline or molecular binding effects in the thermalization properties of the moderator are neglected, infinite homogeneous media calculations^{47/} with this model have yielded spectra which are essentially consistent with those measured experimentally.

The cross section for scattering from an energy E' to an energy E through an angle with a cosine of μ may be derived from the short collision time approximation^{48/} applied to the single oscillational mode of the translational motion of the scattering particle. For the situation where E' is greater than E , this results in^{49/}

$$\sigma(E' \rightarrow E, \mu) = \frac{\sigma_b}{4} \left[\frac{EA}{E' \pi TX} \right]^{1/2} \exp \left[\frac{-A}{4TX} (E-E') + \frac{X}{A} \right]^2 , \quad (5.1)$$

^{41/} M. S. Nelkin, "Scattering of Slow Neutrons by Water," Phys. Rev. 119, 741-746 (1960).

^{42/} A. Radkowsky, "Temperature Dependence of the Thermal Transport Mean Free Path," Physics Quarterly Report, (April, May, June, 1950), ANL-4476, p. 89, Argonne National Laboratory (July, 1950).

^{43/} H. D. Brown and D. S. St. John, "Neutron Energy Spectrum in D_2O ," DP-33 (1954).

^{44/} The Scattering Law, Proceedings of the Brookhaven Conference on Neutron Thermalization, BNL 719, Vol. I, Brookhaven National Laboratory (1962).

where $\sigma(E' \rightarrow E, \mu)$ is in barns/(eV-unit cosine). The bound atom cross section in barns is σ_b , T is the moderator temperature in electron volts, and A is the ratio of the scattering nucleus mass to the neutron mass. The quantity X is related to the momentum transfer in that

$$X = E+E' - 2\mu\sqrt{EE'} . \quad (5.2)$$

A similar result can be obtained for upscattering in energy by employing the principle of detailed balance, Eq. (2.5) as is discussed below.

The scattering kernel is found by the angular integration of Eq. (5.1),

$$\sigma(E' \rightarrow E) = \int_{-1}^1 \sigma(E' \rightarrow E, \mu) d\mu . \quad (5.3)$$

This operation can be carried out analytically and it results in the formulation of the Wilkins' heavy gas model^{50/} for the scattering kernel. For down scattering in energy,

^{45/} E. P. Wigner and J. E. Wilkins, Jr., see Footnotes 39 and 40.

^{46/} M. S. Nelkin, see Footnote 41.

^{47/} L. G. de Sobrino and M. Clark, Jr., "A Study of the Wilkins Equation," Nucl. Sci. Eng. 10, 388 (1961); "Comparison of the Wilkins Equation with Experiments on Water Systems," Nucl. Sci. Eng. 10, 377 (1961).

^{48/} M. S. Nelkin, see Footnote 41.

^{49/} F. D. Federighi and D. T. Goldman, "KERNEL and PAM - Programs for Use in the Calculation of the Thermal Scattering Matrix for Chemically Bound Systems," KAPL-2225, Knolls Atomic Power Laboratory (1962).

^{50/} J. E. Wilkins, Jr., see Footnote 40.

$E' \geq E$, the monatomic gas scattering kernel is expressed in barns/eV as^{51/}

$$\sigma(E' \rightarrow E) = \frac{\sigma_f \eta^2}{2E'} \left(\text{ERF}(\eta z - \rho z') + \text{ERF}(\eta z + \rho z') + \exp(z'^2 - z^2) [\text{ERF}(\eta z' - \rho z) - \text{ERF}(\rho z + \eta z')] \right), \quad (5.4)$$

where

$$z^2 = E/T, \quad (5.5)$$

$$z'^2 = E'/T, \quad (5.6)$$

$$\eta = \frac{1}{2}(A+1)A^{-1/2}, \quad (5.7)$$

and,

$$\rho = \frac{1}{2}(A-1)A^{-1/2}. \quad (5.8)$$

$\text{ERF}(z)$ is the error function defined by

$$\text{ERF}(z) = \frac{2}{\sqrt{\pi}} \int_0^z e^{-y^2} dy, \quad (5.9)$$

while σ_f is the free atom scattering cross section for the moderating medium.

$$\sigma_f = \sigma_b \left(\frac{A}{A+1} \right)^2. \quad (5.10)$$

The scattering kernel for upscattering, $E' < E$, is calculated utilizing detailed balance as expressed in Eq. (2.5).

In the case where one is considering moderation by hydrogen, Eq. (5.4) reduces to the Wigner-Wilkins model for

a gas of mass one.^{52/} Then for $E' \geq E$,

$$\sigma(E' \rightarrow E) = \frac{\sigma_f}{E'} \operatorname{ERF}(z) . \quad (5.11)$$

The use of the monatomic gas model has another advantage in that the scattering cross section defined by

$$\sigma_s(E) = \int_0^{\infty} \sigma(E \rightarrow E') dE' , \quad (5.12)$$

is an analytic function given by

$$\sigma_s(E) = \sigma_f \left[\left(1 + \frac{1}{2y^2} \right) \operatorname{ERF}(z) + \frac{e^{-y^2}}{\sqrt{\pi}y} \right] , \quad (5.13)$$

where

$$y^2 = \frac{EA}{T} . \quad (5.14)$$

This analytic function for the scattering cross section is useful because it allows one to check on the accuracy of the numerical integration scheme employed. This aspect is more fully discussed in Sec. 5.2.

The calculations performed utilizing the monatomic gas model for the scattering kernel are discussed in Chap. 7. Calculation of the error function necessary in the computations of this kernel is detailed in Appendix C.

^{51/} M. J. Poole, M. S. Nelkin, and R. S. Stone, "The Measurement and Theory of Reactor Spectra," Progress in Nuclear Energy, Series I, Vol. 2, pp. 91-164, Pergamon Press, New York, London, Paris, and Los Angeles, 1958.

^{52/} E. P. Wigner and J. E. Wilkins, Jr., see Footnote 39.

5.2 The Nelkin Water Kernel

The second mathematical model for the scattering kernel utilized in these calculations is that proposed by Nelkin^{53/} for protons bound in water. Although the computer calculation of the Nelkin water kernel takes a relatively long time, its use is justified in that infinite homogeneous media thermal spectra calculated with this model are in good agreement with those measured experimentally.^{54/} In addition, diffusion coefficients calculated with the Nelkin model^{55/} agree well with measured values.^{56/}

Physically, the mathematical approximation proposed by Nelkin for water treats the scattering molecule translation with the free gas model utilizing a translator mass (M) of 18. The effects of the atomic motions within the molecule are approximated by simple harmonic oscillations, the phonon frequencies of which determine the relative strength of the interaction with a particular oscillator. The oscillators treated are as follows: A hindered rotational oscillator of mass (M_r) 2.32 and frequency (Ω_r) corresponding to an energy ($\omega_r = \hbar\Omega_r$) of 0.06 eV, where \hbar is Planck's Constant divided by 2π ; a vibrational oscillator of mass (M_v) 5.84 and an energy (ω_1) of 0.205 eV; and a

^{53/} M. S. Nelkin, see Footnote 41.

^{54/} J. R. Beyster, et al., "Measurement of Neutron Spectra in Water, Polyethylene, and Zirconium Hydride," Nucl. Sci. Eng. 9, 168 (1961).

second vibrational oscillator of mass ($M_{V2} = M_V/2$) 2.92 and energy (ω_2) of 0.481 eV. Different mathematical approximations may be made to treat the translational, vibrational and rotational modes, dependent upon the incident neutron energy and the energy or momentum transfer. However, a single expression may be used to characterize the differential scattering kernel for scattering from an energy E' to an energy E ($E' \geq E$) through an angle with a cosine of μ . Parameters within the Nelkin water kernel then change dependent upon the specific approximation made,

$$\begin{aligned} \sigma(E' \rightarrow E, \mu) &= \frac{\sigma_b}{4} \sqrt{\frac{E}{E' \chi \xi \pi}} \quad e^{-\frac{X}{A}} \sum_{m=0}^{mm} \frac{1}{m!} \left(\frac{2X}{M_V \omega_2} \right)^m \\ &\sum_{l=0}^{ll} \frac{1}{l!} \left(\frac{X}{M_V \omega_1} \right)^l \sum_{n=-\infty}^{\infty} e^{\frac{n\omega}{2T}} I_n(z) \exp \left[-\frac{1}{4X\xi} (E-E' \right. \\ &\left. + \frac{X}{M} + m\omega_2 + l\omega_1 + n\omega)^2 \right] . \end{aligned} \quad (5.15)$$

55/ G. P. Calame, "Diffusion Parameters of Water for Various Scattering Kernels," Nucl. Sci. Eng. 19, 189 (1964).

56/ E. Starr and J. Koppel, "Determination of Diffusion Hardening in Water," Nucl. Sci. Eng. 14, 224 (1962).

Equation (5.15) gives the differential scattering kernel in barns/(eV-unit cosine) with σ_b as the bound atom cross section in barns. The $I_n(z)$ are the modified Bessel functions of the first kind and order n. As before, the quantity X is given by

$$X = E + E' - 2\mu \sqrt{EE'} . \quad (5.16)$$

One may allow for all of the transitions for the translational and rotational modes, while utilizing a phonon expansion for the first ($\omega_1 = .205$ eV) vibrational mode and the elastic (unexcited) limit for the second ($\omega_2 = .481$ eV) vibrational mode by inserting the following values into Eq. (5.15):

$$\frac{1}{A} = \frac{1}{\omega_r M_r \tanh(\omega_r/2T)} + \frac{1}{M_v \omega_1} + \frac{2}{M_v \omega_2} ,$$

$$\xi = T/M ,$$

$$z = \frac{X}{M \omega \sinh(\omega/2T)} , \quad (5.17)$$

$$\frac{1}{M} = \frac{1}{M} ,$$

$$mm = 0 ,$$

$$\ell\ell = 2 ,$$

$$\omega = \omega_r ,$$

and,

$$M = M_r ,$$

where T is the moderator temperature in eV. The phonon expansion for the second vibrational mode is included if m_m is set equal to 2 in the above set of parameters.

To allow for all transitions of the translational and first vibrational modes, while treating the rotational mode with the short collision time approximation and the second vibrational mode with a phonon expansion, the following parameters are inserted into Eq. (5.15):

$$\begin{aligned} \frac{1}{A} &= \frac{1}{M_V \omega_1} + \frac{2}{M_V \omega_2} , \\ \xi &= \frac{T}{M} + \frac{\omega_r}{M_r} \left(\frac{1}{e^{\omega_r/T} - 1} + \frac{1}{2} \right) , \\ z &= \frac{X}{M \omega \sinh(\omega/2T)} , \\ \frac{1}{\bar{M}} &= \frac{1}{M} + \frac{1}{M_r} , \end{aligned} \tag{5.18}$$

$$m_m = 2 ,$$

$$\ell \ell = 0 ,$$

$$\omega = \omega_1$$

and

$$M = M_V .$$

The oxygen present in the water is accounted for by adding the monatomic gas model with mass 16, Eq. (5.1), to the Nelkin water kernel, Eq. (5.15).

Angular integration of the differential scattering kernel, $\sigma(E' \rightarrow E, \mu)$, was performed numerically to obtain the scattering kernel in the form utilized in lattice calculations. For the non diagonal terms in the scattering matrix ($E' \neq E$), the Gauss quadrature formula was used for the angular integration:

$$\begin{aligned} \sigma(E' \rightarrow E) &= \int_{-1}^1 \sigma(E' \rightarrow E, \mu) d\mu \\ &\approx \sum_{k=1}^{kk} w_k \left[\sigma(E' \rightarrow E, \mu_k) + \sigma(E' \rightarrow E, -\mu_k) \right], \end{aligned} \quad (5.19)$$

where w_k is the weighting coefficient corresponding to μ_k , a zero of the Legendre polynomials.^{57/} For terms where the energy transfer is large ($E \ll E'$), an eight point ($kk = 4$) integration is used, while for small energy transfers where the fine structure of the differential kernel is a rapidly varying function of angle, a sixteen point ($kk = 8$) quadrature integration is performed.

Calculation of the scattering kernel diagonal terms ($E = E'$), where there is no energy transfer, requires some

^{57/} A. N. Lowan, N. Davis, and A. Levinson, "Tables of the Zeros of the Legendre Polynomials of Order 1-16 and the Weight Coefficients for Gauss's Mechanical Quadrature Formula," Bull. Am. Math. Soc. 48, 739 (1942).

modification of the above procedure. Inspection of Eq. (5.15) shows that for $E' = E$, $X = 2E(1-\mu)$, and there is a singularity in the differential scattering kernel at $\mu = 1$.

The use of the Gaussian quadrature angular integration scheme introduces numerical errors in this situation. Therefore the following calculational technique is utilized as suggested by Federighi and Goldman.^{58/} Equation (5.15) is considered in the limit as X goes to zero (μ goes to 1). The singularity is subtracted from the differential kernel and integrated analytically, the remainder being integrated with the sixteen point Gaussian quadrature rule. The analytically integrated singularity is then added to the result. This process is indicated below:

$$\sigma(E \rightarrow E) = \int_{-1}^1 f(\mu) d\mu + \frac{\sigma_b}{4\sqrt{\pi\xi}} \int_{-1}^1 \frac{d\mu}{\sqrt{2E(1-\mu)}} , \quad (5.20)$$

where,

$$f(\mu) = \sigma(E \rightarrow E, \mu) - \frac{\sigma_b}{4\sqrt{\pi\xi X}} , \quad (5.21)$$

and $X = 2E(1-\mu)$. The diagonal terms are then approximated by

^{58/} F. D. Federighi and D. T. Goldman, see Footnote 49.

$$\sigma(E \rightarrow E) = \sum_{k=1}^8 w_k [f(\mu_k) + f(-\mu_k)] + \frac{\sigma_b}{2\sqrt{\pi\xi E}} . \quad (5.22)$$

In the calculations of the Nelkin water kernel made for incorporation into the lattice studies Eqs. (5.17) were utilized for incident energies, E' , less than 0.33 eV, while Eqs. (5.18) were used for E' greater than 0.33 eV. This is essentially the same approximation made by Honeck for the water kernel calculations incorporated in THERMOS.^{59/} The phonon expansion for the second vibrational mode along with Eqs. (5.17) is not used because only a small increase in accuracy at higher incident energies is accomplished with a large (by a factor of 3) increase in computer time through its utilization.

Figure 5.1 shows the results of a calculation which utilized both Eqs. (5.17) and (5.18) in Eq. (5.15) for an incident energy of 0.366 eV. The results are expressed in barns/unit lethargy, $E\sigma(E' \rightarrow E)$, for down scattering, $E' \geq E$. However, the basic difference between the two approximations is plainly evident in Fig. 5.1. By considering all transitions for the hindered rotator, Eqs. (5.17), a scattering kernel is predicted with a complicated fine energy structure having oscillations at energy

^{59/} H. C. Honeck, "THERMOS - A Thermalization Transport Theory Code for Reactor Lattice Calculations," BNL 5826, Brookhaven National Laboratory (1961).

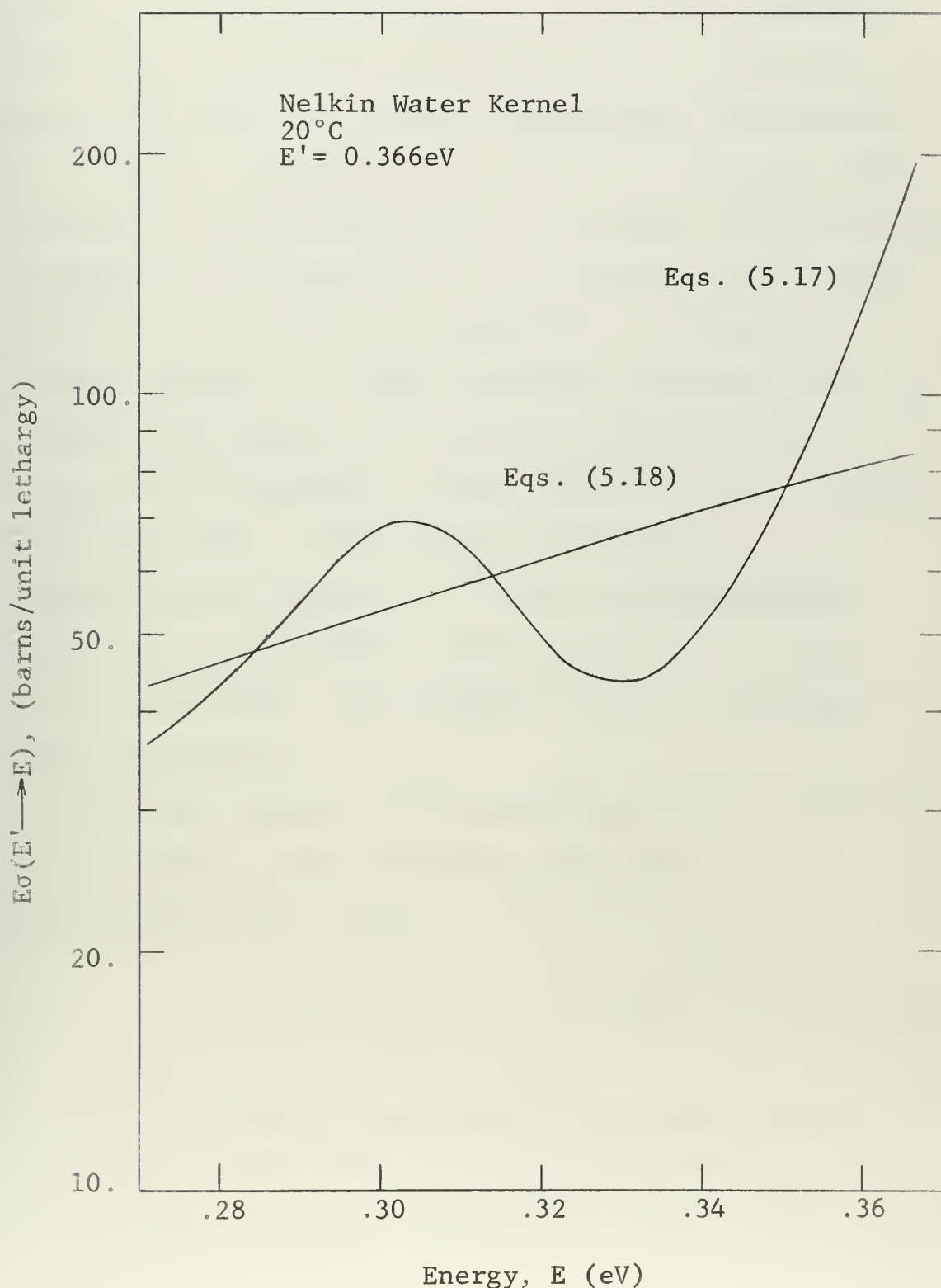


Figure 5.1 Approximations Used in the Calculation of the Nelkin Water Kernel

intervals ($E' - E$) equal to the frequency of the rotator, $\omega_r = 0.06$ eV. In going to the short collision time approximation for the hindered rotator, Eqs. (5.18), this fine structure is considerably smoothed, however the cross section derived by the energy integration of the kernel, Eq. (5.12), is essentially the same for both models. The choice of 0.33 eV as the energy above which Eqs. (5.18) will be used and below which Eqs. (5.17) will be used is made with this fact in mind, but primarily on the basis of computer economy. In order to predict accurate cross sections utilizing all transitions for the hindered rotator, it is necessary to use a fine energy mesh in the calculations ($\Delta E < .06$ eV), but if one is interested in energies in the range up to 1.0 eV this means that an excessively large number of energy points must be used in the calculation. This problem is further discussed below and in Chap. 7.

The first moment of the scattering kernel, $\sigma_1(E' \rightarrow E)$ is calculated for down scattering utilizing the same techniques as above, where,

$$\sigma_1(E' \rightarrow E) = \int_{-1}^1 \mu \sigma(E' \rightarrow E, \mu) d\mu . \quad (5.23)$$

As before, a sixteen point Gaussian quadrature angular integration is made for the off diagonal terms when the energy transfer is small, while eight points is considered

sufficient for large energy transfers. The diagonal terms, $E' = E$, for the first moment are calculated using the function defined in Eq. (5.21):

$$\begin{aligned} \sigma_1(E \rightarrow E) &= \int_{-1}^1 \mu f(\mu) d\mu + \frac{\sigma_b}{4\sqrt{\pi\xi}} \int_{-1}^1 \frac{\mu d\mu}{\sqrt{2E(1-\mu)}} , \\ &\approx \sum_{k=1}^8 w_k \left[\mu_k f(\mu_k) - \mu_k f(-\mu_k) \right] + \frac{\sigma_b}{6\sqrt{\pi\xi E}} . \end{aligned} \quad (5.23)$$

The upscattering terms for both the scattering kernel and its first moment are calculated using detailed balance, Eq. (2.5). It is to be noted that a slight, but acceptable inconsistency is introduced in this manner, since the use of detailed balance means that in the up-scattering portion of the scattering matrices, the approximation used, Eqs. (5.17) or Eqs. (5.18), actually depends on the neutron final energy rather than its initial energy.

Energy integration was performed on the scattering kernel and its first moment to determine the average cosine of the scattering angle, $\bar{\mu}(E)$:

$$\bar{\mu}(E) = \frac{\int_0^{E_c} \sigma_1(E \rightarrow E') dE'}{\int_0^{E_c} \sigma(E \rightarrow E') dE'} . \quad (5.24)$$

A trapezoidal rule numerical integration scheme, Appendix C, is used for this calculation and the results are shown in Fig. 5.2. Figure 5.2 also shows the transport cross section of water as calculated using the expression

$$\sigma_{tr}(E) = \sigma_a(E) + \sigma_s(E)[1 - \bar{\mu}(E)] . \quad (5.25)$$

In the energy integration of the scattering kernel, Eq. (5.12), to obtain the scattering cross section, $\sigma_s(E)$, certain numerical inaccuracies were encountered. Specifically, numerical integration of the Nelkin water utilizing the trapezoidal integration scheme discussed in Appendix C consistently yields scattering cross sections which were higher than those measured experimentally^{60/} for energies greater than 0.1 eV. Essentially the same percentage error is seen when the numerically integrated monatomic gas kernel is compared with the analytic expression for the cross section given by Eq. (5.13). These numerical errors are attributable to the fact that at higher incident energies, the diagonal terms of the scattering matrix are large compared with the first off diagonal terms for the energy mesh used in the calculation as discussed in Chap. 7. Use of the trapezoidal integration rule in this region therefore yields scattering cross sections for both kernels which are higher

^{60/} D. Hughes and B. Schwartz, "Neutron Cross Sections," BNL 325, 2nd ed., Brookhaven National Laboratory (1958).

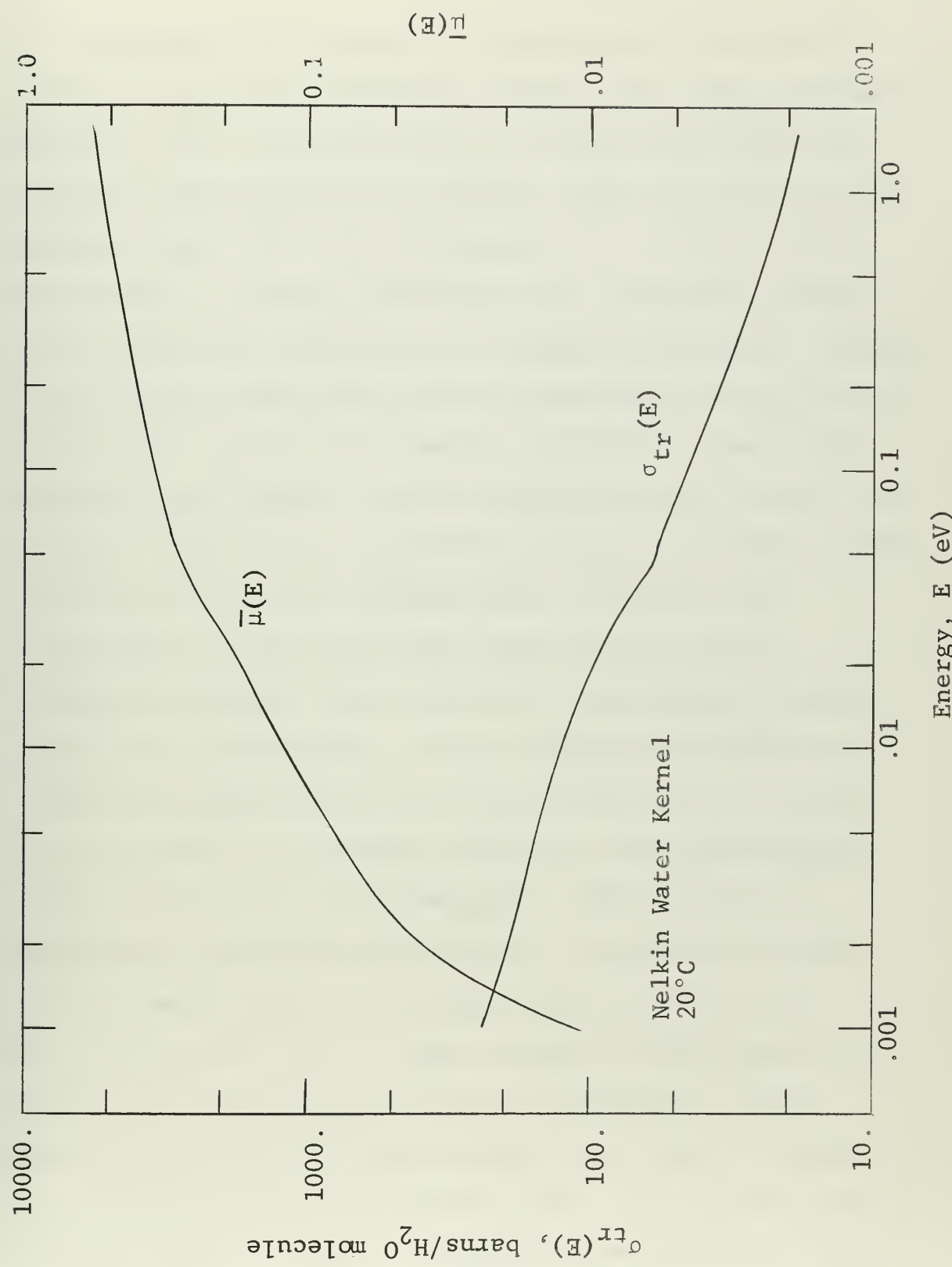


Figure 5.2 The Average Cosine of the Scattering Angle and the Transport Cross Section for Water

than experimentally measured or analytically calculated values. Auxiliary calculations showed that good agreement between $\sigma_s(E)$ calculated with the Nelkin water kernel and measured experimentally or between $\sigma_s(E)$ calculated by the monatomic gas model and $\sigma_s(E)$ given by Eq. (5.13) could be obtained by either utilizing a much finer energy mesh or by using more sophisticated integration schemes. However, both of these approaches create large increases in the computational time since the kernel calculation time is proportional to n^2 where n is the number of energy points considered, and the more complicated integration schemes which involve the fitting of exponentials or higher order polynomials to the calculated kernel points require additional computer time due to the uneven energy spacing used in the calculations. It is therefore desirable to retain the simplicity of the trapezoidal rule and correct for its inability to handle accurately the large diagonal terms encountered at high energies. This is done by recognizing that the actual value of the diagonal terms, $E' = E$, has no effect on the spectrum calculated with Eq. (2.1) or Eq. (2.9). This is seen by substituting the definition of the scattering cross section, Eq. (2.2) into Eq. (2.1) or (2.9) and letting E go to E' . Furthermore, integration of both sides of Eq. (2.1) or Eq. (2.9) over the energy variable E indicates the scattering cross section used in calculations must be the one derived from

the scattering kernel by the numerical integration scheme.

Since some of the integral properties that are to be calculated are strongly dependent upon the use of an accurate scattering cross section, we propose to modify the calculated diagonal terms in such a way that the scattering cross section calculated with the trapezoidal numerical integration scheme will equal the measured values for the Nelkin water kernel and Eq. (5.13) for the monatomic gas model. Thus, the diagonal terms, $\sigma^*(E \rightarrow E)$, utilized in the calculations will be given by:

$$\sigma^*(E \rightarrow E) = C(E)\sigma(E \rightarrow E), \quad (5.26)$$

where $\sigma(E \rightarrow E)$ is calculated using Eq. (5.22). The correction factors, $C(E)$, are easily found for the trapezoidal integration rule from the difference between the measured or analytic scattering cross section and the scattering cross section using the diagonals, $\sigma(E \rightarrow E)$. These correction factors are assumed to be temperature independent and those calculated for room temperature may therefore be applied to the diagonals, $\sigma(E \rightarrow E)$ calculated at any temperature. It is to be noted that this technique is not applied to the calculation of $\bar{\mu}(E)$, Eq. (5.24), since the most important effect is the relative magnitude of the correctly calculated values of $\sigma_1(E' \rightarrow E)$ and $\sigma(E' \rightarrow E)$.

Appendix B gives a listing of the scattering matrix as calculated using the Nelkin water model. The physical

temperatures of 20°C and 40°C are considered.

The source of thermal neutrons, $S(E)$, due to down scattering from energies above the thermal cutoff energy, E_c , can be calculated in accordance with Eq. (2.3) by taking the short collision time approximation on all of the modes of oscillation in the Nelkin model. Assuming a $1/E$ flux above E_c and neglecting upscattering, Eq. (2.3) yields an unnormalized source of:

$$S(E) = \text{ERF}\sqrt{E/T_e} , \quad (5.27)$$

where $\text{ERF}(z)$ is defined in Eq. (5.9).

The effective temperature, T_e , is given by:

$$T_e = \frac{T}{M} + \frac{\bar{E}_r}{M_r} + \frac{\bar{E}_1}{M_v} + \frac{2\bar{E}_2}{M_v} , \quad (5.28)$$

where the \bar{E} 's are given for each mode of oscillation as:

$$\bar{E} = \omega \left(\frac{1}{e^{\omega/T} - 1} + \frac{1}{2} \right) . \quad (5.29)$$

Because of the relative magnitudes of ω_1 and ω_2 , T_e may be approximated by:

$$T_e = \frac{T}{M} + \frac{\omega_1}{2M_v} + \frac{\omega_2}{M_v} + \frac{\omega_r}{M_r} \left(\frac{1}{e^{\omega_r/T} - 1} + \frac{1}{2} \right) . \quad (5.30)$$

At a physical temperature of 20°C the effective temperature has a value of 0.1169 eV.

CHAPTER 6

THERMAL LATTICE SPECTRA AND INTEGRAL PROPERTIES

Having selected appropriate mathematical models for the scattering kernel, Eq. (5.4) or Eqs. (5.15) and (5.19), and for the relative fuel absorption, $f(E)/[1-f(E)]$, Eqs. (3.8) and (4.21), one proceeds to look for solutions to Eq. (2.9), which is rearranged below.

$$\bar{\phi}^m(E) = \frac{\bar{S}(E) + \int_0^{E_c} \Sigma(E' \rightarrow E) \bar{\phi}^m(E') dE'}{\Sigma_s^m(E) + \Sigma_a^m(E) \left[1 + \frac{f(E)}{1 - f(E)} \right]}, \quad (6.1)$$

where $\bar{S}(E)$ is given in its unnormalized form by Eq. (5.27) and,

$$\Sigma(E' \rightarrow E) = N\sigma(E' \rightarrow E), \quad (6.2)$$

N being the number density of the moderator. Solution of Eq. (6.1) for the spatially averaged, energy dependent thermal flux in the moderator is accomplished with Program COUTH (Cornell University Thermalization), a Fortran 63 code written for use with the Control Data Corporation 1604 digital computer. A Fortran statement of COUTH appears in Appendix E, while the numerical methods employed are discussed in Appendix C. This chapter describes the lattice variables and integral parameters calculated in COUTH. The results of a set of actual lattice calculations are described in Chap. 7.

Determination of the spatially averaged flux in the moderator through the solution of Eq. (6.1) leads to the calculation of several other useful quantities. The spatially averaged thermal flux in the fuel, $\bar{\phi}^f(E)$, and in the cladding, $\bar{\phi}^c(E)$, may be determined from the moderator spectrum by equating absorption rates in the various regions. Utilizing the relationships in Eqs. (4.53) and (4.54),

$$\bar{\phi}^f(E) = \frac{V^m}{V^f} \frac{\Sigma_a^m(E)}{\Sigma_a^f(E)} \left[\frac{f(E)}{1-f(E)} \right] \cdot \left[\frac{J_o(E)(1-P_{rv}(E))}{P_{rv}(E)(1-P_e(E))} \right] \bar{\phi}^m(E) , \quad (6.3)$$

where V^m and V^f are the volumes of the moderator and fuel respectively, $\Sigma_a^f(E)$ is the fuel absorption cross section, $\Sigma_a^m f \bar{\phi}^m / (1-f)$ is the absorption rate in the fuel element, and $J_o(1-P_{rv})/(1-P_e)P_{rv}$ is the ratio of absorptions in the fuel meat to absorptions in the fuel element. Similarly for the cladding:

$$\bar{\phi}^c(E) = \frac{V^m}{V^c} \frac{\Sigma_a^m(E)}{\Sigma_a^c(E)} \left[\frac{f(E)}{1-f(E)} \right] \cdot \left[1 - \frac{J_o(E)(1-P_{rv}(E))}{P_{rv}(E)(1-P_e(E))} \right] \bar{\phi}^m(E) , \quad (6.4)$$

where V^c is the cladding volume and $\Sigma_a^c(E)$ is the cladding absorption cross section.

Average neutron velocities in each region of the cell may now be defined utilizing the relationship between

neutron density and flux,

$$\bar{N}(E) = \bar{\phi}(E)/v(E) , \quad (6.5)$$

where $v(E)$ is the neutron velocity. The average velocity in the moderator, \bar{v}_m , is then expressed as

$$\bar{v}_m = \frac{\int_0^{E_c} v(E) \bar{N}^m(E) dE}{\int_0^{E_c} \bar{N}^m(E) dE} = \frac{\int_0^{E_c} \bar{\phi}^m(E) dE}{\int_0^{E_c} \bar{\phi}^m(E)/v(E) dE} . \quad (6.6)$$

Similar expressions define the average velocities in the fuel, \bar{v}_f , and in the cladding, \bar{v}_c .

Definitions of disadvantage factors follow directly by expressing the total spatially averaged neutron density, \bar{N} , as shown below for the moderator:

$$\bar{N}^m = \int_0^{E_c} \bar{N}^m(E) dE = \int_0^{E_c} \bar{\phi}^m(E)/v(E) dE . \quad (6.7)$$

Using analogous expressions for the total densities in the fuel, \bar{N}^f , and the cladding, \bar{N}^c , one can calculate neutron density disadvantage factors for the moderator, δ_n^m ;

$$\delta_n^m = \bar{N}^m/\bar{N}^f , \quad (6.8)$$

and for the cladding δ_n^c ;

$$\delta_n^c = \bar{N}^c/\bar{N}^f . \quad (6.9)$$

The disadvantage factors are related to the familiar flux disadvantage factors through the relationships:

$$\delta_{\phi}^m = \bar{\phi}^m / \bar{\phi}^f = \bar{v}_m \delta_n^m / \bar{v}_f , \quad (6.10)$$

and

$$\delta_{\phi}^c = \bar{\phi}^c / \bar{\phi}^f = \bar{v}_c \delta_n^c / \bar{v}_f , \quad (6.11)$$

where m, c, and f again refer to moderator, cladding, and fuel, and

$$\bar{\phi}^m = \int_0^{E_c} \bar{\phi}^m(E) dE . \quad (6.12)$$

In terms of quantities already defined the thermal utilization, f, and the more basic quantity, η_f , may be determined, where

$$f = \frac{\text{thermal absorption rate in the fuel rod}}{\text{thermal absorption rate in the cell}} , \quad (6.13)$$

and,

$$\eta_f = \frac{\text{thermal fission neutron production rate in the cell}}{\text{thermal absorption rate in the cell}} . \quad (6.14)$$

These definitions lead to the following expressions:

$$f = \frac{V^f \int_0^{E_c} \Sigma_a^f(E) \bar{\phi}^f(E) dE}{V^m \int_0^{E_c} \Sigma_a^m(E) \left[1 + \frac{f(E)}{1-f(E)} \right] \bar{\phi}^m(E) dE}, \quad (6.15)$$

and,

$$\eta f = \frac{\nu V^f \int_0^{E_c} \Sigma_a^f(E) \bar{\phi}^f(E) / [1+\alpha(E)] dE}{V^m \int_0^{E_c} \Sigma_a^m(E) \left[1 + \frac{f(E)}{1-f(E)} \right] \bar{\phi}^m(E) dE}, \quad (6.16)$$

where ν is the number of fission neutrons produced per thermal fission, and $\alpha(E)$ is the energy dependent capture to fission ratio for the fuel.

A thermal neutron lifetime, τ_t , may be defined as the ratio of the total number of thermal neutrons in the cell to the thermal absorption rate in the cell,

$$\tau_t = \frac{\bar{N}^m V^m + \bar{N}^c V^c + \bar{N}^f V^f}{V^m \int_0^{E_c} \Sigma_a^m(E) \left[1 + \frac{f(E)}{1-f(E)} \right] \bar{\phi}^m(E) dE}, \quad (6.17)$$

where \bar{N} is defined by Eq. (6.7) for each region.

Since one of the prime concerns in reactor calculations is the accurate determination of various reaction rates, it is desirable to define average thermal cross sections which are suitable for use in calculations utilizing the thermal flux or the 2200 meter/second flux. In terms of the spatially averaged flux or neutron density in a given region, a reaction rate, RR, per unit volume of the region is expressed by:

$$RR = \int_0^{E_c} \Sigma(E) \bar{\phi}(E) dE = \int_0^{E_c} \Sigma(E) \bar{N}(E) v(E) dE . \quad (6.18)$$

As before, superscripts on the variables will denote the region considered (m = moderator, c = cladding, f = fuel), while subscripts will denote the interaction considered (a = absorption, s = scattering, t = total, tr = transport, f = fission). Thus, the thermal absorption rate in the moderator will be given by

$$RR_a^m = \int_0^{E_c} \Sigma_a^m(E) \bar{\phi}^m(E) dE = \int_0^{E_c} \Sigma_a^m(E) \bar{N}^m(E) v(E) dE . \quad (6.19)$$

In the notation of Wescott,^{61/} reaction rates may now be formulated in terms of an effective cross section, $\hat{\Sigma}$, and

^{61/} C. H. Wescott, "The Specification of Neutron Flux and Effective Cross Sections," AECL 352 (1956).

a mean cross section, $\bar{\Sigma}$, for use in a calculation with the spatially averaged 2200 meter per second flux, $\bar{\phi}_o$, and the spatially averaged thermal flux, $\bar{\phi}_T$, respectively. A given reaction rate is now defined by

$$RR = \widehat{\Sigma} \bar{\phi}_o = \bar{\Sigma} \bar{\phi}_T , \quad (6.20)$$

where,

$$\bar{\phi}_o = \bar{N}v_o = v_o \int_0^{E_c} \bar{N}(E)dE = v_o \int_0^{E_c} \bar{\phi}(E)/v(E)dE , \quad (6.21)$$

and,

$$\bar{\phi}_T = \bar{N}\bar{v} = \int_0^{E_c} \bar{N}(E)v(E)dE = \int_0^{E_c} \bar{\phi}(E)dE . \quad (6.22)$$

The velocity v_o denotes 2200 m/sec, while \bar{v} is the mean velocity defined by Eq. (6.6). This leads to the definition of the effective cross section as:

$$\widehat{\Sigma} = \frac{\int_0^{E_c} \Sigma(E)\bar{\phi}(E)dE}{v_o \int_0^{E_c} \bar{N}(E)dE} , \quad (6.23)$$

while the mean cross section is defined as

$$\bar{\Sigma} = \frac{\int_0^{E_c} \Sigma(E) \bar{\varphi}(E) dE}{\int_0^{E_c} \bar{\varphi}(E) dE} . \quad (6.24)$$

Consideration of Eqs. (6.23) and (6.24) shows that $\hat{\Sigma}v_o = \bar{\Sigma}v$. Applying this nomenclature to absorption rate per unit volume of the moderator as an example yields:

$$RR_a^m = \hat{\Sigma}_a^m \bar{\varphi}_o^m = \bar{\Sigma}_a^m \bar{\varphi}_T^m , \quad (6.25)$$

where

$$\hat{\Sigma}_a^m = \frac{\int_0^{E_c} \Sigma_a^m(E) \bar{\varphi}^m(E) dE}{v_o \int_0^{E_c} \bar{\varphi}^m(E) / v(E) dE} , \quad (6.26)$$

$$\bar{\Sigma}_a^m = \frac{\int_0^{E_c} \Sigma_a^m(E) \bar{\varphi}^m(E) dE}{\int_0^{E_c} \bar{\varphi}^m(E) dE} , \quad (6.27)$$

$$\bar{\varphi}_o^m = v_o \int_0^{E_c} \bar{\varphi}^m(E) / v(E) dE , \quad (6.28)$$

$$\bar{\varphi}_T^m = \int_0^{E_c} \bar{\varphi}^m(E) dE , \quad (6.29)$$

and,

$$\hat{\Sigma}_a^m v_o = \bar{\Sigma}_a^m \bar{v}_m . \quad (6.30)$$

This approach is extended to define effective and mean cross sections for the homogenized cell, $\hat{\Sigma}^h$ and $\bar{\Sigma}^h$, subscripts denoting the interaction considered. In this manner

$$\begin{aligned} \hat{\Sigma}^h &= \frac{\int_0^{E_c} dE \left[V^m \Sigma^m(E) \bar{\varphi}^m(E) + V^c \Sigma^c(E) \bar{\varphi}^c(E) + V^f \Sigma^f(E) \bar{\varphi}^f(E) \right]}{v_o \int_0^{E_c} \frac{dE}{v(E)} \left[V^m \bar{\varphi}^m(E) + V^c \bar{\varphi}^c(E) + V^f \bar{\varphi}^f(E) \right]} , \\ &\quad (6.31) \end{aligned}$$

and,

$$\begin{aligned} \bar{\Sigma}^h &= \frac{\int_0^{E_c} dE \left[V^m \Sigma^m(E) \bar{\varphi}^m(E) + V^c \Sigma^c(E) \bar{\varphi}^c(E) + V^f \Sigma^f(E) \bar{\varphi}^f(E) \right]}{\int_0^{E_c} dE \left[V^m \bar{\varphi}^m(E) + V^c \bar{\varphi}^c(E) + V^f \bar{\varphi}^f(E) \right]} . \\ &\quad (6.32) \end{aligned}$$

The mean velocity of neutrons in the homogenized cell is defined as

$$\bar{v}_h = \frac{\int_0^{E_c} dE \left[v_{\phi}^{m-m}(E) + v_{\phi}^{c-c}(E) + v_{\phi}^{f-f}(E) \right]}{v_o \int_0^{E_c} \frac{dE}{v(E)} \left[v_{\phi}^{m-m}(E) + v_{\phi}^{c-c}(E) + v_{\phi}^{f-f}(E) \right]}, \quad (6.33)$$

so that,

$$\hat{\Sigma}^h v_o = \bar{\Sigma}^h \bar{v}_h. \quad (6.34)$$

To complete the calculation of the thermal parameters, one would like to define a thermal diffusion area, L^2 , for the homogenized cell in a meaningful way. In the one velocity, one region problem, L^2 may be defined unambiguously as

$$L^2 = D/\Sigma_a, \quad (6.35)$$

where $D = 1/3\Sigma_{tr}$. However, in the polyenergetic, homogenized cell problem, one must decide whether L^2 in Eq. (6.35) should be calculated utilizing mean or effective cross sections, and whether D should be calculated by averaging the transport cross section or the transport mean free path.

Larrimore^{62/} has indicated the desirability of utilizing the mean homogenized cross section, $\bar{\Sigma}_a^h$, in the calculation of L^2 . He also notes that several authors^{63, 64, 65/} argue in favor of averaging the transport mean free path, while Sjøstrand^{66/} has shown a physical basis for averaging the transport cross section in the determination of D. The paradox between these two approaches has recently been clarified by Pomraning^{67/} and on the basis of that discussion this work averages the reciprocal of a homogenized transport cross section, $\Sigma_{tr}^h(E)$, over a homogenized spectrum in the determination of the diffusion coefficient, D. The homogenized transport cross section is defined as

$$\Sigma_{tr}^h(E) = \frac{\Sigma_{tr}^m(E)\bar{\phi}^m(E)V^m + \Sigma_{tr}^c(E)\bar{\phi}^c(E)V^c + \Sigma_{tr}^f(E)\bar{\phi}^f(E)V^f}{\bar{\phi}^m(E)V^m + \bar{\phi}^c(E)V^c + \bar{\phi}^f(E)V^f}, \quad (6.36)$$

while the homogenized flux, $\bar{\phi}^h(E)$, is defined by

$$\bar{\phi}^h(E) = \frac{\bar{\phi}^m(E)V^m + \bar{\phi}^c(E)V^c + \bar{\phi}^f(E)V^f}{V^m + V^c + V^f}. \quad (6.37)$$

^{62/} J. A. Larrimore, "Temperature Coefficients of Reactivity in Homogenized Thermal Nuclear Reactors," Massachusetts Institute of Technology Thesis (1962).

^{63/} A. M. Weinberg and E. P. Wigner, The Physical Theory of Neutron Chain Reactors, p. 514, The University of Chicago Press, Chicago, 1958.

^{64/} C. D. Petrie, M. L. Storm, and P. F. Zweifel, "Calculation of Thermal Group Constants for Mixtures Containing Hydrogen," Nucl. Sci. Eng. 2, 728-744 (1957).

The diffusion coefficient is then expressed as

$$D = \frac{\frac{1}{3} \int_0^{E_c} \bar{\phi}^h(E) / \Sigma_{tr}^h(E) dE}{\int_0^{E_c} \bar{\phi}^h(E) dE} . \quad (6.38)$$

The thermal diffusion area is calculated from

$$L^2 = D / \bar{\Sigma}_a^h , \quad (6.39)$$

where $\bar{\Sigma}_a^h$ is defined by Eq. (6.32).

The calculation of all of the parameters and variables discussed in this chapter is carried out by program COUTH. The results derived from these calculations for an actual lattice system are discussed in Chap. 7.

65/ K. S. Singwi and L. S. Kothari, "Transport Cross Section of Thermal Neutrons in Solid Moderators," Second Geneva Conference Proceedings, 16, 325 (1958).

66/ N. G. Sjøstrand, "Definition of the Diffusion Constant in One-Group Theory," J. Nucl. Energy, Part A, Reactor Science, 151 (1960).

67/ G. C. Pomraning, "On the Energy Averaging of the Diffusion Coefficient," Nucl. Sci. Eng. 19, 250 (1964).

CHAPTER 7

APPLICATION OF THE METHOD TO ACTUAL LATTICES

7.1 Room Temperature Calculations

In this chapter we discuss the numerical results obtained with program COUTH when the cell theory formulated in Secs. 2.1 and 2.3 is applied to an actual lattice system. The aim of this work is to calculate at various temperatures, the spatially averaged thermal spectra, and the integral parameters defined in Chap. 6 for all of the cores incorporated in the Cornell University Zero Power Reactor facility.^{68,69/} The Cornell ZPR cores are light water moderated and utilize high density, low enrichment uranium dioxide fuel, clad in aluminum. Several water to uranium oxide volume ratios (nominally 1:1, 1.5:1, 2:1, 3:1 and 4:1) are provided with sets of grid plates which vary the spacing (lattice pitch) between the fuel elements arranged in a hexagonal array. More specifically, the fuel rods consist of 0.60 inch diameter uranium dioxide fuel of density 10.38 gm/cc, enriched to 2.096 atom per cent of U²³⁵. The fuel rods, formed by 48 one inch long fuel pellets, are clad in 0.028 inch thick aluminum to form a fuel element with an outside diameter of 0.666 inches. A list of the parameters of the various lattices is given in Appendix A.

^{68/} D. D. Clark, "The Cornell University Nuclear Reactor Laboratory," CURL-1, Cornell University (1961).

Initial calculations have been carried out utilizing as a scattering kernel both the Nelkin water kernel, Eq. (5.15), and the monatomic gas model, Eq. (5.11), for a gas of mass one. The two physical temperatures of 20°C and 40°C have been considered. The results of an elementary study utilizing the monatomic gas model have previously been reported.^{70/}

In the solution of the neutron balance equation, Eq. (6.1), to determine the spatially averaged moderator flux, $\bar{\phi}^m(E)$, the heterogeneous effects of the lattice are accounted for by the relative fuel absorption, $f(E)/[1-f(E)]$, as given in terms of escape probabilities by Eq. (2.29). The moderator escape probabilities, $P_s(E)$ and $P_m(E)$, are given by Eqs. (3.4) and (3.6), respectively. This yields Eq. (3.8) for the relative fuel absorption. The fuel element escape probability to be used in Eq. (3.8) is calculated by means of Eq. (4.21), which in turn requires the calculations indicated by Eqs. (4.22), (4.19), and (4.8). Equation (4.8) calculates the fuel rod escape probability utilizing the parabolic flux approximation.

^{69/} S. S. Berg, "Initial Experiments on the Cornell University Zero Power Reactor Cores," Cornell University Thesis (1964).

^{70/} K. B. Cady and C. R. Mac Vean, "A Simplified Formulation of Space-Energy Cell Theory," Trans. Am. Nucl. Soc. 6, 234-235 (1963).

The source of neutrons due to down scattering from energies above E_c is that given by Eq. (5.27), normalized to one neutron per second per unit volume of the moderator. That is,

$$\bar{S}(E) = \frac{\text{ERF}\sqrt{E/T_e}}{\int_0^{E_c} \text{ERF}\sqrt{E/T_e}} . \quad (7.1)$$

The calculations were performed utilizing an energy mesh containing forty-five energy points ranging from 0.001 eV to a thermal cutoff energy, E_c , of 1.609 eV. In the stipulation of a useful energy mesh a compromise must be reached between several conflicting requirements. In the first place, a reasonable range of energies must be covered. Secondly, the total number of energy mesh points, n , may not be too large, since the computer time necessary for the calculation of the scattering kernel increases as n squared. Furthermore, it is desirable to have a finely spaced energy mesh in the region above the thermal energy, $E_0 = kT$, where the $1/E$ tail joins that part of the spectrum resembling a Maxwellian. Finally, the use of the Nelkin water kernel places certain restrictions on the size of the energy spacing, ΔE , between the energy points in the mesh. With the use of the approximation allowing for all transitions of the hindered rotator, Eqs. (5.17) (utilized for incident neutron energies less than 0.33 eV) it is

necessary to use a ΔE which is less than the frequency ($\omega_r = 0.06$ eV) of the hindered rotator. This requirement insures that the fine structure of the water kernel is preserved in the calculations and that energy integration of the scattering kernel will yield a fairly accurate scattering cross section. In order to satisfy this requirement, the energy spacings utilized in the calculations are less than one quarter of ω_r or .015 eV for all energies below 0.33 eV. In light of these restrictions, the energy mesh used in the calculations consists of 35 energy points below $E = .33$ eV with 34 energy intervals corresponding to equal intervals in velocity. Each of these low energy velocity intervals corresponds to $0.1 v_o$ or 220 m/sec. For energies above $E = 0.33$ eV the ten energy intervals correspond to velocity intervals which exponentially increase from 220 m/sec to 2200 m/sec as energy increases. A complete listing of the energy mesh utilized is given in Appendix B.

The U^{235} absorption and fission cross sections used are those compiled by Suich.^{71/} The absorption cross sections for U^{238} , the moderator and the cladding are all assumed to be $1/v$ and the 2200 m/s values of these cross sections are given in Appendix A. The scattering cross

^{71/} J. Suich, "Temperature Coefficients in Heterogeneous Reactor Lattices," Massachusetts Institute of Technology Thesis (1963).

sections for all of the materials other than the moderator are calculated utilizing the analytic expression, Eq. (5.13), derived from the monatomic gas model. Scattering cross sections for the moderator are computed by integration of the scattering kernel in accordance with Eq. (5.12). The use of the monatomic gas model yields a water scattering cross section given by Eq. (5.13), while the use of the Nelkin water kernel results in the scattering cross section given by BNL 325.^{72/} The free atom scattering cross sections used are given in Appendix A.

The transport cross sections are calculated using

$$\Sigma_{tr}(E) = \Sigma_a(E) + \Sigma_s(E) [1 - \bar{\mu}(E)] . \quad (7.2)$$

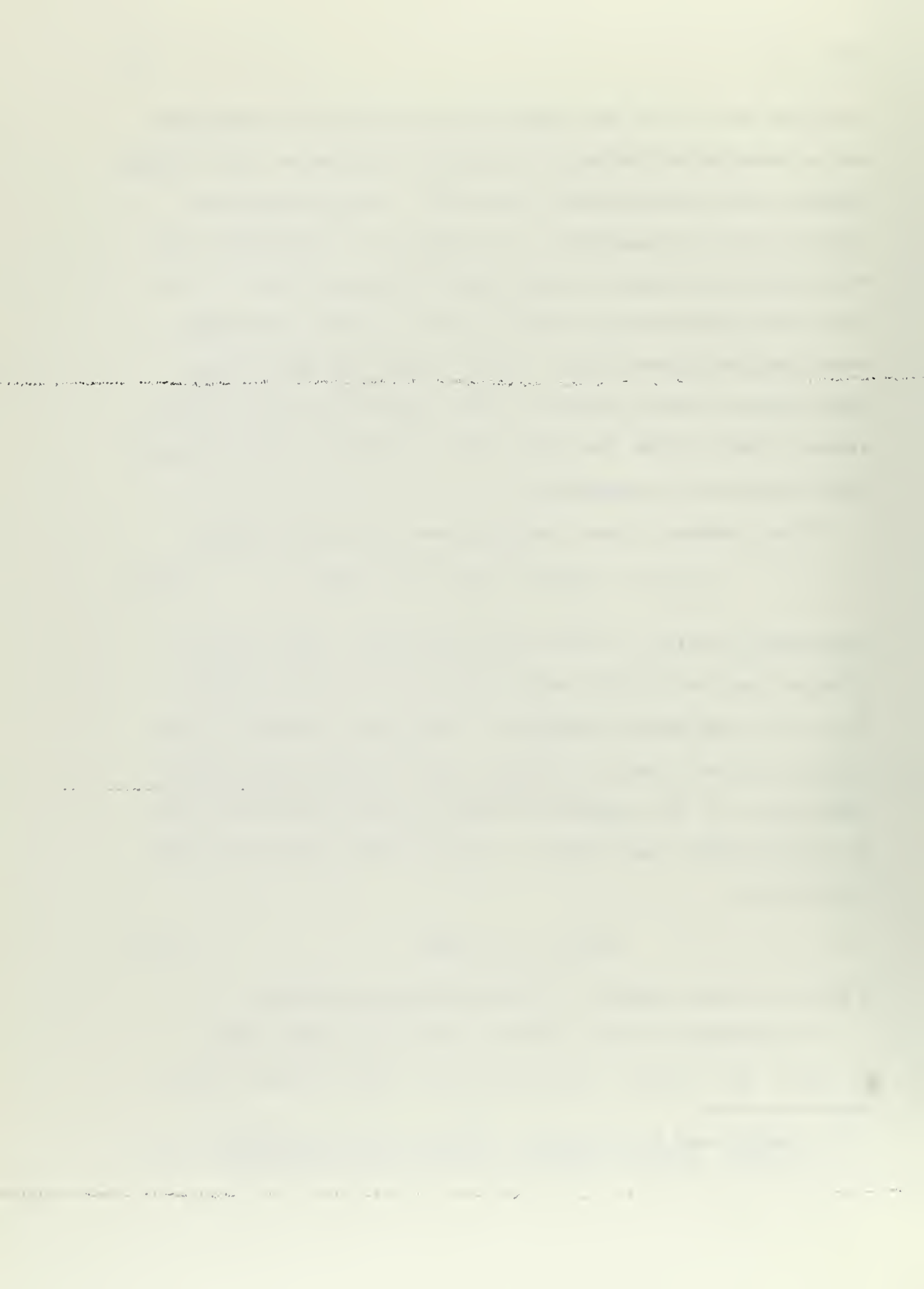
The average cosine of the scattering angle, $\bar{\mu}(E)$, is calculated from the Nelkin water kernel, Eq. (5.24) and Fig. (5.2), for the water moderator. The water transport cross section derived from the Nelkin model is also used in the calculation of the moderator escape probabilities with use of the monatomic gas kernel. For all other materials $\bar{\mu}(E)$ is given by

$$\bar{\mu}(E) = \bar{\mu} = 2/3A , \quad (7.3)$$

A being the mass number of the scattering material.

Calculation of the relative fuel absorption $f(E)/[1-f(E)]$, Eq. (2.29), using the $P_s(E)$ shown in Fig. (3.1),

^{72/}D. Hughes and B. Schwartz, "Neutron Cross Sections," BNL 325, 2nd Ed., Brookhaven National Laboratory (1958).



the $P_m(E)$ shown in Fig. (3.2), and the $P_e(E)$ shown in Fig. (4.2), yields the apparent lattice absorption cross section, $\Sigma_a^m(E) \left[1 + f(E)/[1-f(E)] \right]$. This quantity is shown in Fig. 7.1 for the five Cornell ZPR cores. Comparison with the absorption cross section of pure water, $\Sigma_a^m(E)$, shows the non $1/v$ behavior of this apparent cross section as well as the effect of the 0.273 eV resonances in U^{235} . It is this non $1/v$ behavior which yields a temperature coefficient of the thermal utilization, f .

The apparent lattice absorption cross section shown in Fig. (7.1) is substituted into the neutron balance equation, Eq. (6.1), along with either the monatomic gas or Nelkin water scattering cross section. The computer solution of Eq. (6.1) is discussed in Appendix C, the result of the solution being the spatially averaged moderator spectrum, $\bar{\phi}^m(E)$, evaluated at the discrete energy points in the energy mesh used. Figure 7.2 shows the results of this calculation utilizing the Nelkin water kernel for the five water to uranium oxide volume ratios of the Cornell ZPR. Since all of the results are normalized to one neutron per second slowing down per unit volume of the moderator, Fig. 7.2 shows the flux suppression as well as the spectral hardening experienced in the tighter (lower water to oxide volume ratios) cores. The difference between moderator spectra predicted with the monatomic gas model and the Nelkin water kernel is shown in Fig. 7.3 where the $\bar{\phi}^m(E)$

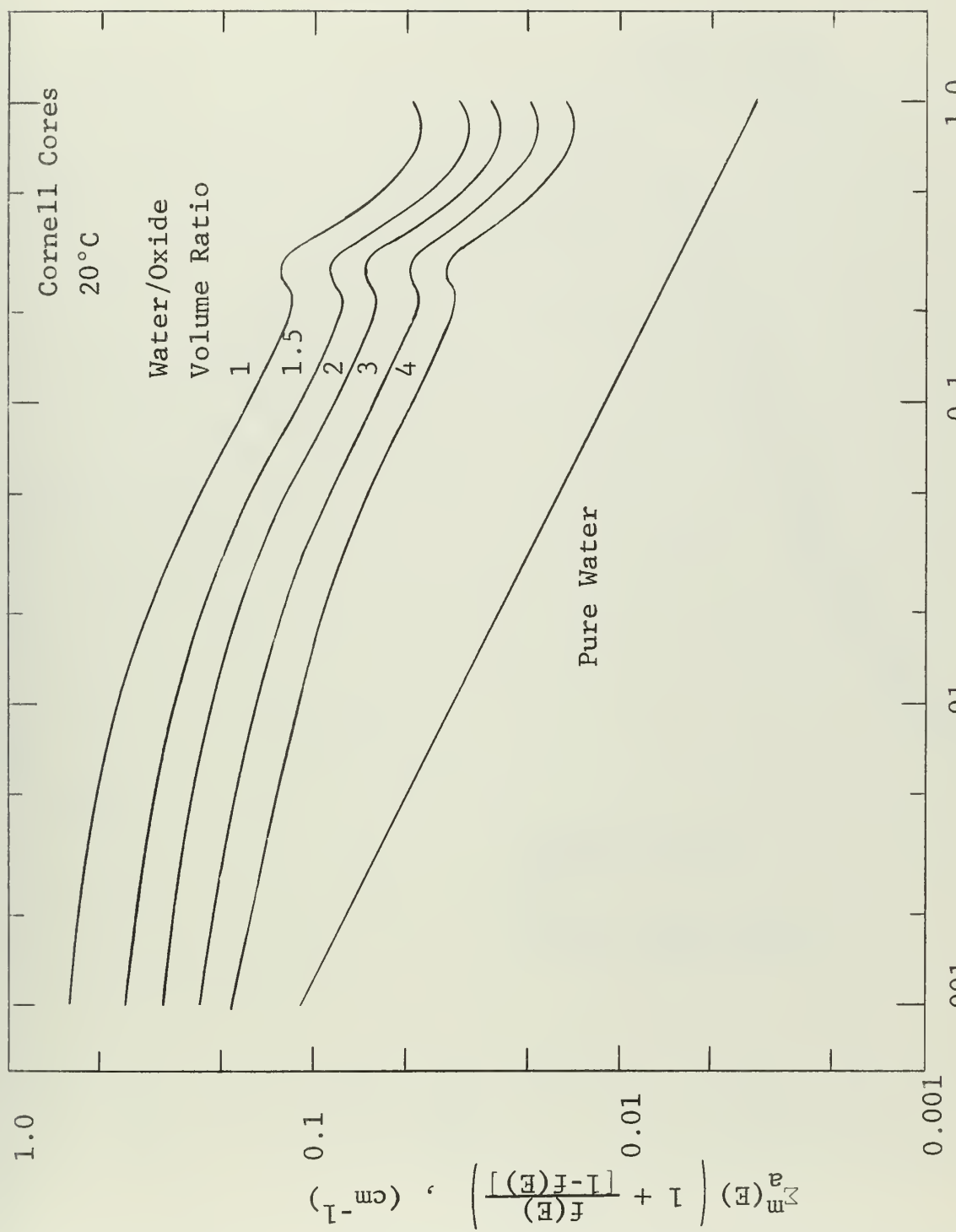


Figure 7.1 Apparent Lattice Absorption Cross Section

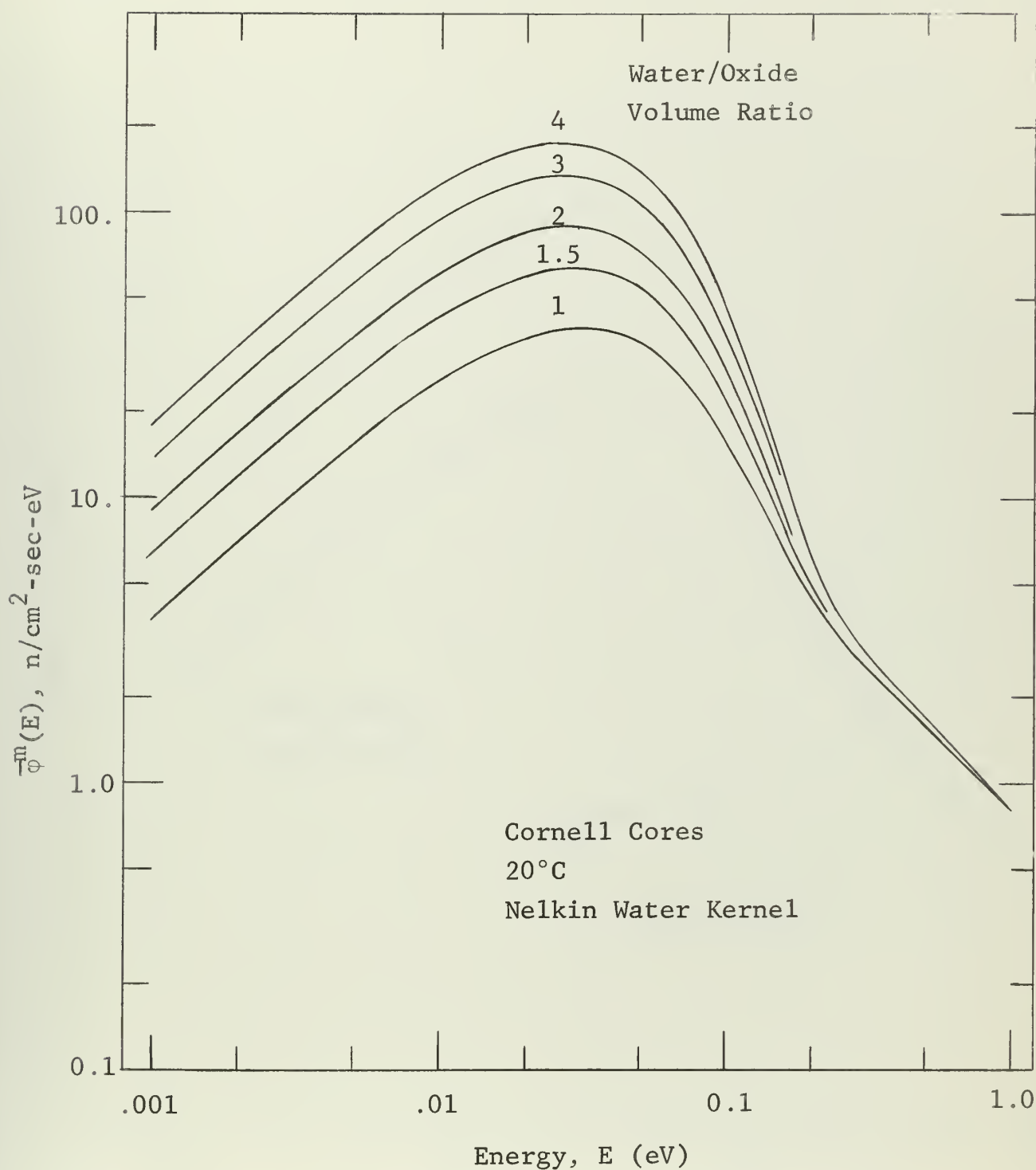


Figure 7.2 Spatially Averaged Moderator Thermal Spectra

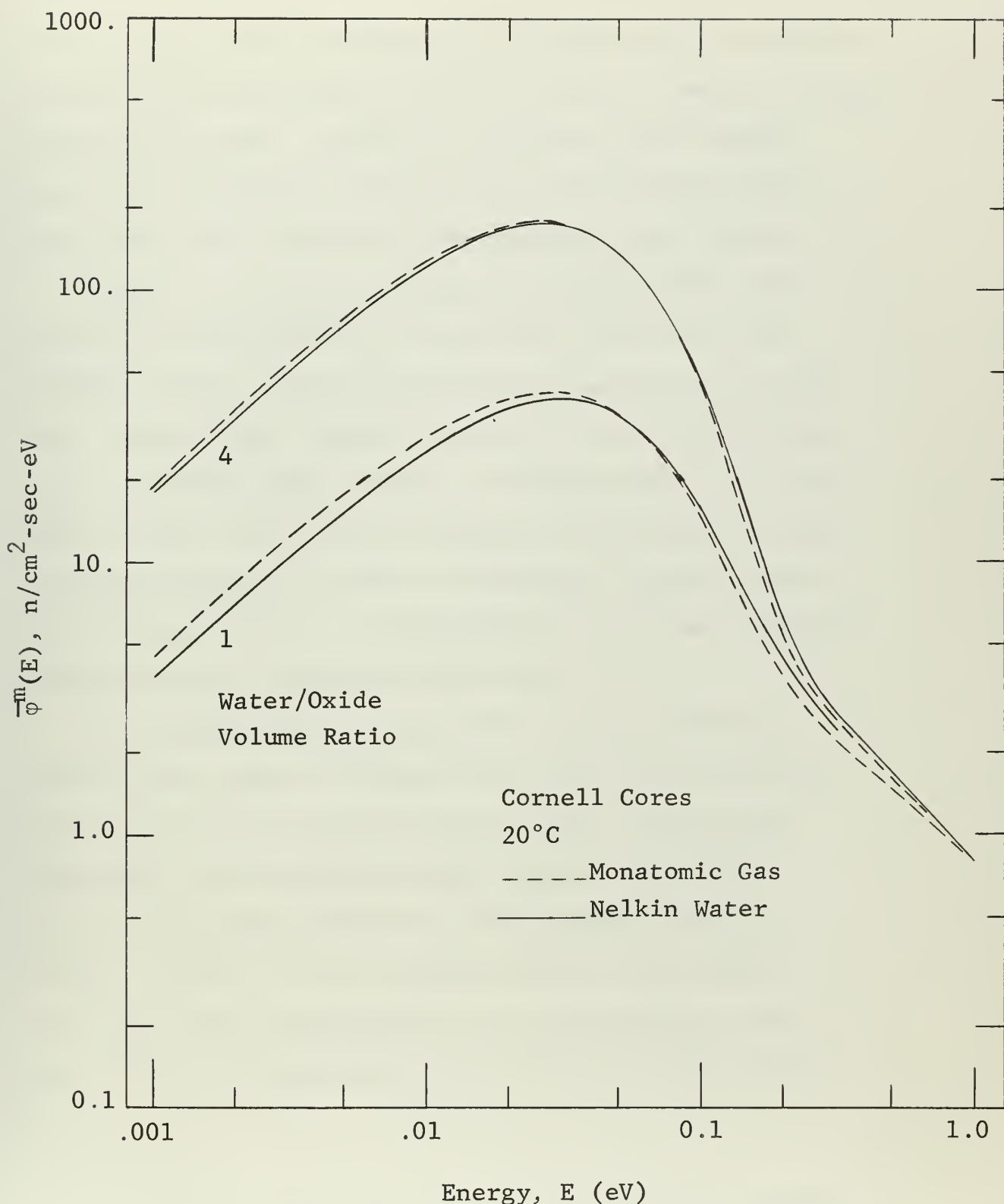


Figure 7.3 Comparison of the Moderator Spectra Predicted with the Nelkin Water and Monatomic Gas Models

predicted by these two models are plotted for the extreme lattices of the ZPR; that is the 1:1 and 4:1 water to oxide volume ratio cores. Figure 7.3 indicates that harder spectra are predicted with the use of the Nelkin water kernel than with the use of the monatomic gas kernel.

Using the spatially averaged moderator flux, the spatially averaged fluxes in the fuel, $\bar{\phi}^f(E)$, and the cladding, $\bar{\phi}^c(E)$, may be calculated using Eqs. (6.3) and (6.4) respectively. Results typical of this calculation using the Nelkin water kernel are shown in Fig. 7.4 where $\bar{\phi}^m(E)$, $\bar{\phi}^c(E)$, and $\bar{\phi}^f(E)$ are plotted for the ZPR 3:1 core. Spectrum hardening as well as depression, giving rise to disadvantage factors, is experienced as one goes from the moderator to the cladding to the fuel.

The average neutron velocities in the moderator, cladding, and fuel as defined in Eq. (6.6) are shown in Fig. 7.5 for all of the ZPR cores, these calculations being made with the Nelkin water kernel. Again the spectral hardening produced in the tighter cores is evident. Figure 7.5 also shows that for the tighter cores \bar{v}_c is well represented by the relationship which Honeck^{73/} has verified for the Brookhaven uranium metal cores,

^{73/}H. C. Honeck, "The Calculation of the Thermal Utilization and Disadvantage Factor in Uranium/Water Lattices," Nucl. Sci. Eng. 18, 49-68 (1964).

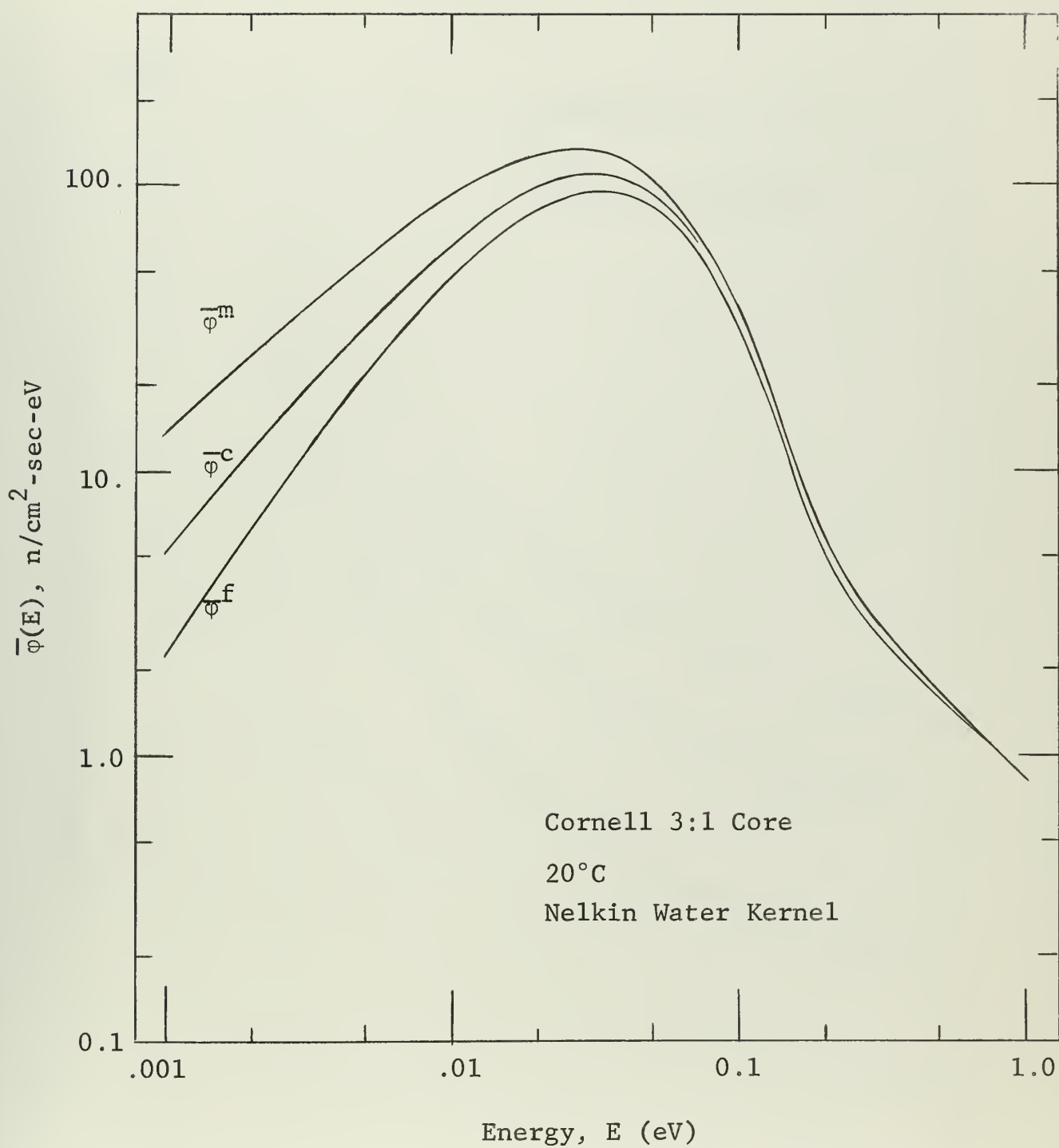


Figure 7.4 Spatially Averaged Cell Spectra

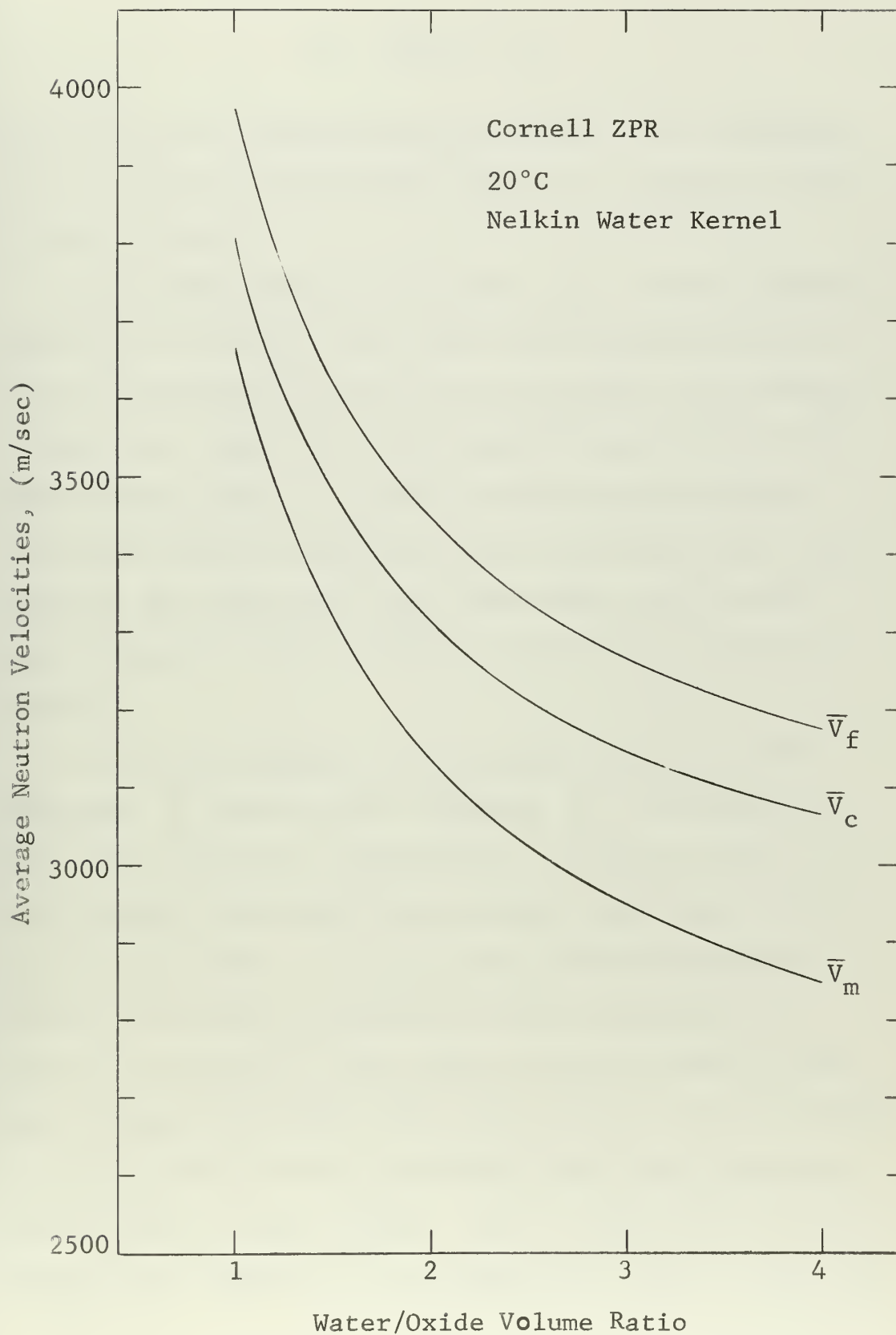


Figure 7.5 Average Neutron Velocities

$$\bar{v}_c = \frac{1}{2}(\bar{v}_f + \bar{v}_m) . \quad (7.4)$$

The error in the result predicted by Eq. (7.4) increases with the water to oxide volume ratio to a maximum of 1.8% for the 4:1 core.

The average neutron velocities, \bar{v}_h , for the homogenized cell, Eq. (6.33), are shown for calculations with both the monatomic gas model and the Nelkin water kernel in Fig. 7.6. Again the harger spectra predicted by the Nelkin water kernel is evident as the average neutron velocities for the homogenized cell calculated with the monatomic gas model are lower than those given by the Nelkin model by 5.4% for the 1:1 core and 2.4% for the 4:1 core.

The neutron density disadvantage factors for the moderator, δ_n^m , and for the cladding, δ_n^c , as defined in Eqs. (6.8) and (6.9) respectively, are shown in Fig. 7.7 as calculated with both the monatomic gas kernel and the Nelkin water model. In this case, the discrepancies between the results computed with the two models is entirely attributed to the softer spectra produced with the monatomic gas model since the transport cross section for water used in both calculations was that calculated with the Nelkin water kernel. The δ_n^m predicted with the monatomic gas kernel are 1.4% higher for the 1:1 core and

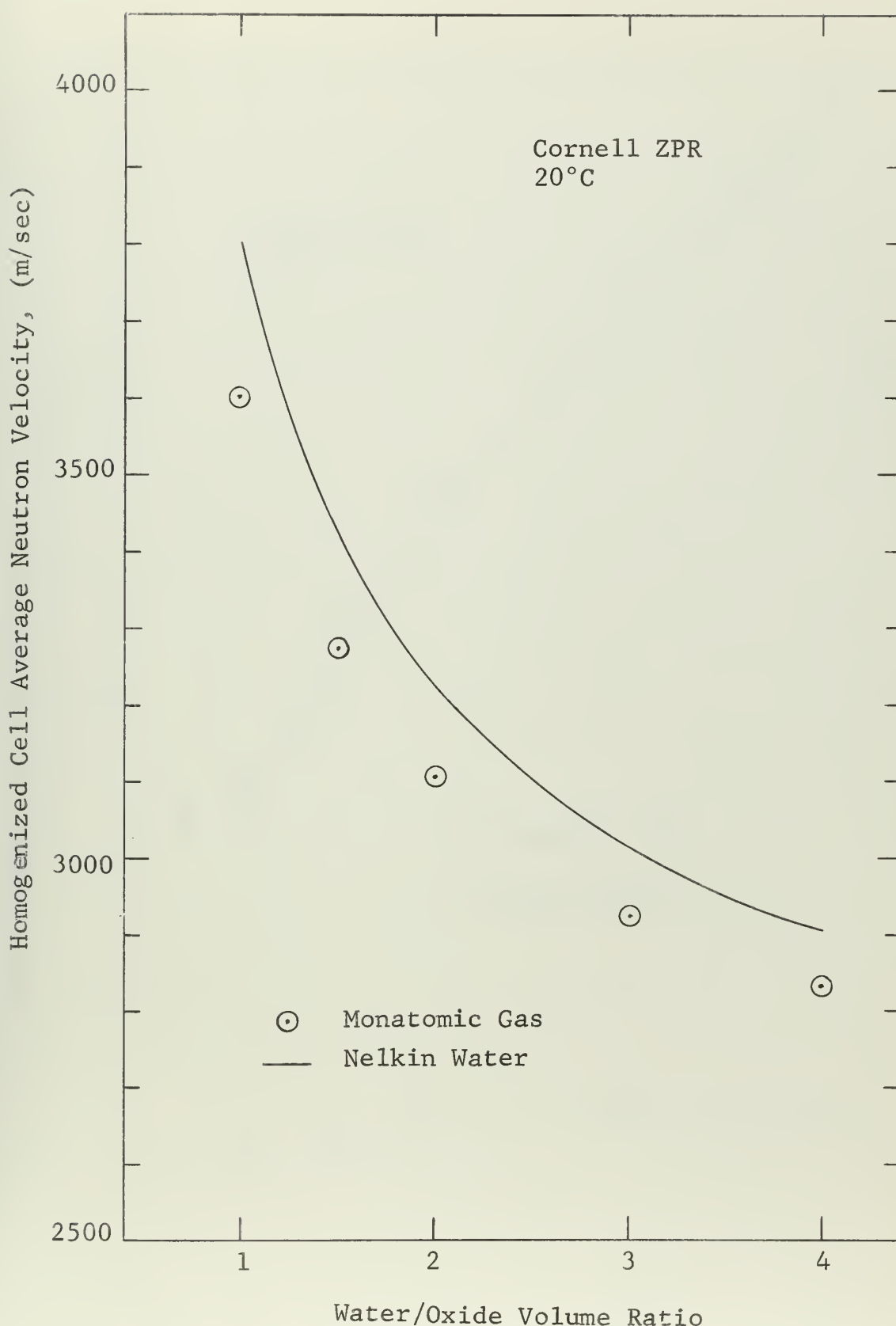


Figure 7.6 Average Neutron Velocity for the Homogenized Cell

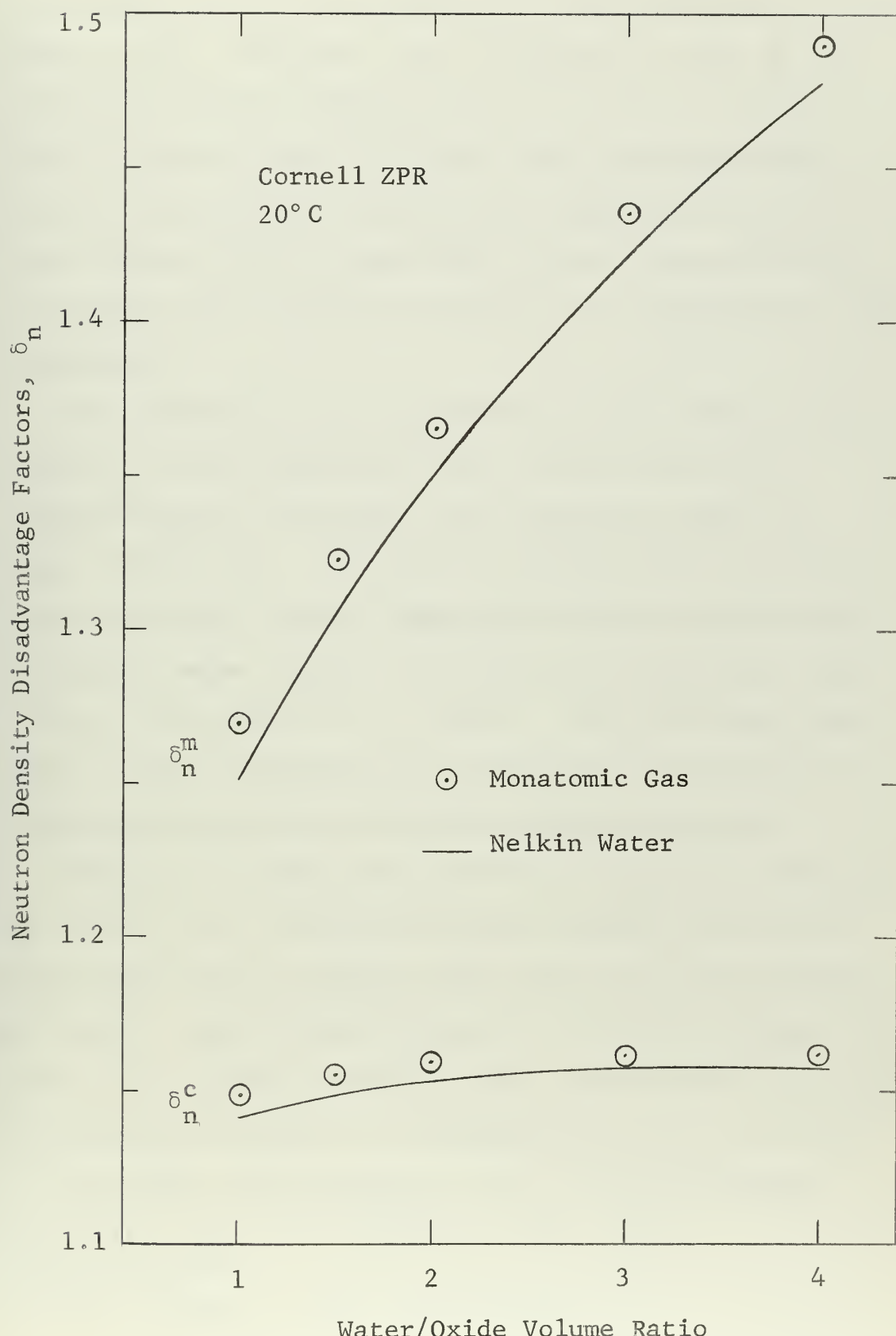


Figure 7 Neutron Density Disadvantage Factors

0.8% higher for the 4:1 core than those calculated with the Nelkin model. Similarly, the differences in the δ_n^c calculated by the two models is 0.8% for the 1:1 core and 0.3% for the 4:1 core. The fact that the disadvantage factors monotonically increase as a function of water to oxide volume ratio is expected^{74/} since a non-reflecting cylindrical cell boundary condition is incorporated in this formulation.

The results of the calculation of the thermal utilization, f , and ηf defined by Eqs. (6.15) and (6.16) respectively for the Nelkin water model are shown in Figs. 7.8 and 7.9. The results predicted with the monatomic gas model closely approximate those computed with the Nelkin water kernel, the differences being less than 0.2% for all cases of f , η , and ηf . This indicates that these integral properties are essentially insensitive to the scattering model used in the averaging process.

Figure 7.10 shows the variation of thermal lifetimes, Eq. (6.17), as a function of water to oxide volume ratio calculated with the Nelkin water kernel and the monatomic gas model. Again relatively small variations, always less than 0.4%, between the Nelkin water and monatomic gas kernel calculations are present. The lifetimes are seen to decrease in the tighter cores because of the increased apparent absorption, Fig. 7.1, present in these cores.

^{74/} H. C. Honeck, p. 56, see Footnote 73.

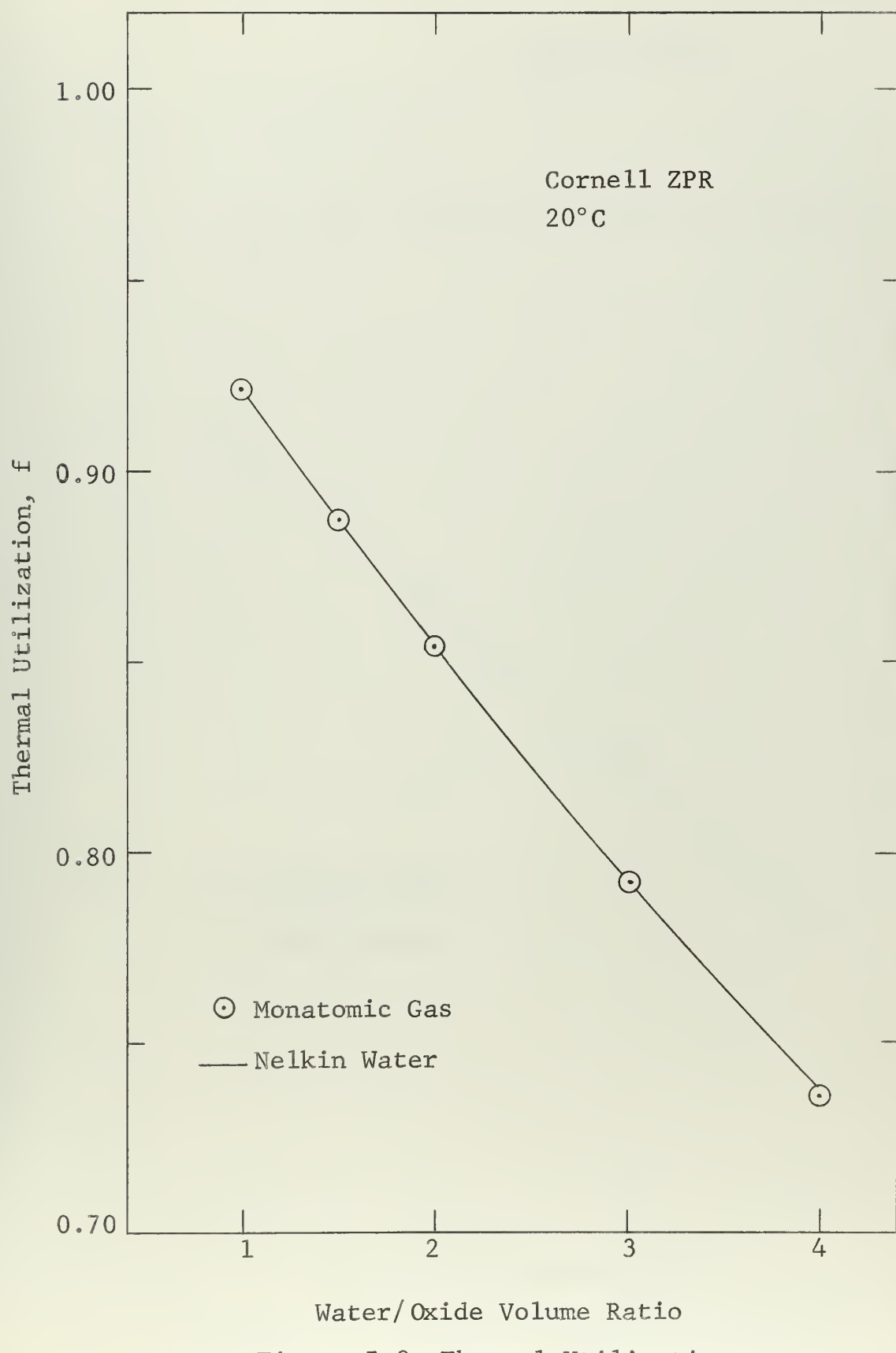
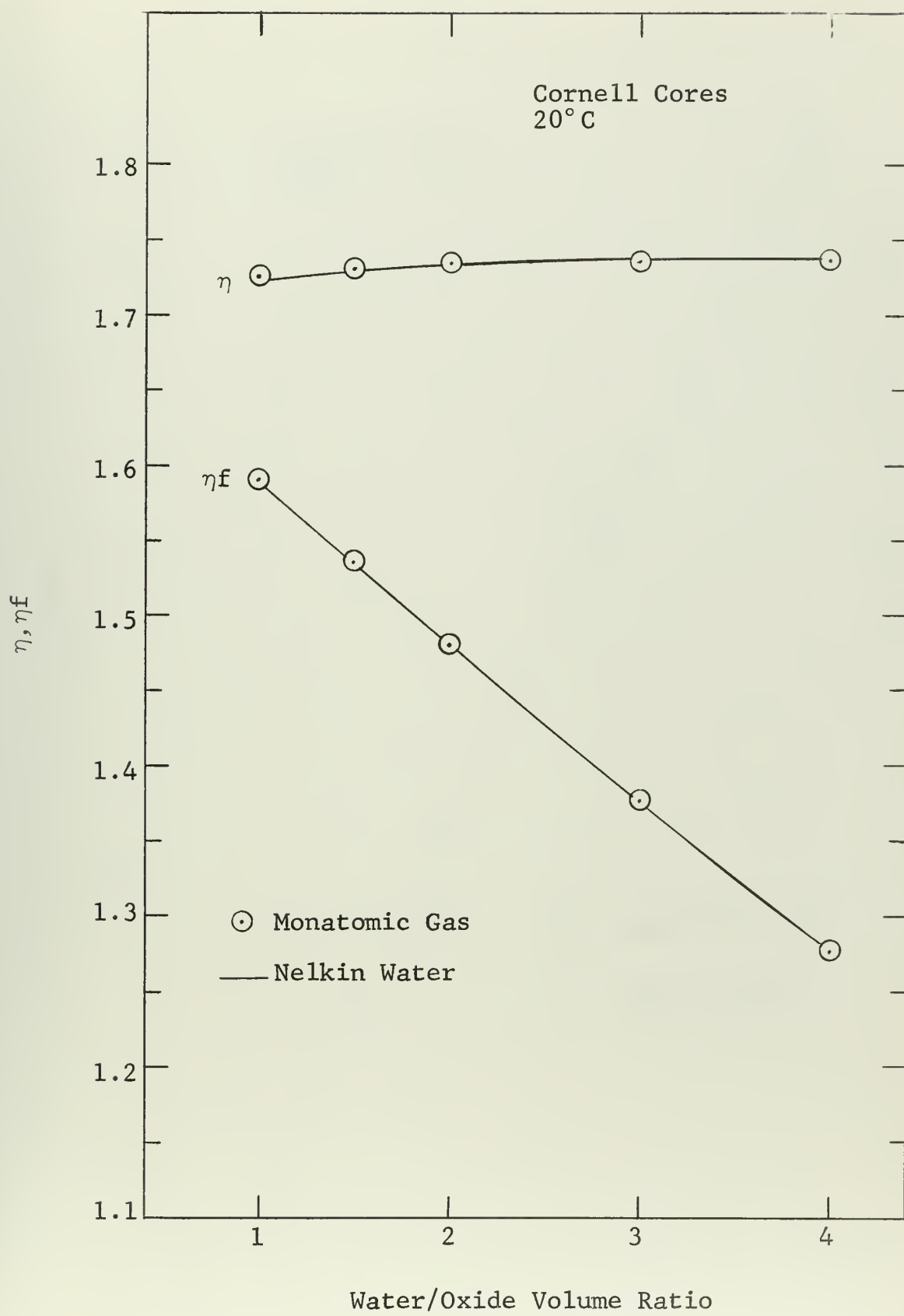


Figure 7.8 Thermal Utilization

Figure 7.9 Integral Properties, η and η_f

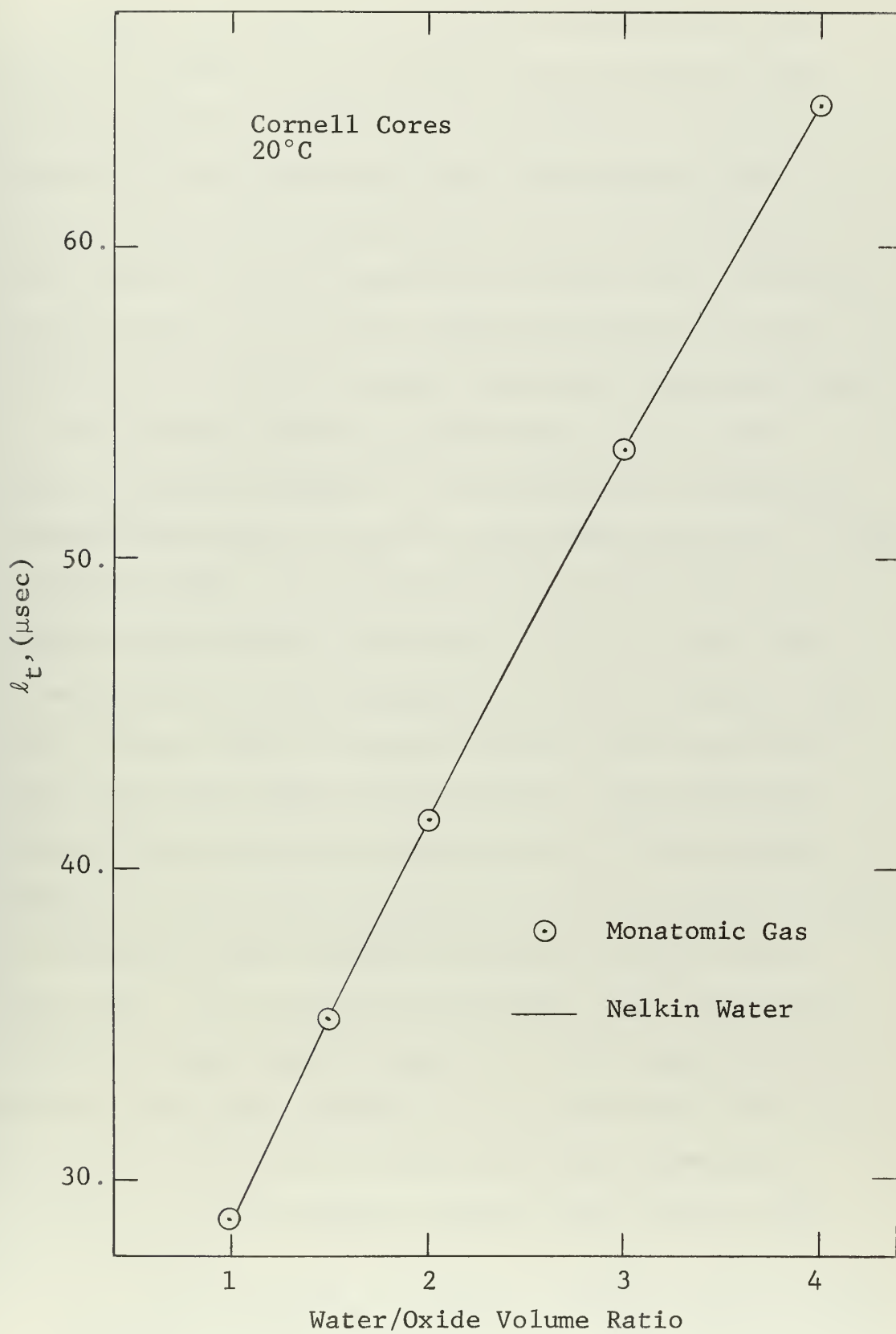


Figure 7.10 Thermal Lifetime

Figure 7.11 shows the effective absorption cross section, $\hat{\Sigma}_a^h$, Eq. (6.31), and the mean absorption cross section, $\bar{\Sigma}_a^h$, Eq. (6.32), for the homogenized cell as calculated using the Nelkin water and monatomic gas models. Variations encountered in the calculation of these results when the monatomic gas model was utilized were less than 0.4% for the effective absorption cross sections and 2.0% for the mean absorption cross sections.

The thermal diffusion coefficient, D, and the thermal diffusion length, L, as calculated by averaging a homogenized mean free path in accordance with Eq. (6.38) are shown in Fig. 7.12 using both the Nelkin water and monatomic gas kernels. From Fig. 7.12 it is seen that the monatomic gas model predicts a D which is about 3.0% less, and an L which is about 4.0% less than those calculated with the Nelkin water kernel. The differences between these results are strictly due to the relative hardness of the spectra predicted by the two models, since the transport cross sections utilized were the same in both cases. It is still not clear how these calculated diffusion lengths would compare with those measured in a buckling experiment; however, it is noteworthy that the minimum in L for the 2:1 core is the same phenomenon measured for the Brookhaven uranium metal lattices.^{75/}

^{75/} R. L. Hellens and H. C. Honeck, "Summary and Preliminary Analysis of the BNL Slightly Enriched Uranium, Water Moderated Lattice Measurements," Light Water Lattices, p. 54, International Atomic Energy Agency, Vienna (1962).

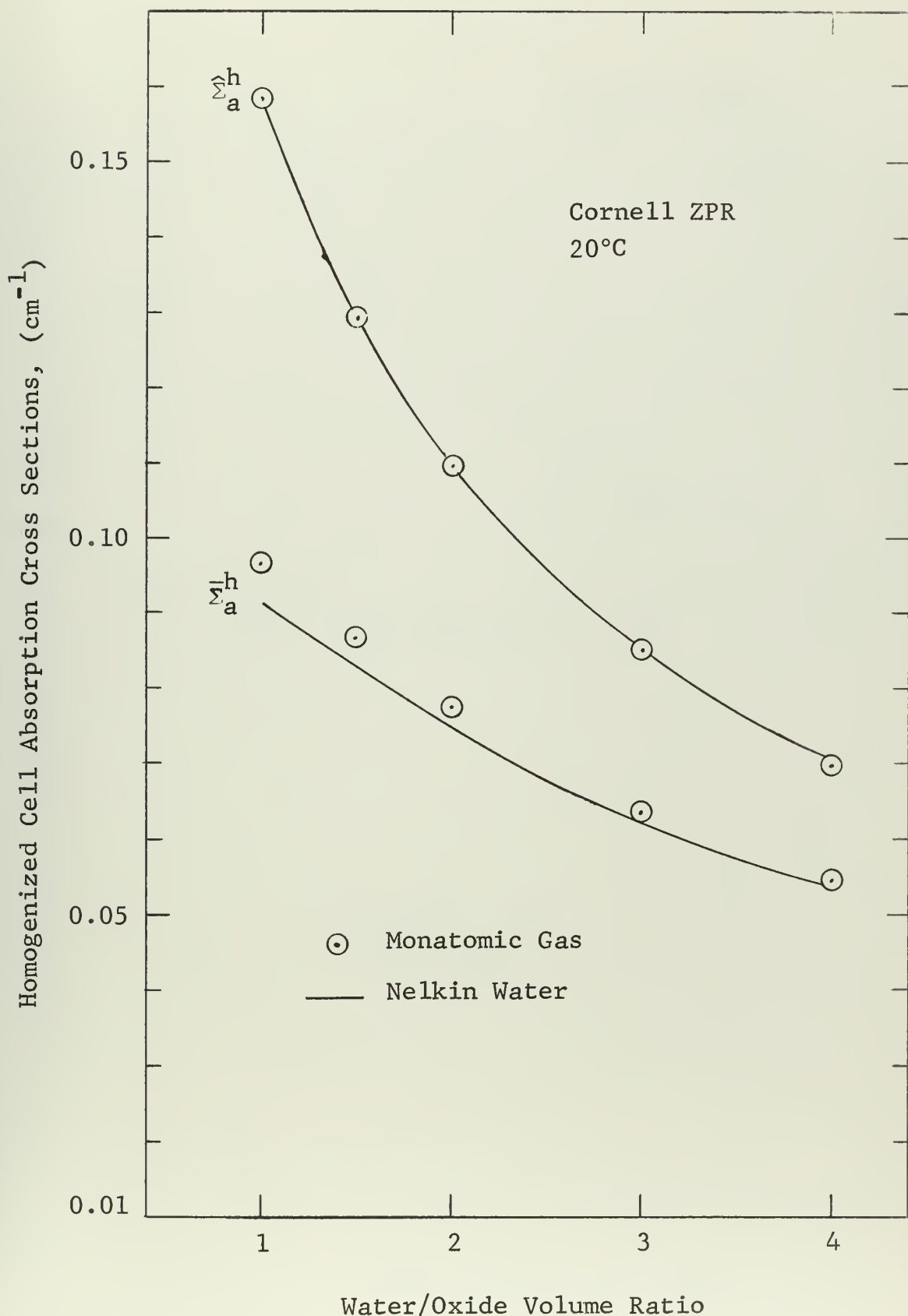


Figure 7.11 Effective and Mean Absorption Cross Sections for Homogenized Cell

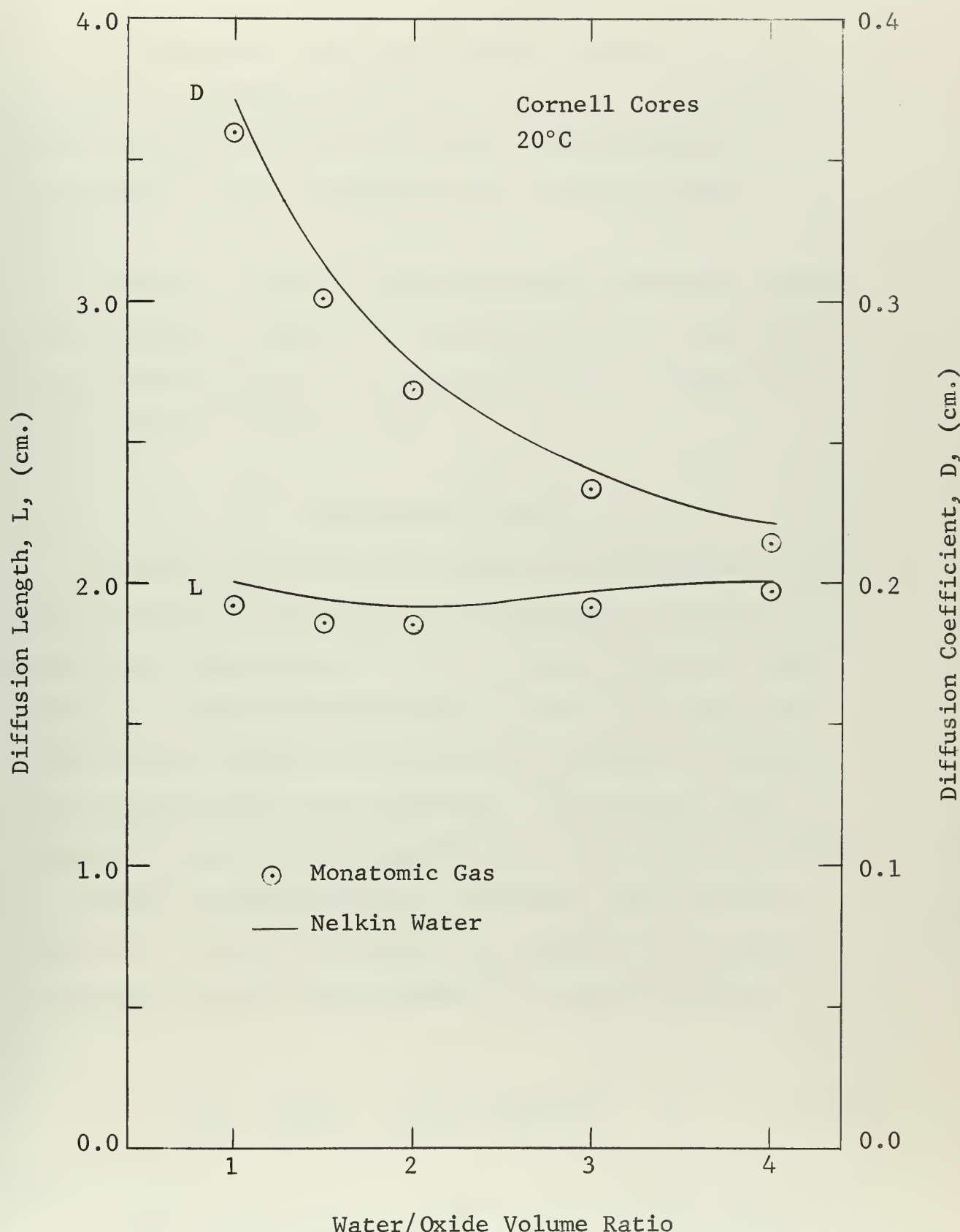


Figure 7.12 Thermal Diffusion Coefficient and Length for the Homogenized Cell

This also indicates that the customary receipe for calculating a homogenized diffusion area, $L^2 = (1-f) L_o^2$, ^{76/} lacks validity in that it predicts a monotonically increasing L^2 with increasing water to oxide volume ratios.

A tabular listing of the parameters presented in this section appear in Appendix B as calculated with the Nelkin water kernel at 20°C. A discussion of the accuracy of these results is given in Chap. 8.

7.2 Temperature Coefficients

In order to estimate the effect of temperature on the various integral parameters defined in Chap. 6 and presented for 20°C in Sec. 7.1, all of the calculations were remade at a physical temperature of 40°C. In these calculations any changes in the fuel and cladding densities and dimensions have been neglected. In addition, the expansion of grid plate supporting the fuel elements leading to a change in the equivalent cell radius has also been neglected. All of the results are expressed in terms of temperature coefficients defined for a given variable, x , as

$$\frac{1}{x} \frac{\Delta x}{\Delta T} = \frac{1}{x(20^\circ)} \cdot \frac{x(40^\circ) - x(20^\circ)}{20} \text{ } ^\circ\text{C}^{-1}. \quad (7.5)$$

^{76/} A. M. Weinberg and E. P. Wigner, The Physical Theory of Neutron Chain Reactors, p. 724, The University of Chicago Press, Chicago, 1958.

The temperature coefficient of the average neutron velocity in the homogenized cell, \bar{v}_h , Eq. (6.33), is shown in Fig. 7.13 for both models of the scattering kernel. This indicates that although the Nelkin model predicts a harder homogenized spectrum at room temperature, the monatomic gas spectra hardens at a faster rate with increasing temperature. It is therefore possible to postulate that at some elevated temperature the integral parameters dependent primarily on the degree of spectral hardening will be the same for both models of the scattering kernel. The temperature coefficient of \bar{v}_h predicted with the monatomic gas model is 23.8% higher for the 1:1 core and 7.8% higher for the 4:1 core than those predicted by the Nelkin water kernel.

Figure 7.14 shows the temperature coefficients of the moderator and cladding disadvantage factors, δ_n^m and δ_n^c , these parameters having been defined in Eqs. (6.8) and (6.9) respectively. As expected, they are negative; the effects of harder spectra being seen in Fig. 7.7. The monatomic gas model predicts larger negative temperature coefficients because of the greater relative spectral hardening encountered with that model. The maximum difference between the scattering models occurs in the 1:1 core where the temperature coefficient of δ_n^m predicted by the monatomic gas model is 30% higher than the prediction by the Nelkin water kernel. In the case of δ_n^c the results differ by 20%.

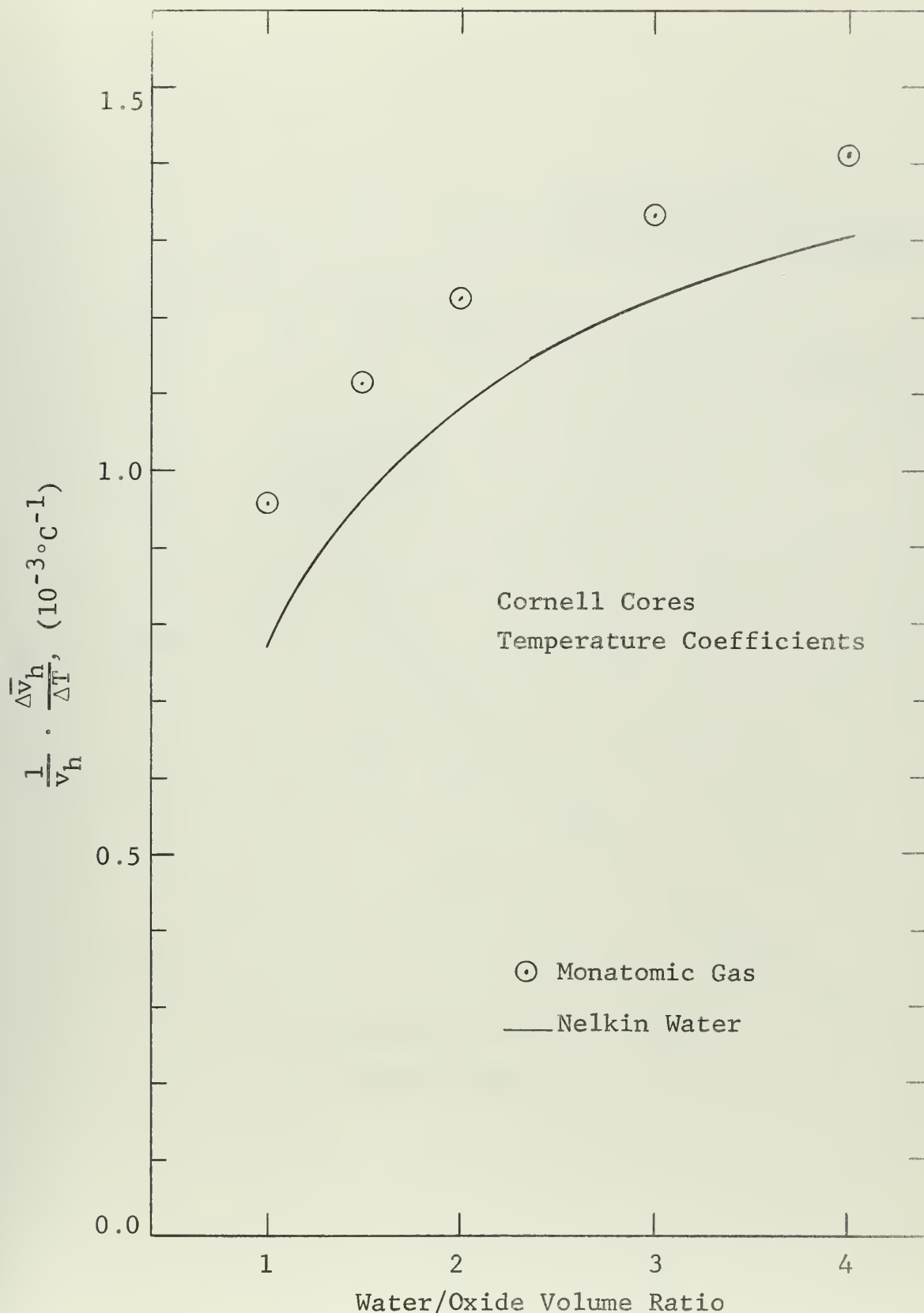


Figure 7.13 Temperature Coefficient of the Average Neutron Velocity for the Homogenized Cell

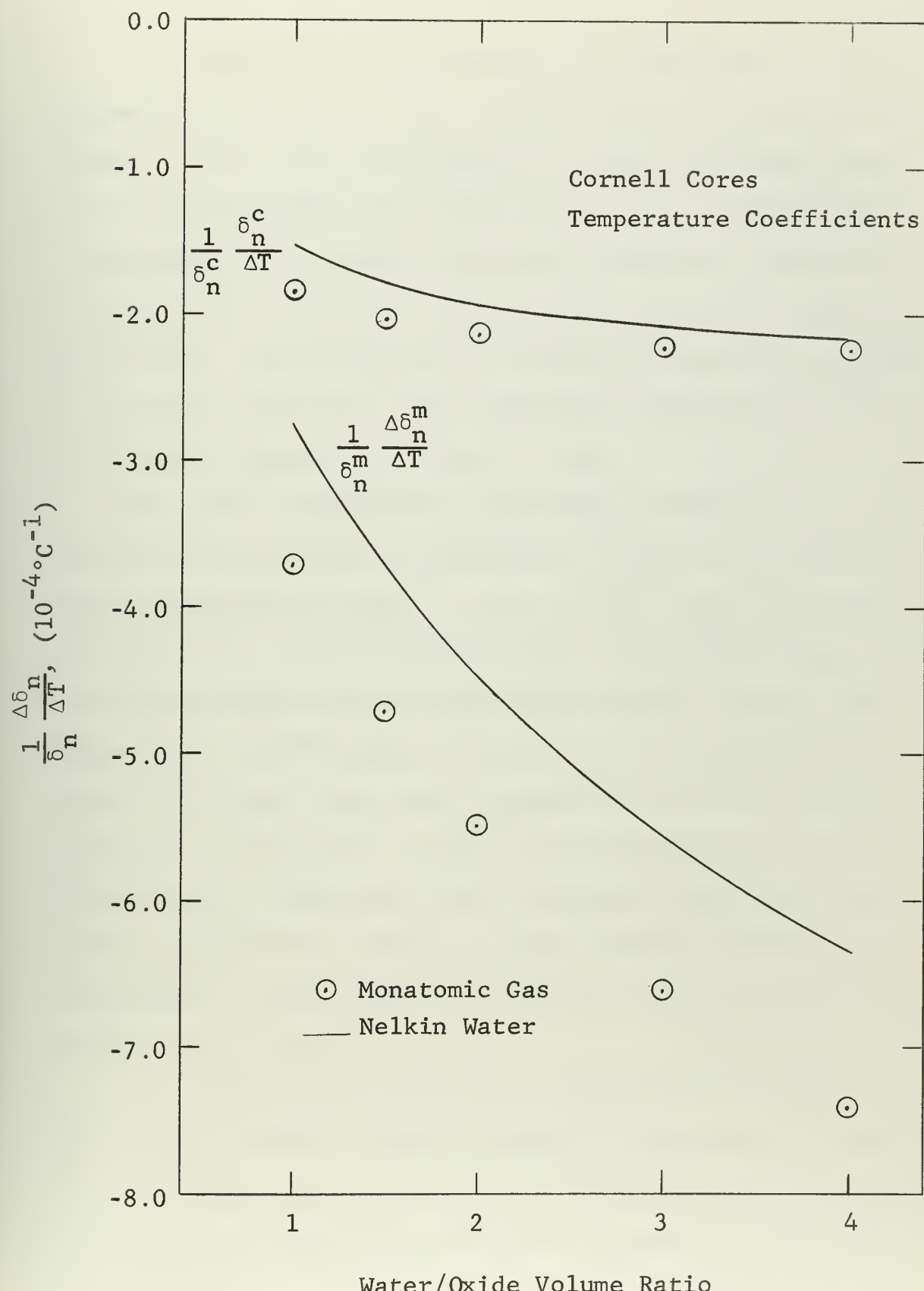


Figure 7.14 Temperature Coefficients of the Neutron Density Disadvantage Factors

The variation of the temperature coefficients of the thermal utilization, f , Eq. (6.15), and ηf , Eq. (6.16) is shown in Fig. 7.15, the difference between the two curves for each scattering model being equal to the temperature coefficient of η . Again the results predicted are more positive with the use of the monatomic gas model because of the greater relative spectral hardening given by that model. It is to be noted that the temperature coefficient of ηf is slightly negative for the 1:1 core.

The final temperature coefficients worthy of note are those of the diffusion coefficient, D , Eq. (6.38), and the thermal diffusion length, L , Eq. (6.39). These are shown in Fig. 7.16; the difference between the monatomic gas and the Nelkin water models being quite evident. Again, the temperature coefficients predicted by the monatomic gas model are higher than those produced by the Nelkin water kernel. The deviation is the most pronounced for the 1:1 core where the monatomic gas results are higher than the Nelkin water kernal results by the following percentages: temperature coefficient of D , 68%; and temperature coefficient of L , 34%.

The differences between the monatomic gas and the Nelkin water kernel results are more pronounced for the D and L temperature coefficient calculations than for any of the other parameters previously discussed. This may be attributed to the fact that these calculations are

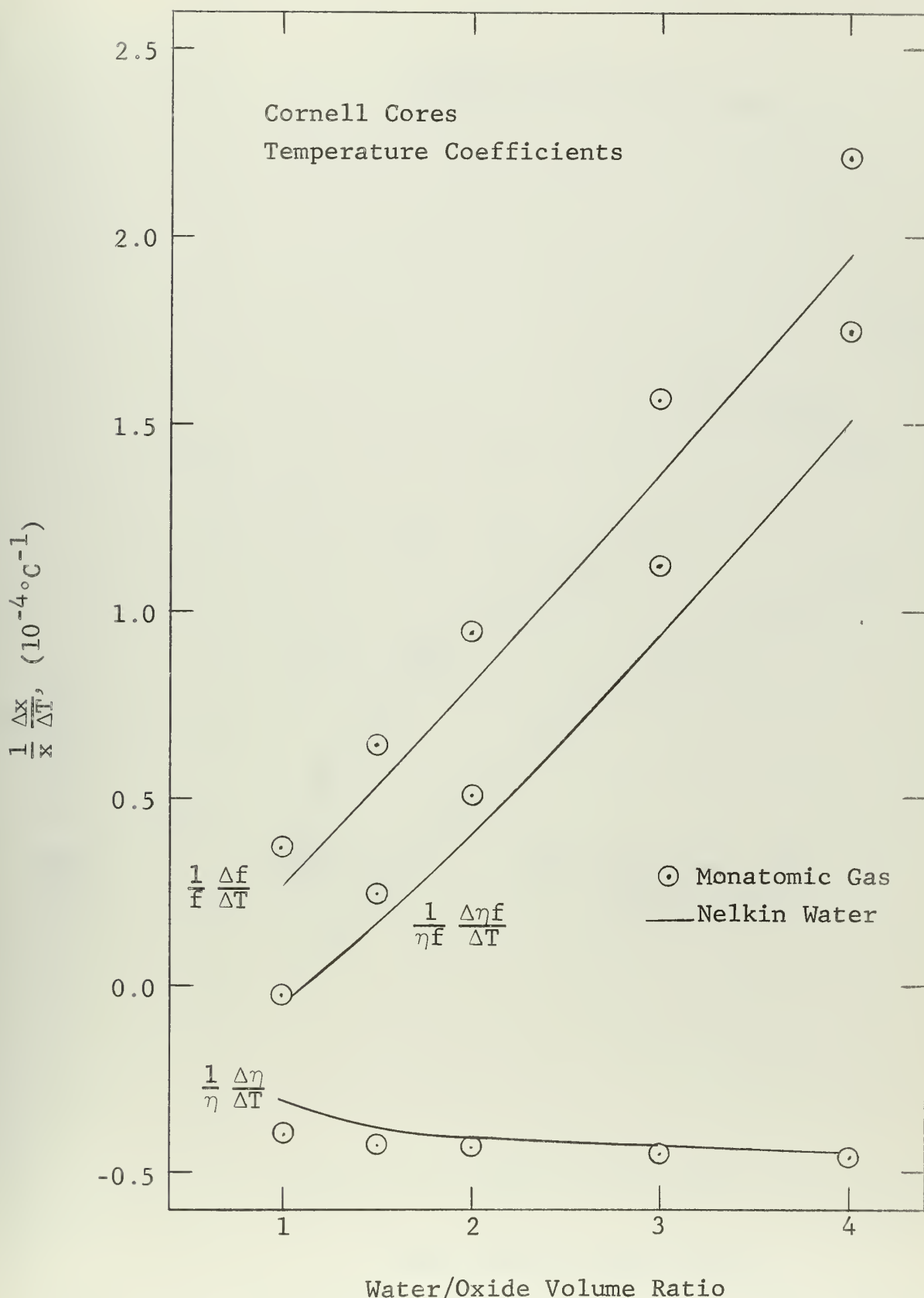


Figure 7.15 Temperature Coefficients of the Integral Properties, f and ηf

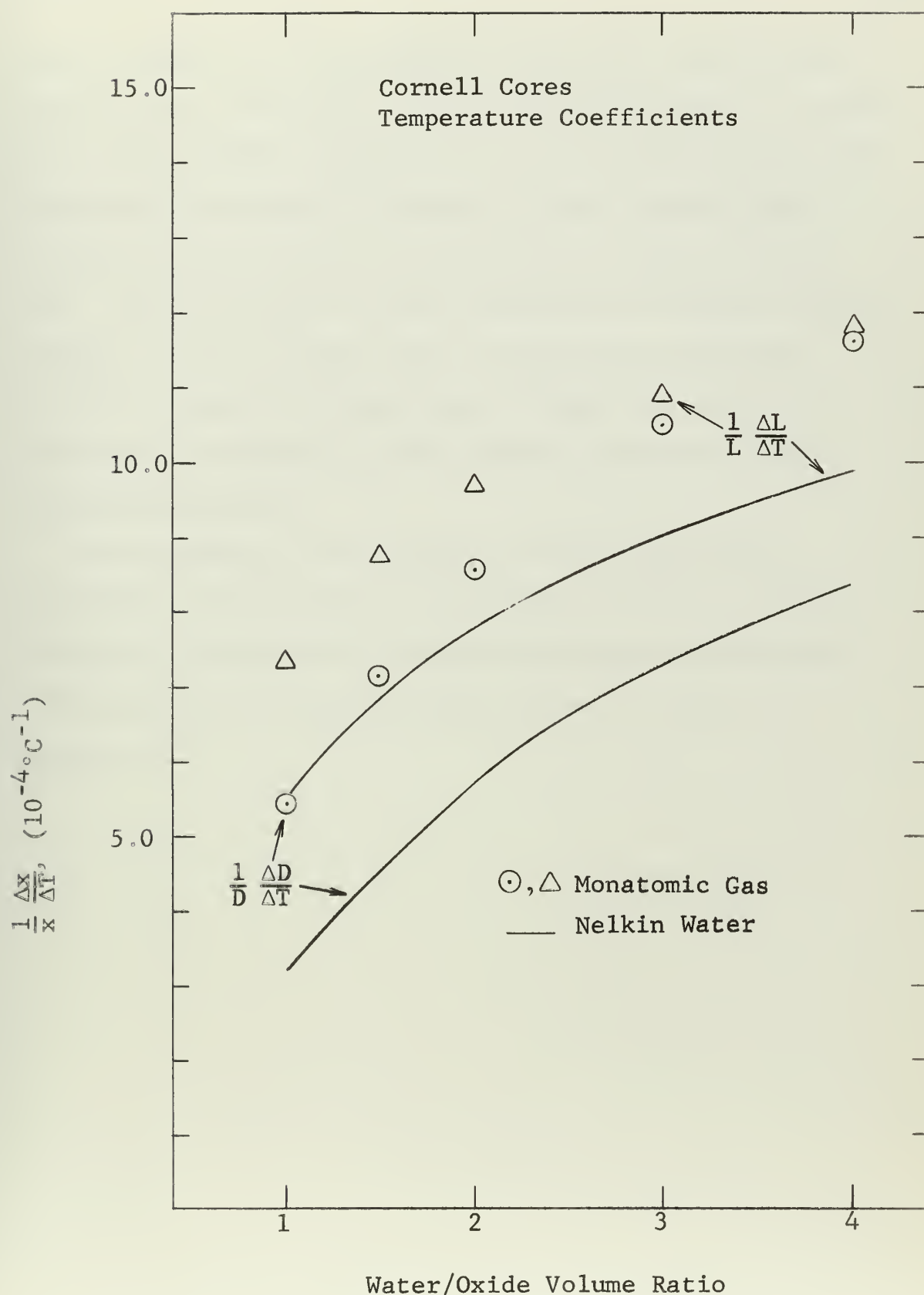
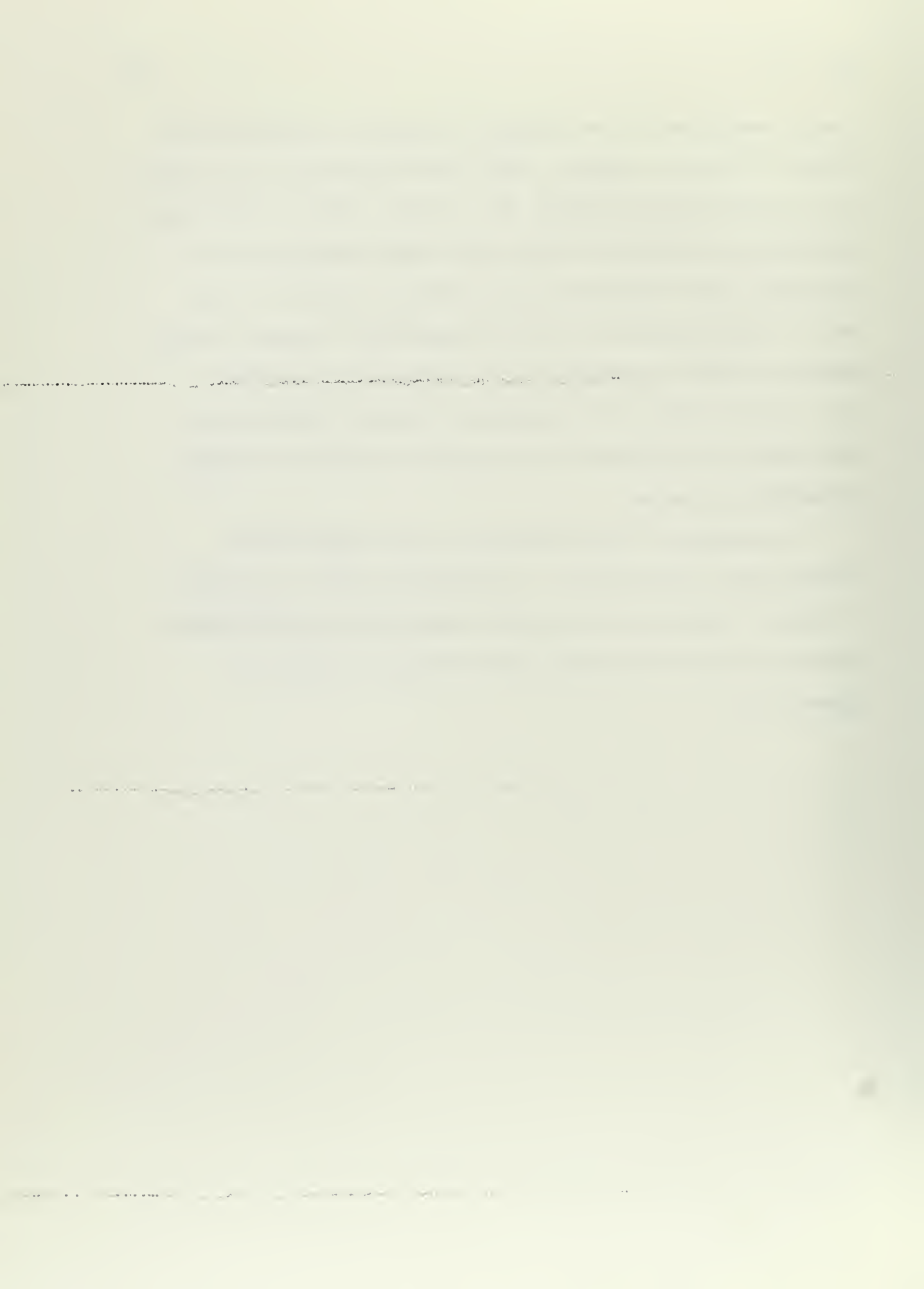


Figure 7.16 Temperature Coefficients of the Thermal Diffusion Coefficient and Length for the Homogenized Cell

doubly sensitive to the degree of spectral hardening predicted by the two models, since the homogenized cell transport cross section, $\Sigma_{tr}^h(E)$, Eq. (6.36), used in these calculations is derived by flux and volume weighting the transport cross sections of the various regions in the cell. The reciprocal of this homogenized transport cross section is then averaged over a homogenized spectrum, Eq. (6.37), making the resultant D highly sensitive to the degree of hardness in the spectra utilized in these averaging processes.

An estimate of the accuracy of the temperature coefficient calculations is discussed in Chap. 8, while a tabular listing of all of the temperature coefficients calculated with the Nelkin water kernel is given in Appendix B.



CHAPTER 8

ACCURACY OF THE RESULTS

In an attempt to estimate the accuracy of the results predicted with program COUTH, as presented in Chap. 7 and listed in Appendix B, two lines of approach have been utilized. The first of these involved the calculation by COUTH of several integral properties of the Brookhaven uranium dioxide lattices, a comparison then being made between these results and those calculated by Honeck^{77/} with the THERMOS transport theory code. The second of these was an investigation of the sensitivity of the Cornell ZPR results to changes in the inputs to the COUTH code such as the densities, cross sections, and dimensions of various regions within the lattice cell.

The Brookhaven cores^{78/} studied are generically related to the Cornell ZPR cores in that they are light water moderated and utilize low enrichment uranium dioxide fuel. Five water to uranium oxide volume ratios are provided, these being 1.291:1, 1.600:1, 2.050:1, 2.803:1, and 4.000:1. The fuel rods are 0.444 inches in diameter and clad with 0.028 inch thick stainless steel giving the fuel element an outside diameter of 0.500 inches. The uranium dioxide fuel is enriched to 3.0 atom per cent, its density being 9.3 gm/cc.

^{77/} H. C. Honeck, "The Calculation of the Thermal Utilization and Disadvantage Factor in Uranium/Water Lattices," Nucl. Sci. Eng. 18, 49-68 (1964).

The integral thermal parameters compared are the thermal utilization, f , the ratio of the number of fission neutrons produced to the number of thermal neutrons absorbed in the fuel, η , and the moderator neutron density disadvantage factor, δ_n^m . The THERMOS calculation of these parameters utilizes a thirty point energy mesh ranging from 0.00025 to 0.632 eV, while COUTH uses a 41 point energy mesh ranging from 0.001 to 0.645 eV, as discussed in Sec. 7.1. Both programs utilize the same cross section input data and both perform their calculations utilizing a Nelkin water model for the scattering kernel at 20°C.

A comparison between the results predicted by THERMOS, using integral transport theory, and COUTH, using the simplified cell theory, are shown in Fig. 8.1 for the thermal utilization, f . In Fig. 8.1 it is seen that the f 's calculated with the two codes compare very well, the maximum deviation in the results occurring in the 4.0:1 core where the THERMOS f is 0.39% higher than the f calculated with COUTH.

The results of the calculation of η by COUTH and THERMOS are seen in Fig. 8.2 to be even closer than those for f . In this case the maximum difference between the results predicted by the two techniques is found in the 1:1 core, the THERMOS result here being 0.19% higher than the COUTH estimate.

78/ H. C. Honeck, see Footnote 77.

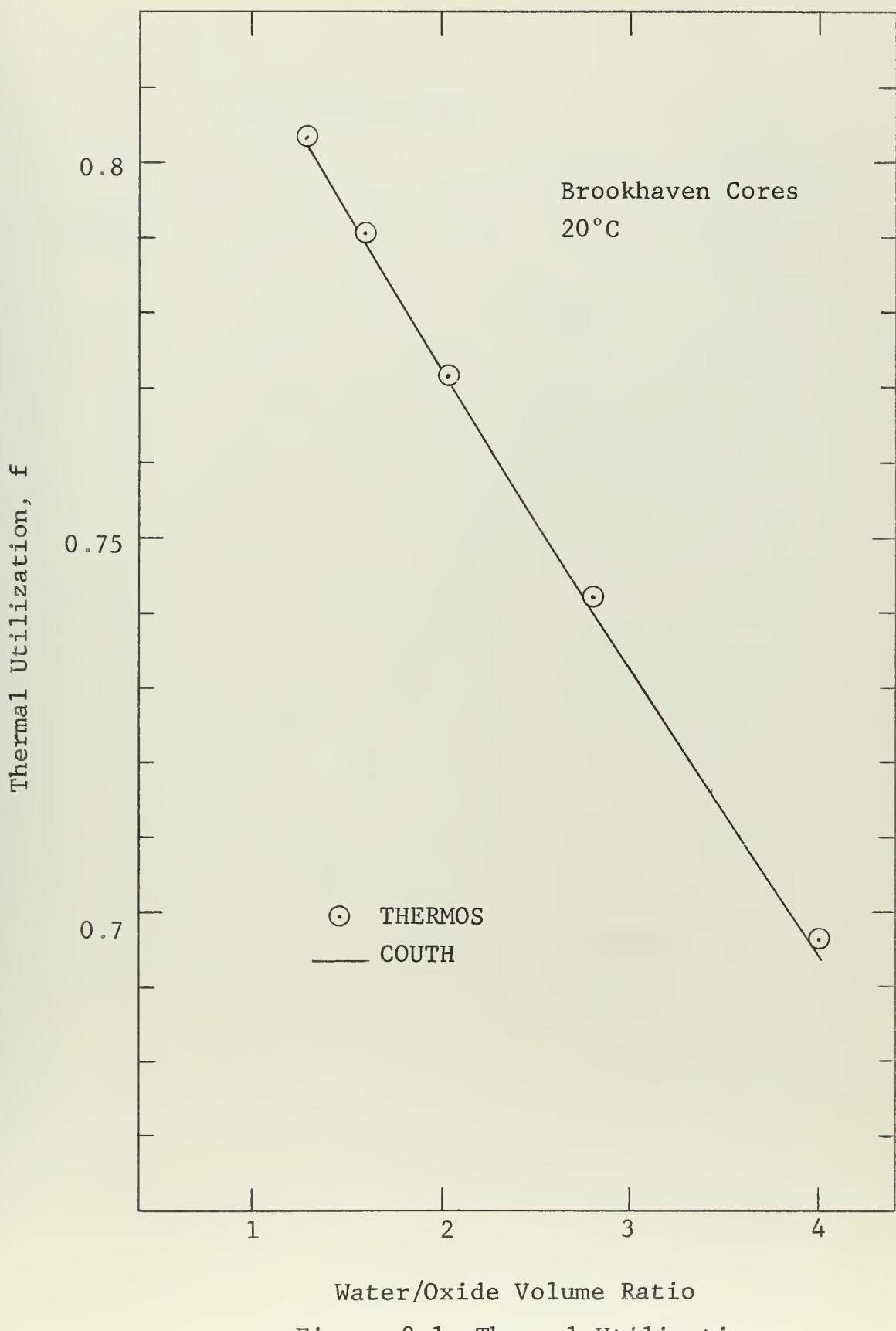
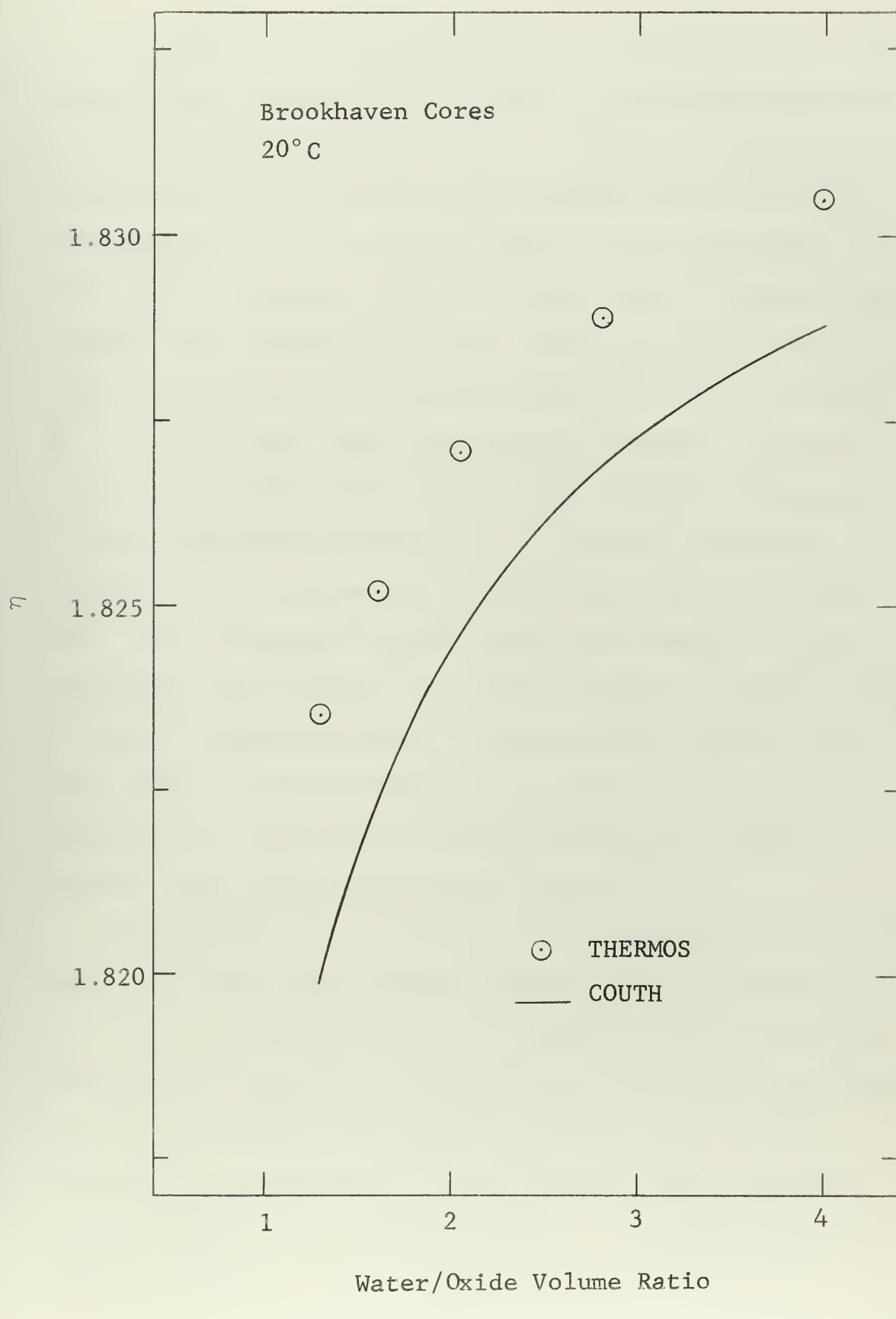


Figure 8.1 Thermal Utilization

Figure 8.2 Integral Property, η

In the case of the moderator disadvantage factor, δ_n^m , the agreement between the two codes is not quite as close as in the calculations of f and η . Figure 8.3 shows the results derived, indicating that THERMOS predicts higher disadvantage factors for the tighter cores than COUTH, while this role is reversed with the larger water to oxide volume ratios. The THERMOS δ_n^m for the 1.29:1 core is 0.62% higher than the COUTH number, while for the 4.0:1 core the COUTH δ_n^m is 0.97% higher than that given by THERMOS. Honeck^{79/} assigns a combined uncertainty to the THERMOS calculation of the disadvantage factor of 1.5%, meaning the COUTH calculation of this parameter has an uncertainty less than 2.5%. The deviations between COUTH and THERMOS in this calculation are believed to be attributable to COUTH's use of simple diffusion theory in the moderator region, combined with an overestimation of the fuel element escape probability. Resolution of these differences requires further study and is discussed in Chap. 9.

The parametric study made on the Cornell ZPR for 20°C using the Nelkin water kernel investigated the sensitivity of the calculated parameters to changes in the input data. Changes were made in the fuel density, the fuel enrichment, the fuel rod radius, the cladding radius, the cladding scattering and absorption cross sections, the moderator density, and lattice spacing or pitch. In an attempt to

^{79/} H. C. Honeck, p. 60, see Footnote 77.

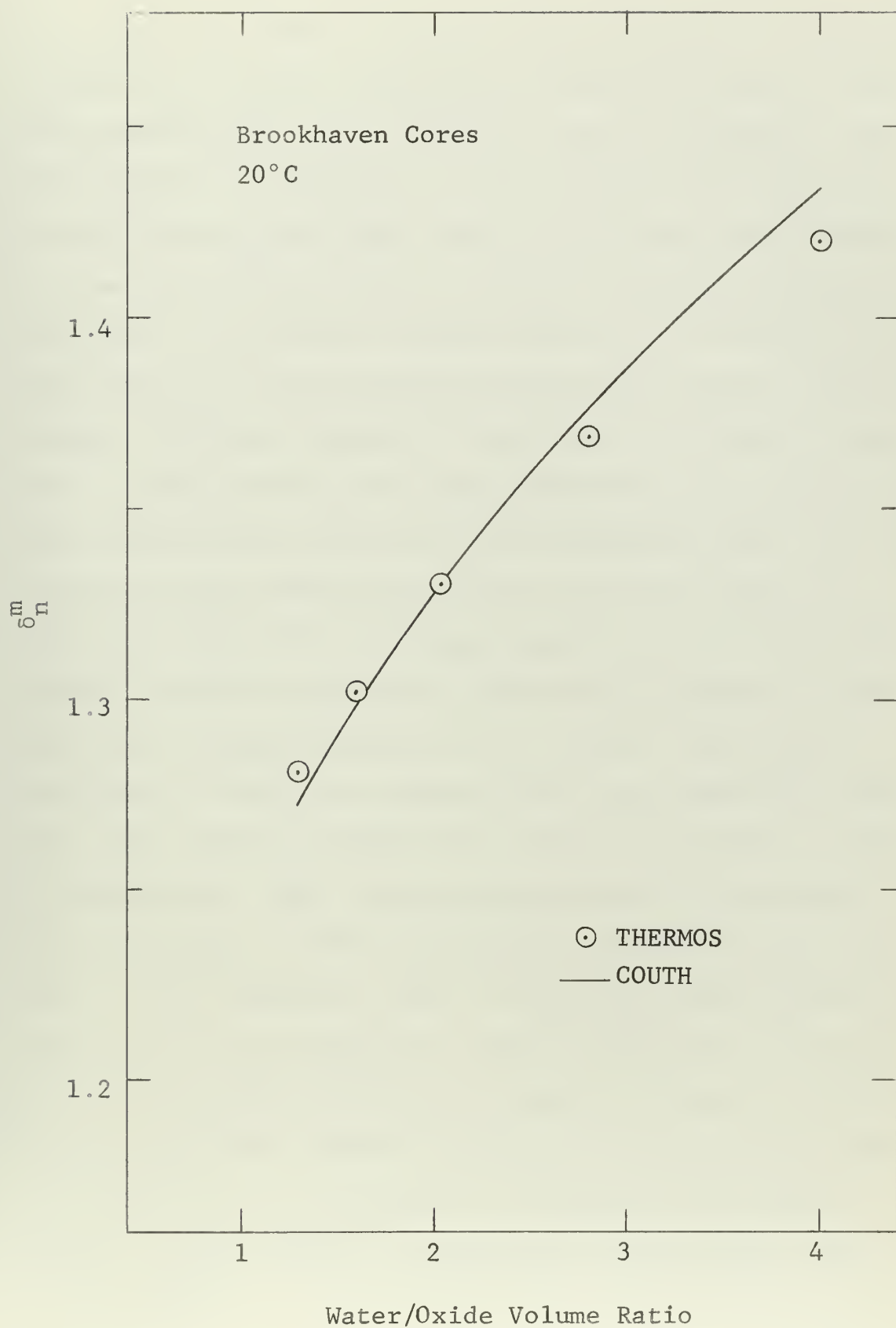


Figure 8.3 Neutron Density Moderator Disadvantage Factor

determine the effect of using various numerical integration schemes, the results utilizing an integration method which fit exponentials, i.e., straight lines on log paper, were also studied. The effect of these changes were noted for several parameters, these being: The thermal utilization, f ; the ratio of the number of fission neutrons produced to the number of neutrons absorbed thermally in the cell, η_f ; the moderator neutron density disadvantage factor, δ_n^m ; the thermal diffusion length, L ; the thermal lifetime τ_t ; the mean neutron velocity for the homogenized cell, \bar{v}_h ; and the mean total cross section for the homogenized cell, $\bar{\Sigma}_t^h$. The results of the parameter variation study are shown in Table 8.1 where the percentage changes in the input parameters required to produce a positive 0.1% change in the resultant integral properties are listed. The results presented in Table 8.1 represent the most sensitive cases, the error analysis having been carried out on the 1:1 and 4:1 ZPR cores. Thus the percentage changes shown which involve changes in the fuel element parameters come from the 1:1 core analysis, since a relatively large portion of the unit cell is composed of fuel for this core. The 1:1 core is also most sensitive to changes in lattice pitch. On the other hand results from the 4:1 core are given for the sensitivity of parameters to changes in the water density, water playing a relatively more important role in this core.

TABLE 8.1

PERCENTAGE CHANGES IN INPUT PARAMETERS REQUIRED TO CHANGE INTEGRAL PROPERTIES
BY +0.1 PERCENT

INPUT PARAMETERS	INTEGRAL PROPERTIES					
	f	ηf	δ_m^n	L	ℓ_t	\bar{v}_h $\sum t$
Fuel Density	+1.64	+1.92	+0.57	-0.28	-0.13	+0.47
Fuel Enrichment	+1.89	+0.47	+0.74	-0.48	-0.15	+0.55
Fuel Radius	+0.69	+0.81	-1.43	+0.85	-0.10	+0.19
Cladding Radius	+1.25	+1.85	+0.45	+0.07	-1.47	+0.14
Cladding Scattering Cross Section	-500.	-1000.	+58.8	-7.46	-100.	-333.
Cladding Absorption Cross Section	-12.5	-12.3	+166.	-34.48	-14.49	+50.
Lattice Pitch	-0.10	-0.34	+0.23	-0.18	+0.05	-0.08
Water Density	-1.35	-1.56	+1.14	-0.16	-1.45	-0.39

The use of the numerical integration scheme involving the fitting of exponentials rather than straight lines as in the trapezoidal integration rule produces the following maximum percentage changes in the integral parameters: f , 0.004%; ηf , .009%; δ_n^m , 0.12%; L , 1.1%; ℓ_t , .069%; \bar{v}_h , 0.12%; and $\bar{\Sigma}_t^h$, 2.5%. The large percentage change in $\bar{\Sigma}_t^h$ may attribute to the fact that the numerical integration scheme using exponentials predicts scattering cross sections for water by integrating the scattering kernel which are as much as 3.0% higher than the experimentally measured values.

Table 8.1 shows that the numerical results are essentially insensitive to the cladding cross section data, while they are most sensitive to the lattice pitch. The actual tolerances given^{80/} for the Cornell ZPR lattice pitches are less than 0.10% so that the output parameters will vary no more than about 0.2% because of variations in this dimension. The fuel element parameter, density, enrichment, fuel rod radius, and fuel element radius are known to within 0.5% and reference to Table 8.1 indicates that in general variations of the thermal integral properties will be less than 0.5%.

In light of the results of comparing the predictions of the THERMOS and COUTH codes and the results of the input parametric studies, the following probable uncertainties may be assigned to the 20°C calculations performed

by COUTH utilizing the Nelkin water kernel as a scattering model.

1. f , η , and ηf ; 0.5%.
2. Disadvantage factors for the moderator and cladding, 2.0%.
3. Thermal lifetimes; 3.0%.
4. Mean velocities; 3.0%.
5. Averaged cross sections, including the calculation of D and L ; 5%.

With regard to the room temperature calculations made utilizing the monatomic gas model, the deviations from the Nelkin water kernel results were quoted in Chap. 7. Using these percentages, one can then assign the following probable uncertainties to the 20°C monatomic gas calculations.

1. f , η , and ηf ; 0.8%.
2. Moderator and cladding disadvantage factors; 4.0%.
3. Thermal lifetimes; 4.0%.
4. Mean velocities; 8.0%.
5. Averaged cross sections, including the diffusion coefficient and length; 10.0%.

On the basis of these two sets of uncertainties, one must reconcile the accuracy obtained with the computer time required for a given calculation. A monatomic gas scattering kernel, in the form of a 45 by 45 matrix takes only two and one half minutes of computer calculation, while the Nelkin

water scattering kernel takes on the order of fifteen minutes. Thus if one is undertaking a detailed temperature study wherein multiple scattering kernels must be calculated, use of the monatomic gas model is advocated for one primarily interested in f and ηf . However, if emphasis is to be placed on the other integral parameters, and in particular the averaged cross sections, then the more complicated Nelkin model should be used.

The assignment of uncertainties to the temperature coefficients presented in Chap. 7 presents a slightly different problem. In this case one must estimate the uncertainties in a calculation at a given temperature and then estimate the uncertainty in the degree of spectral hardening predicted by a certain model. The fact that the THERMOS and COUTH results at room temperature are in agreement for all values of water to fuel volume ratios indicates that COUTH can adequately handle spectral hardening effects if the scattering kernel model can predict the appropriate temperature changes in the energy transfer process. We therefore, *a priori*, assign uncertainties to the temperature coefficient calculations as being twice those stated above for the room temperature calculations with both the Nelkin water model and the monatomic gas kernel.

80/ S. S. Berg, "Initial Experiments on the Cornell University Zero Power Reactor Cores," Cornell University Thesis (1964).

CHAPTER 9

SUMMARY AND CONCLUSIONS

A simplified polyenergetic cell theory has been formulated for use in the determination of the spatially averaged energy dependent thermal fluxes in the various regions of a lattice cell. The derived spectra are then utilized in the calculations of the thermal integral parameters and average cross sections required for reactor computations.

The cell theory, as formulated, postulates an infinite moderator region with the absorption cross section of this region appropriately modified to account for the neutron leakage into and absorption by the fuel element in the actual lattice. The modifications to the moderator absorption cross section, have been formulated both in general terms an in terms of moderator and fuel element escape probabilities, the latter approach offering physical transparency and ease of calculation.

Analytic expressions for the escape probabilities have been presented, integral transport theory having been applied in the fuel element region, while diffusion theory was utilized in the moderator region. Using these analytic expressions the theory was applied to actual lattices in the form of the Cornell University Zero Power Reactor cores to determine room temperature parameters and their temperature coefficients.

In an attempt to estimate the accuracy of these results, the method was also applied to the Brookhaven uranium dioxide cores and the results then compared with those predicted by multigroup transport methods. The remarkably good comparison between these two sets of calculations in conjunction with a parametric study which yielded a relatively low sensitivity of the calculated parameters to changes in the input data has led to the assignment of rather small uncertainties in the results calculated with the simplified cell theory.

Although the estimated uncertainties tend to instill confidence in the calculational results, one must insure that these events are not just fortuitous and that the simplified cell theory is in fact predicting behaviors which closely approximate the physical processes taking place.

In this regard, there are three areas in which further work is necessary in the simplified cell theory as presently formulated. The first of these concerns the validity of the assumptions made in the calculations of the moderator escape probabilities, or alternatively, in the calculation of gradient of the moderator flux at the fuel element surface. In these calculations it was assumed that the shape of the flux in the moderator was given by monoenergetic diffusion theory applied at each energy point. Although multigroup transport calculations have given some

support to this assumption, its accuracy can certainly be questioned particularly in the tighter cores where fuel element spacing becomes comparable with a mean free path. Thus there is a need to accurately determine the flux gradient, or more precisely, the net current as a function of energy at the fuel element moderator interface. Any study such as this should include the effects of a non uniform spatial source of slowing down neutrons. The use of multigroup transport theory specifically oriented toward this problem is suggested for this future study.

The second area of concern involves the calculation of the fuel rod escape probability. In the expression utilized in these calculations an isotropic flux was assumed incident upon the fuel rod. This in turn leads to escape probabilities which are too large; the flux in an actual lattice is more peaked toward the rod. The use of smaller escape probabilities for the fuel rod would lead to larger values of f and η_f , along with larger values for the calculated disadvantage factors. Thus there is need for at least a parametric study utilizing all of the analytic approximations for the fuel rod escape probability presented. One could then turn his attention to variations caused with changes in angular distribution of the neutrons incident on the fuel element.

The final area where further study is needed concerns the calculation of temperature coefficients. The immediate need is to compare temperature coefficients calculated with integral transport theory with those predicted by the simplified cell theory as was done with the room temperature case. However, if both calculations utilize the same scattering model, it is believed the comparison of the temperature coefficient computations will be comparable with those for room temperature, since the simplified cell theory has demonstrated its ability to handle spectral hardening in five different cores at 20°C. The accuracy of the temperature coefficient results thus reduces to a question of how well the scattering model predicts spectral hardening as a function of temperature. This question is perhaps best answered by the comparison of pure moderator spectra predicted by the model at various temperatures with those measured experimentally.

APPENDIX A
LATTICE PARAMETERS FOR THE CORNELL UNIVERSITY ZERO POWER
REACTOR

This section details the input parameters which were utilized by program COUTH in the calculations described in Chap. 7 for the Cornell University Zero Power Reactor cores. Appendix D deals with the Fortran FORMATS used in COUTH for reading data into the program.

Table A.1 lists the fuel element parameters for the Cornell ZPR while Table A.2 gives the dimensional parameters of the five hexagonal lattices of the ZPR. Material concentrations and cross sections are given in Table A.3. The absorption cross sections, σ_a , listed are evaluated at $E_0 = .0253$ eV while the scattering cross sections given are the free atom values, σ_f . The number of neutrons produced per thermal fission for U^{235} , v , is 2.43 while the value of the U^{235} fission cross section at E_0 is 580.9 barns.^{81/} Appendix B gives a complete listing as a function of energy for the scattering and transport cross sections of water, the absorption, fission, and scattering cross sections of U^{235} , and the scattering cross sections of U^{238} and oxygen.

^{81/} H. C. Honeck, "The Calculation of Thermal Utilization and Disadvantage Factor in Uranium/Water Lattices," Nucl. Sci. Eng. 18, 66 (1964).

TABLE A.1

CORNELL UNIVERSITY ZERO POWER REACTOR FUEL ELEMENT
PARAMETERS ^{a/}

Fuel Material	Uranium Dioxide
Fuel Rod Diameter, in:	0.600±0.003
Fuel Density, gm/cc:	10.381±0.52%
Fuel Enrichment, Weight Percent U ²³⁵ :	2.070±0.10
Fuel Enrichment, Atom Percent U ²³⁵ :	2.096±0.90
Oxygen to Uranium Number Ratio:	2.01:1
Fuel Molecular Weight:	270.26(physical)
Cladding Material:	6061-76 aluminum
Cladding Density, gm/cc:	2.70
Cladding Inner Diameter, in:	0.610±0.002
Cladding Thickness, in:	0.028±0.003
Fuel Element Diameter, in:	0.666±.006

^{a/} S. S. Berg, "Initial Experiments on the Cornell University Zero Power Reactor Cores," Cornell University Thesis (1964).

TABLE A.2

CORNELL UNIVERSITY ZERO POWER REACTOR LATTICE PARAMETERS

	1:1	1.5:1	Nominal Water/Oxide Volume Ratio	3:1	4:1
Lattice Pitch, in. ^{a/}	0.8560	0.9470	1.0300	1.1770	1.3090
Equivalent Cell Radius, cm.	1.1416	1.2629	1.3736	1.5696	1.7457
Fuel Element Radius, cm.	0.8458	0.8458	0.8458	0.8458	0.8458
Fuel Rod Radius, cm.	0.7620	0.7620	0.7620	0.7620	0.7620
Water Area, cm ² .	1.8465	2.7632	3.6800	5.4927	7.3261
Cladding Area, cm ² .	0.3621	0.3621	0.3621	0.3621	0.3621
Fuel Rod Area, cm ² .	1.8242	1.8242	1.8242	1.8242	1.8242
Actual Water/Oxide Volume Ratio.	1.0122:1	1.5148:1	2.0174:1	3.0111:1	4.0162:1

^{a/} D. D. Clark, "The Cornell University Nuclear Reactor Laboratory," CURL-1, Cornell University (1961).

TABLE A.3

CORNELL UNIVERSITY ZERO POWER REACTOR MATERIAL CONCENTRATIONS AND CROSS SECTIONS

Material	Concentration (atoms/barn-cm)	$\sigma_a(E_0)^{a/}$ (barns)	$\sigma_f^{a/}$ (barns)
U^{235}	4.8498×10^{-4}	679.0	10.0
U^{238}	2.2654×10^{-2}	2.71	8.3
Oxygen in UO_2	4.6510×10^{-2}	0.0	3.76
Aluminum	6.0205×10^{-2}	0.230	1.40
Hydrogen in H_2O		0.328	20.4
20°C	6.6746×10^{-2}		
40°C	6.6346×10^{-2}		
Oxygen in H_2O		0.0	3.76
20°C	3.3373×10^{-2}		
40°C	3.3173×10^{-2}		

^{a/} H. C. Honeck, "The Calculation of the Thermal Utilization and Disadvantage Factor in Uranium/Water Lattices," Nucl. Sci. Eng. 18, 66 (1964).

APPENDIX B

NUMERICAL RESULTS FOR THE CORNELL UNIVERSITY ZERO POWER REACTOR

Chapter 7 discussed some of the results of the calculations made on the Cornell University Zero Power Reactor using the simplified cell theory as incorporated in COUTH. This section presents all of the results in a tabular form derived from the calculations utilizing the Nelkin water model for the scattering kernel.

Table B.1 lists the energy, velocity and lethargy mesh used in the calculations by COUTH. The derivation of this mesh is discussed in Sec. 7.1, and all of the calculations are carried out using the lethargy mesh.

Table B.2 gives the scattering kernel in matrix form as derived from the Nelkin water model, Eq. (5.15), for a physical moderator temperature of 20°C. The scattering matrix is expressed in barns/unit lethargy and it is related to the scattering matrix in barns/eV by,

$$\sigma(u_j \rightarrow u_i) = E_i \sigma(E_j \rightarrow E_i) . \quad (B.1)$$

The subscripted indices i and j correspond to the lethargy and energy points listed in Table B.1. The diagonal terms of the scattering matrix listed in Table B.2 are those calculated with Eq. (5.22) and they are not modified in accordance with Eq. (5.26).

TABLE B.1

ENERGY, VELOCITY, AND LETHARGY MESH UTILIZED BY COUTH

I	ENERGY	DELTA E	VELOCITY	DELTA V	LETHARGY	DELTA U
1	1.609E 000	3.782E-001	17547.0	2200.0	.0000	.2679
2	1.231E 000	2.644E-001	15347.0	1747.5	.2679	.2418
3	9.647E-001	1.873E-001	13599.5	1388.1	.5097	.2153
4	7.794E-001	1.344E-001	12211.4	1102.6	.7250	.1893
5	6.450E-001	9.770E-002	11108.7	875.8	.9143	.1642
6	5.473E-001	7.189E-002	10232.9	695.7	1.0785	.1408
7	4.754E-001	5.350E-002	9537.2	552.6	1.2194	.1194
8	4.219E-001	4.022E-002	8984.6	439.0	1.3387	.1002
9	3.817E-001	3.051E-002	8545.6	348.7	1.4389	.0833
10	3.512E-001	2.333E-002	8197.0	277.0	1.5222	.0687
11	3.279E-001	1.796E-002	7920.0	220.0	1.5910	.0563
12	3.099E-001	1.746E-002	7700.0	220.0	1.6473	.0580
13	2.924E-001	1.695E-002	7480.0	220.0	1.7053	.0597
14	2.755E-001	1.644E-002	7260.0	220.0	1.7650	.0615
15	2.590E-001	1.594E-002	7040.0	220.0	1.8245	.0635
16	2.431E-001	1.543E-002	6820.0	220.0	1.8900	.0656
17	2.277E-001	1.493E-002	6600.0	220.0	1.9556	.0678
18	2.128E-001	1.442E-002	6380.0	220.0	2.0234	.0702
19	1.983E-001	1.391E-002	6160.0	220.0	2.0936	.0727
20	1.844E-001	1.341E-002	5940.0	220.0	2.1643	.0755
21	1.710E-001	1.290E-002	5720.0	220.0	2.2418	.0784
22	1.581E-001	1.240E-002	5500.0	220.0	2.3203	.0816
23	1.457E-001	1.189E-002	5280.0	220.0	2.4019	.0851
24	1.338E-001	1.138E-002	5060.0	220.0	2.4870	.0889
25	1.224E-001	1.088E-002	4840.0	220.0	2.5759	.0930
26	1.116E-001	1.037E-002	4620.0	220.0	2.6690	.0976
27	1.012E-001	9.866E-003	4400.0	220.0	2.7666	.1026
28	9.132E-002	9.360E-003	4180.0	220.0	2.8691	.1081
29	8.106E-002	8.854E-003	3960.0	220.0	2.9773	.1143
30	7.311E-002	8.348E-003	3740.0	220.0	3.0916	.1212
31	6.476E-002	7.842E-003	3520.0	220.0	3.2128	.1291
32	5.602E-002	7.336E-003	3300.0	220.0	3.3419	.1380
33	4.958E-002	6.830E-003	3080.0	220.0	3.4799	.1482
34	4.275E-002	6.324E-003	2860.0	220.0	3.6281	.1601
35	3.643E-002	5.818E-003	2640.0	220.0	3.7882	.1740
36	3.061E-002	5.313E-003	2420.0	220.0	3.9622	.1906
37	2.530E-002	4.807E-003	2200.0	220.0	4.1529	.2107
38	2.049E-002	4.301E-003	1980.0	220.0	4.3636	.2356
39	1.619E-002	3.795E-003	1760.0	220.0	4.5991	.2671
40	1.240E-002	3.289E-003	1540.0	220.0	4.8662	.3083
41	9.107E-003	2.783E-003	1320.0	220.0	5.1745	.3646
42	6.324E-003	2.277E-003	1100.0	220.0	5.5391	.4463
43	4.048E-003	1.771E-003	880.0	220.0	5.9854	.5754
44	2.277E-003	1.265E-003	660.0	220.0	6.5608	.8109
45	1.012E-003	.0000E 000	440.0	.0	7.3717	.0000

Table B.2 (continued)

	J = 41	42	43	44	45
1	3.845E-23	4.197E-23	4.834E-23	6.060E-23	8.697E-23
2	3.601E-17	1.921E-17	4.527E-17	5.675E-17	.144E-17
3	5.047E-13	F.490E-13	6.333E-13	7.933E-13	1.138E-12
4	4.014E-11	4.355E-11	5.014E-10	6.269E-10	8.943E-10
5	4.531E-08	4.903E-08	5.630E-08	7.027E-08	1.005E-07
6	1.374E-04	1.496E-04	1.702E-04	2.121E-04	3.030E-06
7	1.710E-05	1.841E-05	2.105E-05	2.617E-05	3.734E-05
8	1.125E-04	1.209E-04	1.379E-04	1.713E-04	2.441E-04
9	4.650E-04	4.987E-04	5.683E-04	7.047E-04	1.003E-03
10	1.362E-03	1.460E-03	1.661E-03	2.029E-03	2.929E-03
11	3.032E-01	1.260E-03	3.723E-01	4.624E-03	6.591E-03
12	5.627E-03	4.027E-03	6.866E-03	8.518E-03	1.214E-02
13	1.057E-02	1.127E-02	1.277E-02	1.578E-02	2.241E-02
14	2.066E-02	2.099E-02	2.350E-02	2.909E-02	4.135E-02
15	3.260E-02	3.521E-02	4.034E-02	5.022E-02	7.169E-02
16	5.413E-02	F.787E-02	6.591E-02	8.181E-02	1.166E-01
17	9.518E-02	1.013E-01	1.126E-01	1.382E-01	1.954E-01
18	1.671E-01	1.774E-01	1.999E-01	2.453E-01	3.463E-01
19	2.610E-01	2.875E-01	3.255E-01	4.015E-01	6.776E-01
20	3.639E-01	3.966E-01	4.590E-01	5.767E-01	8.290E-01
21	5.350E-01	F.611E-01	6.321E-01	7.795E-01	1.108E-00
22	9.431E-01	G.584E-01	1.043E-00	1.248E-00	1.732E-00
23	1.672E-00	1.734E-00	1.914E-00	2.300E-00	3.194E-00
24	2.440E-00	2.676E-00	3.069E-00	3.802E-00	5.392E-00
25	2.825E-00	3.207E-00	3.821E-00	4.893E-00	7.115E-00
26	3.061E-00	3.325E-00	3.902E-00	4.998E-00	7.314E-00
27	4.535E-00	4.368E-00	4.614E-00	4.646E-00	5.582E-00
28	8.770E-00	9.255E-00	8.340E-00	9.345E-00	1.233E-01
29	1.582E-01	1.571E-01	1.649E-01	1.895E-01	2.537E-01
30	2.225E-01	2.413E-01	2.693E-01	3.251E-01	4.507E-01
31	2.212E-01	2.672E-01	3.262E-01	4.194E-01	6.075E-01
32	1.511E-01	2.030E-01	2.737E-01	3.807E-01	5.826E-01
33	8.473E-01	1.096E-01	1.546E-01	2.300E-01	3.728E-01
34	6.705E-01	A.096E-01	6.929E-01	9.506E-01	1.530E-01
35	9.994E-01	4.832E-01	5.158E-01	4.643E-01	5.441E-01
36	1.817E-01	1.295E-01	1.545E-01	6.432E-01	5.738E-01
37	3.146E-01	2.221E-01	1.618E-01	1.266E-01	1.164E-01
38	4.957E-01	A.672E-01	2.816E-01	2.324E-01	2.253E-01
39	7.055E-01	F.4A3E-01	4.397E-01	3.816E-01	3.887E-01
40	9.010E-01	7.271E-01	6.117E-01	5.561E-01	5.928E-01
41	1.028E-02	9.585E-01	7.515E-01	7.125E-01	7.910E-01
42	4.590E-01	A.875E-01	A.042E-01	7.910E-01	8.101E-01
43	1.791E-01	1.584E-01	7.317E-01	7.425E-01	8.802E-01
44	5.734E-01	1.191E-01	2.509E-01	5.622E-01	6.827E-01
45	1.318E-01	2.837E-01	6.156E-01	1.413E-01	3.815E-01

Table B.3 gives the Nelkin water kernel scattering matrix for a moderator physical temperature of 40°C. Its format is the same as that described for Table B.2.

Table B.4 lists as a function of energy the scattering cross section, Eq. (2.2), and the transport cross section, Eq. (5.25), for water. The energy dependent scattering cross sections for U²³⁵, U²³⁸, and oxygen are also listed in Table B.4 as calculated using Eq. (5.13) with the parameters listed in Table A.3.

Table B.5 gives as a function of energy the absorption and fission cross sections^{82/} for U²³⁵, as well as the uranium dioxide fuel fission and absorption cross sections. One plus the capture to fission ratio, [1+ $\alpha(E)$], for the fuel is also listed in Table B.5, along with the normalized slowing down source of neutrons, $\bar{S}(E)$, Eq. (7.1), used in the calculations.

Table B.6 through B.10 list the energy dependent thermal spectra calculated by COUTH for a moderator physical temperature of 20°C. The moderator, Eq. (6.1), fuel, Eq. (6.3), and cladding, Eq. (6.4), spectra are given for the five Cornell ZPR cores.

Table B.11 gives the integral properties defined in Chap. 6 for the five ZPR cores at a temperature of 20°C,

^{82/} J. Suich, "Temperature Coefficients in Heterogeneous Reactor Lattices," Massachusetts Institute of Technology Thesis (1963).

Table B.3 (continued)

SCATTERING KERNEL, SIGMA(U(j) TO U(1))/JNIT LETHARGY, KT = .02699, J = 21 TO 30									
	J = 21	22	23	24	25	26	27	28	29
1	2.529E-21	1.673E-21	1.128E-21	7.767E-22	5.453E-22	3.907E-22	2.856E-22	2.131E-22	1.623E-22
2	2.373E-15	1.570E-15	1.059E-15	7.290E-16	5.119E-16	3.668E-16	2.681E-16	2.000E-16	1.523E-16
3	3.402E-11	2.251E-11	1.519E-11	1.045E-11	7.335E-12	5.252E-12	3.836E-12	2.859E-12	2.175E-12
4	2.774E-08	1.841E-08	1.245E-08	8.580E-09	6.029E-09	4.319E-09	3.155E-09	2.350E-09	1.385E-09
5	3.192E-06	2.119E-06	9.904E-07	9.904E-07	9.904E-07	5.001E-07	3.657E-07	2.727E-07	1.607E-07
6	1.044E-04	4.867E-05	4.613E-05	3.163E-05	2.214E-05	1.581E-05	1.152E-05	8.564E-06	6.494E-06
7	1.387E-03	9.106E-04	6.098E-04	4.166E-04	2.904E-04	2.065E-04	1.499E-04	1.109E-04	8.379E-05
8	9.365E-03	4.158E-03	4.130E-03	2.824E-03	1.970E-03	1.401E-03	1.016E-03	7.512E-04	5.666E-04
9	3.889E-02	2.557E-02	1.716E-02	1.716E-02	1.716E-02	1.545E-03	1.411E-03	3.144E-03	1.825E-03
10	1.146E-01	7.502E-02	5.025E-02	3.440E-02	2.403E-02	1.713E-02	1.245E-02	9.223E-03	5.367E-03
11	2.459E-01	1.592E-01	1.126E-01	8.118E-02	5.734E-02	3.969E-02	2.782E-02	2.032E-02	1.550E-02
12	5.255E-01	3.113E-01	1.985E-01	1.399E-01	1.035E-01	7.630E-02	5.515E-02	3.957E-02	2.898E-02
13	9.898E-01	4.510E-01	3.980E-01	2.519E-01	1.750E-01	1.307E-01	9.979E-02	7.546E-02	5.626E-02
14	1.527E-01	1.129E-01	7.962E-01	5.103E-01	3.253E-01	2.221E-01	1.650E-01	1.286E-01	9.400E-02
15	2.963E-01	1.737E-01	1.274E-01	9.563E-01	6.513E-01	4.257E-01	2.881E-01	2.104E-01	1.645E-01
16	6.938E-01	1.525E-01	2.011E-01	1.435E-01	1.124E-01	8.204E-01	5.598E-01	3.818E-01	2.742E-01
17	1.170E-01	7.981E-01	4.221E-01	2.372E-01	1.628E-01	1.296E-01	1.011E-01	7.320E-01	5.674E-01
18	1.253E-01	1.196E-01	9.095E-01	5.074E-01	2.848E-01	1.877E-01	1.476E-01	1.213E-01	9.403E-01
19	2.088E-01	1.295E-01	1.213E-01	1.022E-01	6.101E-01	3.473E-01	2.213E-01	1.682E-01	1.173E-01
20	5.642E-01	2.213E-01	1.324E-01	1.223E-01	1.125E-01	7.310E-01	4.285E-01	2.678E-01	1.945E-01
21	1.791E-02	5.875E-01	2.350E-01	1.372E-01	1.231E-01	1.209E-01	8.684E-01	5.324E-01	2.312E-01
22	1.100E-01	1.787E-02	6.118E-01	2.502E-01	1.429E-01	1.238E-01	1.016E-01	6.627E-01	4.201E-01
23	4.357E-01	9.225E-01	1.781E-02	6.370E-01	2.668E-01	1.497E-01	1.246E-01	1.295E-01	8.207E-01
24	3.337E-01	4.408E-01	8.347E-01	1.775E-02	6.632E-01	2.849E-01	1.577E-01	1.257E-01	1.301E-01
25	3.816E-01	3.214E-01	4.462E-01	8.465E-01	1.767E-02	6.902E-01	3.047E-01	1.670E-01	1.290E-01
26	4.656E-01	3.458E-01	3.117E-01	8.574E-01	1.574E-01	1.574E-01	1.574E-01	1.777E-01	1.296E-01
27	4.042E-01	4.272E-01	3.128E-01	3.022E-01	4.574E-01	8.674E-01	1.749E-01	3.462E-01	3.494E-01
28	2.909E-01	4.027E-01	3.816E-01	2.828E-01	2.943E-01	4.627E-01	8.760E-01	1.736E-01	3.744E-01
29	2.067E-01	2.992E-01	3.898E-01	3.334E-01	2.556E-01	2.873E-01	4.674E-01	8.829E-01	1.722E-02
30	1.591E-01	2.095E-01	3.495E-01	3.631E-01	2.632E-01	2.313E-01	2.808E-01	4.712E-01	8.876E-01
31	1.368E-01	1.518E-01	2.140E-01	3.034E-01	3.232E-01	2.421E-01	2.421E-01	4.738E-01	8.896E-01
32	1.248E-01	1.200E-01	1.488E-01	2.179E-01	2.920E-01	2.746E-01	2.022E-01	1.900E-01	4.747E-01
33	1.109E-01	1.033E-01	1.085E-01	1.487E-01	2.186E-01	2.672E-01	2.232E-01	1.670E-01	2.625E-01
34	9.205E-01	9.095E-01	8.544E-01	1.019E-01	1.498E-01	2.125E-01	2.293E-01	1.744E-01	1.366E-01
35	7.132E-01	7.078E-01	7.126E-01	9.290E-01	9.916E-01	1.567E-01	1.487E-01	2.044E-01	5.643E-01
36	5.221E-01	4.130E-01	5.268E-01	5.524E-01	6.560E-01	9.816E-01	1.438E-01	1.667E-01	1.314E-01
37	3.656E-01	4.565E-01	4.800E-01	4.342E-01	4.450E-01	6.215E-01	9.616E-01	1.297E-01	9.264E-01
38	2.470E-01	2.201E-01	3.631E-01	3.395E-01	3.124E-01	3.867E-01	6.025E-01	8.979E-01	8.853E-01
39	2.122E-01	2.057E-01	2.568E-01	2.543E-01	2.322E-01	2.398E-01	3.588E-01	5.694E-01	7.566E-01
40	1.619E-01	1.329E-01	1.691E-01	1.784E-01	1.916E-01	2.157E-01	2.044E-01	3.353E-01	4.945E-01
41	6.128E-01	7.821E-01	1.031E-01	1.153E-01	1.042E-01	9.085E-01	1.114E-01	1.835E-01	2.906E-01
42	3.434E-01	4.249E-01	5.730E-01	6.734E-01	6.323E-01	5.276E-01	5.737E-01	9.235E-01	1.542E-01
43	1.722E-01	2.061E-01	2.813E-01	3.441E-01	3.757E-01	2.701E-01	4.157E-01	1.215E-01	1.067E-01
44	7.172E-02	8.329E-02	1.142E-01	1.440E-01	1.194E-01	1.453E-01	1.080E-01	2.801E-01	4.350E-01
45	2.111E-02	2.394E-02	3.283E-02	4.229E-02	3.618E-02	4.372E-02	3.104E-02	7.763E-02	1.249E-01

Table B.3 (continued)

SCATTERING KERNEL, SIGMA(U(J) TO U(I))/JUNIT LETHARGY, KT = .02699, J = 31 TO 40									
	J = 31	32	33	34	35	36	37	38	39
I	1.002E-22	8.137E-23	6.752E-23	5.732E-23	4.982E-23	4.438E-23	4.057E-23	3.812E-23	3.696E-23
1	9.40E-17	7.632E-17	6.332E-17	5.374E-17	4.669E-17	4.158E-17	3.801E-17	3.571E-17	3.458E-17
2	1.339E-12	1.045E-12	A.985E-13	7.612E-13	6.603E-13	5.871E-13	5.357E-13	5.025E-13	4.858E-13
3	1.094E-09	A.861E-10	7.245E-10	6.154E-10	5.350E-10	4.312E-10	4.032E-10	3.874E-10	3.686E-10
4	1.274E-07	1.026E-08	9.463E-08	7.135E-08	6.154E-08	5.438E-08	4.931E-08	4.595E-08	4.414E-08
5	3.96E-06	3.194E-06	2.629E-06	2.211E-06	1.902E-06	1.676E-06	1.515E-06	1.408E-06	1.336E-06
6	5.079E-05	4.078E-05	3.345E-05	2.804E-05	2.405E-05	2.113E-05	1.904E-05	1.764E-05	1.664E-05
7	2.423E-04	2.743E-04	2.245E-04	1.788E-04	1.607E-04	1.408E-04	1.266E-04	1.170E-04	1.098E-04
8	1.432E-03	1.149E-03	9.387E-04	7.845E-04	6.705E-04	5.869E-04	5.268E-04	4.860E-04	4.545E-04
9	4.216E-03	3.379E-03	2.765E-03	2.311E-03	1.974E-03	1.727E-03	1.549E-03	1.428E-03	1.353E-03
10	9.71AE-03	7.808E-03	6.336E-03	5.226E-03	4.410E-03	3.823E-03	3.415E-03	3.147E-03	2.996E-03
11	1.750E-02	1.427E-02	1.185E-02	9.971E-03	A.502E-03	7.378E-03	5.981E-03	5.640E-03	5.317E-03
12	3.219E-02	2.542E-02	2.090E-02	1.771E-02	1.536E-02	1.359E-02	1.223E-02	1.126E-02	1.041E-02
13	6.100E-02	4.750E-02	3.782E-02	3.113E-02	2.655E-02	2.341E-02	2.122E-02	1.983E-02	1.879E-02
14	1.080E-01	8.715E-02	7.051E-02	5.743E-02	4.777E-02	4.095E-02	3.635E-02	3.346E-02	3.193E-02
15	1.724E-01	1.444E-01	1.219E-01	1.029E-01	8.721E-02	7.475E-02	6.539E-02	5.888E-02	5.491E-02
16	2.786E-01	2.242E-01	1.898E-01	1.651E-01	1.455E-01	1.293E-01	1.058E-01	9.867E-01	9.499E-02
17	5.042E-01	3.781E-01	2.969E-01	2.502E-01	2.195E-01	1.990E-01	1.843E-01	1.737E-01	1.669E-01
18	9.200E-01	6.990E-01	5.316E-01	4.163E-01	3.417E-01	2.958E-01	2.687E-01	2.541E-01	2.484E-01
19	1.411E-01	1.197E-01	9.587E-01	7.598E-01	6.054E-01	4.951E-01	4.217E-01	3.773E-01	3.509E-01
20	2.846E-01	2.179E-01	1.883E-01	1.731E-01	1.599E-01	1.452E-01	1.300E-01	1.163E-01	9.775E-01
21	5.395E-01	3.631E-01	2.659E-01	2.187E-01	1.987E-01	1.900E-01	1.838E-01	1.773E-01	1.672E-01
22	1.092E-01	4.970E-01	4.777E-01	3.419E-01	2.664E-01	2.305E-01	2.179E-01	2.172E-01	2.223E-01
23	2.321E-01	1.1322E-01	A.963E-01	6.414E-01	4.625E-01	3.493E-01	2.850E-01	2.592E-01	2.190E-01
24	1.267E-01	1.393E-01	1.363E-01	1.130E-01	A.655E-01	6.494E-01	4.944E-01	3.924E-01	3.055E-01
25	1.326E-01	1.219E-01	1.374E-01	1.473E-01	1.150E-01	1.50E-01	1.243E-01	7.387E-01	5.074E-01
26	1.321E-01	1.347E-01	1.206E-01	1.316E-01	1.503E-01	1.564E-01	1.464E-01	1.292E-01	1.119E-01
27	2.042E-01	2.203E-01	1.719E-01	1.422E-01	1.174E-01	1.230E-01	1.445E-01	1.654E-01	1.711E-01
28	4.101E-01	4.321E-01	2.387E-01	1.194E-01	1.149E-01	1.124E-01	1.316E-01	1.604E-01	1.642E-01
29	3.441E-01	4.616E-01	2.393E-01	4.602E-01	2.598E-01	1.593E-01	1.140E-01	1.023E-01	2.070E-01
30	1.834E-02	A.599E-01	4.602E-01	2.598E-01	1.593E-01	1.140E-01	1.140E-01	1.138E-01	1.179E-01
31	6.738E-01	1.659E-01	A.863E-01	4.921E-01	2.837E-01	1.723E-01	1.158E-01	1.430E-01	1.420E-01
32	8.892E-01	4.662E-01	6.115E-01	1.629E-01	9.105E-01	5.252E-01	3.109E-01	1.894E-01	1.218E-01
33	4.734E-01	8.926E-01	3.235E-01	8.719E-01	1.316E-01	1.564E-01	1.464E-01	1.292E-01	1.033E-01
34	2.550E-01	A.314E-01	9.530E-02	9.314E-02	9.590E-01	3.414E-01	1.654E-01	1.737E-01	1.113E-01
35	1.441E-01	2.483E-01	4.616E-01	8.548E-01	1.549E-02	9.477E-01	1.316E-01	3.752E-01	2.389E-01
36	9.427E-01	1.321E-01	2.393E-01	4.494E-01	1.301E-01	1.495E-02	9.577E-01	6.250E-01	4.120E-01
37	6.738E-01	7.393E-01	1.212E-01	2.292E-01	4.317E-01	7.964E-01	1.430E-01	9.597E-01	6.551E-01
38	5.874E-01	4.662E-01	6.115E-01	1.108E-01	2.143E-01	4.075E-01	7.524E-01	1.218E-01	6.820E-01
39	5.367E-01	3.454E-01	5.133E-01	9.990E-01	9.990E-01	1.967E-01	3.760E-01	1.970E-01	9.330E-01
40	4.594E-01	2.327E-01	1.916E-01	2.313E-01	4.320E-01	8.789E-01	1.750E-01	3.369E-01	6.295E-01
41	3.441E-01	2.275E-01	1.281E-01	1.058E-01	1.719E-01	3.567E-01	7.428E-01	1.493E-01	5.499E-01
42	2.221E-01	1.027E-01	8.858E-01	5.145E-01	6.282E-01	1.286E-01	2.030E-01	5.913E-01	2.370E-01
43	1.211E-01	G.919E-01	2.606E-01	2.114E-01	9.103E-01	9.103E-01	2.021E-01	4.310E-01	8.887E-01
44	5.251E-01	4.614E-01	2.798E-01	1.208E-01	6.430E-01	1.017E-01	2.406E-01	5.634E-01	1.264E-01
45	1.574E-01	1.4462E-01	9.392E-02	4.024E-02	1.560E-02	1.879E-02	2.665E-02	1.131E-01	6.023F-01

Table B.3 (continued)

SCATTERING KERNEL, SIGMA(U(J) TO U(I))/JNIT LETHARGY, KT = .0253, J = 41 TO 45						
	J = 41	42	43	44	45	
1	6.745F-025	7.294F-025	8.372F-025	1.045F-024	1.495E-024	
2	1.644F-018	1.778F-018	2.041F-018	2.546E-018	3.643E-018	
3	4.497F-014	4.857F-014	5.571E-014	6.948F-014	9.936E-014	
4	5.728E-014	6.171E-014	7.064E-014	8.794E-014	1.256E-010	
5	9.050F-009	9.721F-009	1.110F-008	1.373F-008	1.966E-008	
6	3.511F-007	3.764F-007	4.285E-007	5.314E-007	7.565E-007	
7	5.232F-006	5.591F-006	6.354E-006	7.863E-006	1.118E-005	
8	3.946F-005	4.205E-005	4.770E-005	5.894E-005	8.369E-005	
9	1.807F-004	1.922F-004	2.176E-004	2.685E-004	3.810F-004	
10	5.716E-004	6.078E-004	6.872E-004	8.471E-004	1.201E-003	
11	1.353F-003	1.446F-003	1.642F-003	2.031F-003	2.886E-003	
12	2.618F-003	2.783F-003	3.152F-003	3.892E-003	5.529F-003	
13	5.170F-003	5.462F-003	6.149F-003	7.553F-003	1.068E-002	
14	9.870F-003	1.051F-002	1.188F-002	1.464E-002	2.073E-002	
15	1.726F-002	1.834F-002	2.116F-002	2.624E-002	3.737E-002	
16	2.959E-002	3.139E-002	3.555E-002	4.394E-002	6.245E-002	
17	5.455F-002	5.686F-002	6.331E-002	7.716E-002	1.085E-001	
18	1.006E-001	1.059E-001	1.184E-001	1.444E-001	2.028E-001	
19	1.623F-001	1.754F-001	2.006F-001	2.487E-001	3.536E-001	
20	2.291E-001	2.489F-001	2.875E-001	3.606E-001	5.179E-001	
21	3.451F-001	3.578F-001	3.996E-001	4.904E-001	6.950E-001	
22	6.411E-004	6.414E-004	6.489E-004	6.154E-004	1.123E-000	
23	1.201F-000	1.234F-000	1.345F-000	1.602E-000	2.209E-000	
24	1.818F-000	1.976F-000	2.254E-000	2.779E-000	3.926E-000	
25	2.104F-000	2.392E-000	2.852E-000	3.653E-000	5.306E-000	
26	2.288F-000	2.445F-000	2.872E-000	3.686E-000	5.406E-000	
27	3.458F-000	3.261F-000	3.391E-000	3.970E-000	5.482E-000	
28	7.108F-000	6.556E-000	6.497E-000	7.157E-000	9.324E-000	
29	1.347F-001	1.318F-001	1.365E-001	1.551F-001	2.056E-001	
30	1.953F-001	2.093F-001	2.326E-001	2.787E-001	3.841E-001	
31	1.956F-001	2.365F-001	2.880E-001	3.693E-001	5.334E-001	
32	1.310F-001	1.777F-001	2.411E-001	3.364E-001	5.153E-001	
33	7.047F-000	9.227F-000	1.319F-001	1.981F-001	3.233E-001	
34	5.499F-000	4.893E-000	5.560E-000	7.208E-000	1.253E-001	
35	8.594F-000	5.611F-000	4.049E-000	3.516E-000	4.038E-000	
36	1.639F-001	1.052F-001	7.091E-001	5.084E-000	4.307E-000	
37	2.949F-001	2.012F-001	1.411E-001	1.05AF-001	9.309E-001	
38	4.797F-001	3.451F-001	2.560F-001	2.036E-001	1.899E-001	
39	7.015F-001	5.300E-001	4.144E-001	3.481E-001	3.428E-001	
40	9.173F-001	7.238F-001	5.942E-001	5.255E-001	5.442E-001	
41	1.065F-002	8.735F-001	7.488E-001	6.938F-001	7.520E-001	
42	4.703F-001	9.187F-001	8.183F-001	7.895F-001	8.904F-001	
43	1.807F-001	3.648F-001	2.571F-001	2.661E-001	8.818E-001	
44	5.682F-000	1.201F-001	2.566F-001	5.815F-001	6.968F-001	
45	1.279F-000	2.813F-000	6.215F-000	1.447E-001	3.944E-001	

TABLE B.4
ENERGY DEPENDENT CROSS SECTIONS

I	ENERGY	H2O SCATTERING CROSS SECTION (BARNs)	H2O TRANSPORT CROSS SECTION (BARNs)	U235 SCATTER CROSS SECTION (BARNs)	U238 SCATTER CROSS SECTION (BARNs)	016 SCATTER CROSS SECTION (BARNs)
1	1.6n93E-001	4.4500F-001	1.8595E-001	1.0000E-001	8.3003E-001	3.7619E-000
2	1.2311E-001	4.4500F-001	1.9453E-001	1.0000E-001	8.3004E-001	3.7624E-000
3	9.6667E-001	4.4599F-001	2.0356E-001	1.0001E-001	8.3005E-001	3.7631E-000
4	7.7941E-001	4.4701F-001	2.1218E-001	1.0001E-001	8.3006E-001	3.7638E-000
5	6.4501E-001	4.5000F-001	2.2092E-001	1.0001E-001	8.3007E-001	3.7646E-000
6	5.4731E-001	4.6000F-001	2.3281E-001	1.0001F-001	8.3008E-001	3.7655E-000
7	4.7542E-001	4.7500F-001	2.4711E-001	1.0001E-001	8.3009E-001	3.7663E-000
8	4.2192E-001	4.9000F-001	2.6133E-001	1.0001E-001	8.3011F-001	3.7671E-000
9	3.8170E-001	5.0500F-001	2.7239E-001	1.0001E-001	8.3012E-001	3.7678E-000
10	3.5119E-001	5.1400F-001	2.8144E-001	1.0002E-001	8.3013E-001	3.7685E-000
11	3.2786E-001	5.2400F-001	2.9057E-001	1.0002E-001	8.3014E-001	3.7691E-000
12	3.0090E-001	5.3011F-001	2.9658E-001	1.0002E-001	8.3014E-001	3.7697E-000
13	2.9244E-001	5.3800F-001	3.0377E-001	1.0002F-001	8.3015E-001	3.7702E-000
14	2.7549E-001	5.4049F-001	3.1048E-001	1.0002F-001	8.3016E-001	3.7709E-000
15	2.5005E-001	5.5400F-001	3.1785E-001	1.0002F-001	8.3017E-001	3.7716E-000
16	2.4311E-001	5.6200F-001	3.2585E-001	1.0002E-001	8.3018E-001	3.7723E-000
17	2.2768E-001	5.7100F-001	3.3454E-001	1.0002F-001	8.3020E-001	3.7732E-000
18	2.1275E-001	5.8001F-001	3.4333E-001	1.0003E-001	8.3021F-001	3.7741E-000
19	1.9333E-001	5.9000F-001	3.5283E-001	1.0003E-001	8.3022E-001	3.7751E-000
20	1.8442E-001	6.0000F-001	3.6246E-001	1.0003E-001	8.3024E-001	3.7762E-000
21	1.7101E-001	6.1000F-001	3.7282E-001	1.0003E-001	8.3026E-001	3.7775E-000
22	1.5811E-001	6.2100F-001	3.8395E-001	1.0003E-001	8.3028E-001	3.7789E-000
23	1.4571E-001	6.3499E-001	3.9773E-001	1.0004E-001	8.3030E-001	3.7806E-000
24	1.3382E-001	6.4500F-001	4.0795E-001	1.0004E-001	8.3033E-001	3.7824E-000
25	1.2244E-001	6.6400F-001	4.2532E-001	1.0004E-001	8.3036E-001	3.7845E-000
26	1.1156E-001	6.7999E-001	4.4176E-001	1.0005E-001	8.3040E-001	3.7868E-000
27	1.0119E-001	6.9500F-001	4.5855E-001	1.0005E-001	8.3044E-001	3.7896E-000
28	9.1325E-002	7.1000F-001	4.7635E-001	1.0006E-001	8.3049E-001	3.7928E-000
29	8.1965E-002	7.3500F-001	5.0055E-001	1.0007E-001	8.3054E-001	3.7956E-000
30	7.3110E-002	7.5499E-001	5.2032E-001	1.0007E-001	8.3061E-001	3.8010E-000
31	6.4762E-002	7.7500F-001	5.4045E-001	1.0008E-001	8.3069E-001	3.8062E-000
32	5.6920E-002	8.0500F-001	5.6793E-001	1.0010E-001	8.3078E-001	3.8126E-000
33	4.9583E-002	8.3500F-001	5.9926E-001	1.0011E-001	8.3090E-001	3.8204E-000
34	4.2753E-002	8.7000F-001	6.4021E-001	1.0013F-001	8.3104E-001	3.8301E-000
35	3.6429E-002	9.2500F-001	7.0206E-001	1.0015E-001	8.3122E-001	3.8422E-000
36	3.0610E-002	9.9000F-001	7.7626E-001	1.0018E-001	8.3145E-001	3.8578E-000
37	2.5298E-002	1.0700F-002	8.6477E-001	1.0021F-001	8.3176E-001	3.8784E-000
38	2.0491E-002	1.1600F-002	9.6555E-001	1.0026E-001	8.3217E-001	3.9062E-000
39	1.6191E-002	1.2500F-002	1.0683F-002	1.0033E-001	8.3274E-001	3.9450E-000
40	1.2396E-002	1.3500F-002	1.1813F-002	1.0044E-001	8.3358E-001	4.0116E-000
41	9.1072E-003	1.4400F-002	1.2684F-002	1.0060E-001	8.3488E-001	4.0888E-000
42	6.3244E-003	1.5600F-002	1.4267E-002	1.0086E-001	8.3702E-001	4.2322E-000
43	4.0476E-003	1.7200F-002	1.6110E-002	1.0134F-001	8.4098E-001	4.4960E-000
44	2.2768E-003	1.9500F-002	1.8825E-002	1.0238F-001	8.4951F-001	5.3910E-000
45	1.0119E-003	2.3700F-002	2.3914E-002	1.0534E-001	8.7390E-001	6.3850E-000

TABLE B.5
ENERGY DEPENDENT CROSS SECTIONS

I	ENERGY	10235 ABSORPTION CROSS SECTION (BARNs)	J235 FISSION CROSS SECTION (BARNs)	FUEL ABSORPTION CROSS SECTION (1/cm)	FUSSION CROSS SECTION (1/cm)	FUEL FISSION CROSS SECTION (1/cm)	1 + ALPHA	SLOWING DOWN SOURCE
1	1.693E-06	1.8E+00E 01	1.290E 01	1.6427E-02	2.6627E-03	2.1438E 00	1.0341E 00	
2	1.231E-06	4.810E 01	4.200E 01	3.2129E-02	2.0369E-02	1.573E 00	7.9101E-01	
3	9.6667E-06	7.170E 01	5.210E 01	4.4705E-02	3.0117E-02	1.4644E 00	6.2110E-01	
4	7.7941E-06	6.230E 01	5.380E 01	4.1275E-02	2.6092E-02	1.5819E 00	5.0067E-01	
5	6.4501E-06	6.980E 01	6.170E 01	4.6011E-02	2.9922E-02	1.5376E 00	4.1408E-01	
6	5.4731E-06	8.150E 01	7.160E 01	5.2725E-02	3.4725E-02	1.5184E 00	3.5090E-01	
7	4.7542E-06	1.010E 02	9.790E 01	6.2702E-02	4.2630E-02	1.4710E 00	3.0415E-01	
8	4.2196E-06	1.2210E 02	1.0570E 02	7.4250E-02	5.1263E-02	1.4464E 00	2.6915E-01	
9	3.8170E-06	1.4670E 02	1.2580E 02	8.6953E-02	6.1011E-02	1.4252E 00	2.4266E-01	
10	3.5119E-06	1.7650E 02	1.4810E 02	1.0208E-01	7.1826E-02	1.4212E 00	2.2245E-01	
11	3.2786E-06	2.0130E 02	1.6620E 02	1.1463E-01	8.0604E-02	1.4286E 00	2.0690E-01	
12	3.0990E-06	2.2430E 02	1.8330E 02	1.2632E-01	8.8888E-02	1.4210E 00	1.9489E-01	
13	2.0244E-06	2.3700E 02	1.8810E 02	1.3300E-01	9.1225E-02	1.4579E 00	1.8316E-01	
14	2.7549E-06	2.3960E 02	1.8840E 02	1.3481E-01	9.1377E-02	1.4544E 00	1.7172E-01	
15	2.5905E-06	2.3916E 02	1.7760E 02	1.3163E-01	8.6135E-02	1.5268E 00	1.6059E-01	
16	2.4311E-06	2.2110E 02	1.6870E 02	1.2655E-01	8.1817E-02	1.5468E 00	1.4975E-01	
17	2.2768E-06	2.1180E 02	1.6690E 02	1.2270E-01	8.0944E-02	1.5159E 00	1.3922E-01	
18	2.1275E-06	2.0780E 02	1.6720E 02	1.2195E-01	8.1089E-02	1.5039E 00	1.2900E-01	
19	1.9833E-06	2.1630E 02	1.7140E 02	1.2377E-01	8.3126E-02	1.4890E 00	1.1910E-01	
20	1.8442E-06	2.1310E 02	1.7570E 02	1.2603E-01	8.5212E-02	1.4797E 00	1.0954E-01	
21	1.7101E-06	2.1870E 02	1.8130E 02	1.2969E-01	8.7928E-02	1.4748E 00	1.0031E-01	
22	1.5801E-06	2.2520E 02	1.8780E 02	1.3378E-01	9.1080E-02	1.4688E 00	9.1439E-02	
23	1.4571E-06	2.1930E 02	1.9630E 02	1.3873E-01	9.4520E-02	1.4572E 00	8.2929E-02	
24	1.3338E-06	2.4290E 02	2.0620E 02	1.4450E-01	1.0000E-01	1.4449E 00	7.4796E-02	
25	1.2244E-06	2.5560E 02	2.1810E 02	1.5187E-01	1.0577E-01	1.4358E 00	6.7053E-02	
26	1.1156E-06	2.7070E 02	2.3100E 02	1.6052E-01	1.1203E-01	1.4328E 00	5.9712E-02	
27	1.0119E-06	2.8960E 02	2.4710E 02	1.7115E-01	1.1984E-01	1.4284E 00	5.2786E-02	
28	9.1325E-06	3.0880E 02	2.6420E 02	1.8208E-01	1.2813E-01	1.4210E 00	4.6287E-02	
29	8.1965E-06	3.3190E 02	2.8430E 02	1.9508E-01	1.3788E-01	1.4148E 00	4.0225E-02	
30	7.3110E-06	3.5560E 02	3.0500E 02	2.0858E-01	1.4792E-01	1.4101E 00	3.4608E-02	
31	6.4762E-06	3.7070E 02	3.3220E 02	2.2455E-01	1.6111E-01	1.4011E 00	2.9445E-02	
32	5.6920E-06	4.1810E 02	3.6000E 02	2.4357E-01	2.8173E-01	1.3958E 00	2.4738E-02	
33	4.9583E-06	4.5600E 02	3.9210E 02	2.6501E-01	1.9016E-01	1.3936E 00	2.0488E-02	
34	4.2753E-06	4.9930E 02	4.2860E 02	2.8938E-01	2.0786E-01	1.3922E 00	1.6694E-02	
35	3.6429E-06	5.4930E 02	4.7120E 02	3.1757E-01	2.2852E-01	1.3896E 00	1.3348E-02	
36	3.0610E-06	6.0700E 02	5.2140E 02	3.5117E-01	2.5287E-01	1.3867E 00	1.0441E-02	
37	2.5299E-06	6.7900E 02	5.8090E 02	3.9070E-01	2.8173E-01	1.3868E 00	7.9565E-03	
38	2.0491E-06	7.6100E 02	6.5290E 02	4.3831E-01	3.1665E-01	1.3842E 00	5.8763E-03	
39	1.6191E-06	8.6720E 02	7.4190E 02	4.9732E-01	3.5981F-01	1.3822E 00	4.1759E-03	
40	1.2396E-06	9.6990E 02	8.5540E 02	5.7264E-01	4.1866E-01	1.3803E 00	2.8270E-03	
41	9.1072E-07	1.1750E 03	1.0060E 03	6.7219E-01	4.8789E-01	1.3777E 00	1.7966E-03	
42	6.3244E-07	1.4190E 03	1.2140E 03	8.1098E-01	5.8877E-01	1.3774E 00	1.0479E-03	
43	4.0476E-07	1.7840E 03	1.5260E 03	1.0187E 00	7.4009E-01	1.3765E 00	5.3996E-04	
44	2.2768E-07	2.3880E 03	2.0430E 03	1.3628E 00	9.9022E-01	1.3754E 00	2.2894E-04	
45	1.0419E-07	3.5920E 03	3.0730E 03	2.0490E 00	1.4904E 00	1.3749E 00	6.8079E-05	

TABLE B.6
SPATIALLY AVERAGED THERMAL SPECTRA FOR THE CORNELL
ZPR 1:1 CORE

I	ENERGY	MODERATOR SPECTRUM	CLADDING SPECTRUM	FUEL SPECTRUM
1	1.6093E 00	5.4517E-01	5.4549E-01	5.3873E-01
2	1.2311E 00	6.1583E-01	6.1323E-01	6.0196E-01
3	9.6667E-01	8.0549E-01	7.9914E-01	7.8064E-01
4	7.7941E-01	1.0053E 00	9.9849E-01	9.7670E-01
5	6.4501E-01	1.2364E 00	1.2265E 00	1.1975E 00
6	5.4731E-01	1.4605E 00	1.4462E 00	1.4084E 00
7	4.7542E-01	1.6733E 00	1.6526E 00	1.6032E 00
8	4.2192E-01	1.8733E 00	1.8446E 00	1.7814E 00
9	3.8170E-01	2.0569E 00	2.0188E 00	1.9400E 00
10	3.5119E-01	2.2251E 00	2.1755E 00	2.0783E 00
11	3.2786E-01	2.4269E 00	2.3654E 00	2.2485E 00
12	3.0990E-01	2.5621E 00	2.4900E 00	2.3562E 00
13	2.9244E-01	2.6780E 00	2.5986E 00	2.4525E 00
14	2.7549E-01	2.8720E 00	2.7858E 00	2.6273E 00
15	2.5905E-01	3.1313E 00	3.0400E 00	2.8708E 00
16	2.4311E-01	3.3868E 00	3.2923E 00	3.1152E 00
17	2.2768E-01	3.6805E 00	3.5815E 00	3.3940E 00
18	2.1275E-01	4.0585E 00	3.9501E 00	3.7445E 00
19	1.9833E-01	4.5281E 00	4.4053E 00	4.1731E 00
20	1.8442E-01	5.0873E 00	4.9465E 00	4.6815E 00
21	1.7101E-01	5.7628E 00	5.5982E 00	5.2910E 00
22	1.5811E-01	6.6162E 00	6.4207E 00	6.0586E 00
23	1.4571E-01	7.7214E 00	7.4837E 00	7.0480E 00
24	1.3382E-01	9.1329E 00	8.8386E 00	8.3053E 00
25	1.2244E-01	1.0860E 01	1.0490E 01	9.8281E 00
26	1.1156E-01	1.2890E 01	1.2422E 01	1.1599E 01
27	1.0119E-01	1.5239E 01	1.4646E 01	1.3619E 01
28	9.1325E-02	1.7990E 01	1.7239E 01	1.5961E 01
29	8.1965E-02	2.1205E 01	2.0247E 01	1.8650E 01
30	7.3110E-02	2.4876E 01	2.3666E 01	2.1683E 01
31	6.4762E-02	2.8784E 01	2.7259E 01	2.4807E 01
32	5.6920E-02	3.2558E 01	3.0676E 01	2.7716E 01
33	4.9583E-02	3.5759E 01	3.3489E 01	3.0001E 01
34	4.2753E-02	3.8132E 01	3.5455E 01	3.1375E 01
35	3.6429E-02	3.9529E 01	3.6405E 01	3.1844E 01
36	3.0610E-02	3.9848E 01	3.6256E 01	3.1277E 01
37	2.5298E-02	3.8994E 01	3.4941E 01	2.9651E 01
38	2.0491E-02	3.6909E 01	3.2445E 01	2.6991E 01
39	1.6101E-02	3.3619E 01	2.8878E 01	2.3436E 01
40	1.2396E-02	2.9266E 01	2.4426E 01	1.9203E 01
41	9.1072E-03	2.4109E 01	1.9449E 01	1.4659E 01
42	6.3244E-03	1.8522E 01	1.4278E 01	1.0146E 01
43	4.0476E-03	1.2954E 01	9.3837E 00	6.1077E 00
44	2.2768E-03	7.8840E 00	5.2262E 00	2.9522E 00
45	1.0119E-03	3.7721E 00	2.1714E 00	9.4648E-01

TABLE B.7
SPATIALLY AVERAGED THERMAL SPECTRA FOR THE CORNELL
ZPR 1.5:1 CORE

I	ENERGY	MODERATOR SPECTRUM	CLADDING SPECTRUM	FUEL SPECTRUM
1	1.6093E 00	5.4770E-01	5.4779E-01	5.4101E-01
2	1.2311E 00	6.2156E-01	6.1843E-01	6.0706E-01
3	9.6667E-01	8.1724E-01	8.0983E-01	7.9108E-01
4	7.7941E-01	1.0217E 00	1.0136E 00	9.9151E-01
5	6.4501E-01	1.2606E 00	1.2488E 00	1.2193E 00
6	5.4731E-01	1.4943E 00	1.4773E 00	1.4387E 00
7	4.7542E-01	1.7191E 00	1.6944E 00	1.6438E 00
8	4.2192E-01	1.9332E 00	1.8988E 00	1.8338E 00
9	3.8170E-01	2.1327E 00	2.0869E 00	2.0055E 00
10	3.5119E-01	2.3190E 00	2.2592E 00	2.1582E 00
11	3.2786E-01	2.5420E 00	2.4673E 00	2.3454E 00
12	3.0990E-01	2.6954E 00	2.6075E 00	2.4673E 00
13	2.9244E-01	2.8287E 00	2.7312E 00	2.5776E 00
14	2.7549E-01	3.0465E 00	2.9399E 00	2.7726E 00
15	2.5905E-01	3.3369E 00	3.2230E 00	3.1436E 00
16	2.4311E-01	3.6304E 00	3.5112E 00	3.3223E 00
17	2.2768E-01	3.9778E 00	3.8511E 00	3.6495E 00
18	2.1275E-01	4.4366E 00	4.2957E 00	4.0722E 00
19	1.9833E-01	5.0247E 00	4.8620E 00	4.6057E 00
20	1.8442E-01	5.7523E 00	5.5615E 00	5.2530E 00
21	1.7101E-01	6.6668E 00	6.4319E 00	6.0845E 00
22	1.5811E-01	7.8577E 00	7.5773E 00	7.1500E 00
23	1.4571E-01	9.4351E 00	9.0828E 00	8.5541E 00
24	1.3382E-01	1.1493E 01	1.1042E 01	1.0376E 01
25	1.2244E-01	1.4078E 01	1.3491E 01	1.2541E 01
26	1.1156E-01	1.7210E 01	1.6444E 01	1.5355E 01
27	1.0119E-01	2.0941E 01	1.9937E 01	1.8538E 01
28	9.1325E-02	2.5381E 01	2.4072E 01	2.2287E 01
29	8.1965E-02	3.0613E 01	2.8896E 01	2.5517E 01
30	7.5110E-02	3.6609E 01	3.4389E 01	3.1500E 01
31	6.4762E-02	4.3073E 01	4.0222E 01	3.6603E 01
32	5.6920E-02	4.9486E 01	4.5898E 01	4.1469E 01
33	4.9583E-02	5.5219E 01	5.0801E 01	4.5509E 01
34	4.2753E-02	5.9821E 01	5.4503E 01	4.8231E 01
35	3.6429E-02	6.2963E 01	5.6618E 01	4.9524E 01
36	3.0610E-02	6.4361E 01	5.6921E 01	4.9103E 01
37	2.5298E-02	6.3762E 01	5.5227E 01	4.6866E 01
38	2.0491E-02	6.0997E 01	5.1480E 01	4.2827E 01
39	1.6191E-02	5.6058E 01	4.5874E 01	3.7230E 01
40	1.2396E-02	4.9154E 01	3.8723E 01	3.1444E 01
41	9.1072E-03	4.0712E 01	3.0685E 01	2.3128E 01
42	6.3244E-03	3.1386E 01	2.0312E 01	1.5852E 01
43	4.0476E-03	2.1971E 01	1.4437E 01	9.3968E 00
44	2.2768E-03	1.3337E 01	7.8532E 00	4.4363E 00
45	1.0119E-03	6.3281E 00	3.1495E 00	1.3728E 00

TABLE B.8

SPATIALLY AVERAGED THERMAL SPECTRA FOR THE CORNELL
ZPR 2:1 CORE

I	ENERGY	MODERATOR SPECTRUM	CLADDING SPECTRUM	FUEL SPECTRUM
1	1.6093E-00	5.4898E-01	5.4887E-01	5.4207E-01
2	1.2311E-00	6.2448E-01	6.2087E-01	6.0946E-01
3	9.6667E-01	8.2325E-01	8.1492E-01	7.9506E-01
4	7.7941E-01	1.0301E-00	1.0209E-00	9.9865E-01
5	6.4501E-01	1.2730E-00	1.2596E-00	1.2298E-00
6	5.4731E-01	1.5118E-00	1.4924E-00	1.4534E-00
7	4.7542E-01	1.7429E-00	1.7148E-00	1.6635E-00
8	4.2102E-01	1.9644E-00	1.9253E-00	1.8593E-00
9	3.8170E-01	2.1725E-00	2.1202E-00	2.0375E-00
10	3.5119E-01	2.3689E-00	2.3003E-00	2.1975E-00
11	3.2786E-01	2.6038E-00	2.5180E-00	2.3936E-00
12	3.0190E-01	2.7681E-00	2.6668E-00	2.5234E-00
13	2.9244E-01	2.9124E-00	2.7996E-00	2.6422E-00
14	2.7549E-01	3.1460E-00	3.0220E-00	2.8501E-00
15	2.5905E-01	3.4581E-00	3.3248E-00	3.1398E-00
16	2.4311E-01	3.7806E-00	3.6399E-00	3.4441E-00
17	2.2768E-01	4.1711E-00	4.0200E-00	3.8096E-00
18	2.1275E-01	4.6967E-00	4.5266E-00	4.2910E-00
19	1.9833E-01	5.3856E-00	5.1862E-00	4.9128E-00
20	1.8442E-01	6.2613E-00	6.0233E-00	5.7007E-00
21	1.7101E-01	7.3914E-00	7.0999E-00	6.7102E-00
22	1.5811E-01	8.8924E-00	8.5271E-00	8.0462E-00
23	1.4571E-01	1.0909E-01	1.0438E-01	9.8308E-00
24	1.3382E-01	1.3573E-01	1.2958E-01	1.2176E-01
25	1.2244E-01	1.6971E-01	1.6151E-01	1.5133E-01
26	1.1156E-01	2.1163E-01	2.0068E-01	1.8739E-01
27	1.0119E-01	2.6233E-01	2.4767E-01	2.3030E-01
28	9.1325E-02	3.2322E-01	3.0376E-01	2.8124E-01
29	8.1965E-02	3.9526E-01	3.6932E-01	3.4019E-01
30	7.3110E-02	4.7797E-01	4.4400E-01	4.0580E-01
31	6.4762E-02	5.6769E-01	5.2359E-01	4.7649E-01
32	5.6920E-02	6.5794E-01	6.0185E-01	5.4377E-01
33	4.9583E-02	7.4071E-01	6.7090E-01	6.0102E-01
34	4.2753E-02	8.0958E-01	7.2462E-01	6.4123E-01
35	3.6429E-02	8.5931E-01	7.5681E-01	6.6199E-01
36	3.0610E-02	8.8511E-01	7.6378E-01	6.5887E-01
37	2.5298E-02	8.8270E-01	7.4250E-01	6.3009E-01
38	2.0491E-02	8.4918E-01	6.9214E-01	5.7580E-01
39	1.6191E-02	7.8403E-01	6.1574E-01	4.9971E-01
40	1.2396E-02	6.8997E-01	5.1782E-01	4.0710E-01
41	9.1072E-03	5.7299E-01	4.0814E-01	3.0762E-01
42	6.3244E-03	4.4241E-01	2.9431E-01	2.0913E-01
43	4.0476E-03	3.0975E-01	1.8818E-01	1.2249E-01
44	2.2768E-03	1.8772E-01	1.0074E-01	5.6906E-00
45	1.0119E-03	8.8666E-00	3.9564E-00	1.7245E-00

TABLE B.9

 SPATIALLY AVERAGED THERMAL SPECTRA FOR THE CORNELL
 ZPR 3:1 CORE

I	ENERGY	MODERATOR SPECTRUM	CLADDING SPECTRUM	FUEL SPECTRUM
1	1.6093E 00	5.5025E-01	5.4979E-01	5.4298E-01
2	1.2311E 00	6.2740E-01	6.2299E-01	6.1154E-01
3	9.6667E-01	8.2930E-01	8.1943E-01	8.0045E-01
4	7.7941E-01	1.0386E 00	1.0275E 00	1.0051E 00
5	6.4501E-01	1.2855E 00	1.2694E 00	1.2394E 00
6	5.4731E-01	1.5295E 00	1.5062E 00	1.4668E 00
7	4.7542E-01	1.7671E 00	1.7333E 00	1.6814E 00
8	4.2192E-01	1.9963E 00	1.9491E 00	1.8824E 00
9	3.8170E-01	2.2135E 00	2.1503E 00	2.0664E 00
10	3.5119E-01	2.4208E 00	2.3379E 00	2.2334E 00
11	3.2786E-01	2.6693E 00	2.5651E 00	2.4384E 00
12	3.0990E-01	2.8464E 00	2.7231E 00	2.5767E 00
13	2.9244E-01	3.0052E 00	2.8671E 00	2.7059E 00
14	2.7549E-01	3.2604E 00	3.1077E 00	2.9308E 00
15	2.5905E-01	3.6043E 00	3.4384E 00	3.2471E 00
16	2.4311E-01	3.9724E 00	3.7952E 00	3.5910E 00
17	2.2768E-01	4.4338E 00	4.2404E 00	4.0184E 00
18	2.1275E-01	5.0712E 00	4.8493E 00	4.5969E 00
19	1.9833E-01	5.9324E 00	5.6662E 00	5.3675E 00
20	1.8442E-01	7.0673E 00	6.7408E 00	6.3797E 00
21	1.7101E-01	8.5809E 00	8.1684E 00	7.7201E 00
22	1.5811E-01	1.0640E 01	1.0106E 01	9.5357E 00
23	1.4571E-01	1.3451E 01	1.2740E 01	1.1999E 01
24	1.3382E-01	1.7220E 01	1.6262E 01	1.5281E 01
25	1.2244E-01	2.2110E 01	2.0796E 01	1.9484E 01
26	1.1156E-01	2.8257E 01	2.6453E 01	2.4701E 01
27	1.0119E-01	3.5816E 01	3.3342E 01	3.1004E 01
28	9.1325E-02	4.4981E 01	4.1626E 01	3.8540E 01
29	8.1965E-02	5.5868E 01	5.1313E 01	4.7266E 01
30	7.3110E-02	6.8387E 01	6.2343E 01	5.7119E 01
31	6.4762E-02	8.2050E 01	7.4117E 01	6.7450E 01
32	5.6920E-02	9.5986E 01	8.5787E 01	7.7509E 01
33	4.9583E-02	1.0909E 02	9.6262E 01	8.6236E 01
34	4.2753E-02	1.2036E 02	1.0458E 02	9.2546E 01
35	3.6429E-02	1.2889E 02	1.0966E 02	9.5918E 01
36	3.0610E-02	1.3381E 02	1.1087E 02	9.5639E 01
37	2.5298E-02	1.3434E 02	1.0771E 02	9.1404E 01
38	2.0491E-02	1.2997E 02	1.0010E 02	8.3273E 01
39	1.6191E-02	1.2054E 02	8.8597E 01	7.1902E 01
40	1.2396E-02	1.0644E 02	7.3949E 01	5.8138E 01
41	9.1072E-03	8.8606E 01	5.7754E 01	4.3530E 01
42	6.3244E-03	6.8496E 01	4.1127E 01	2.9224E 01
43	4.0476E-03	4.7951E 01	2.5877E 01	1.6843E 01
44	2.2768E-03	2.9002E 01	1.3586E 01	7.6744E 00
45	1.0119E-03	1.3635E 01	5.2270E 00	2.2783E 00

TABLE B.10
SPATIALLY AVERAGED THERMAL SPECTRA FOR THE CORNELL
ZPR 4:1 CORE

I	ENERGY	MODERATOR SPECTRUM	CLADDING SPECTRUM	FUEL SPECTRUM
1	1.6093E 00	5.5090E-01	5.5015F-01	5.4333E-01
2	1.2311E 00	6.2890E-01	6.2380F-01	6.1233E-01
3	9.6667E-01	8.3241E-01	8.2121F-01	8.0220E-01
4	7.7941E-01	1.0430E 00	1.0303F 00	1.0078E 00
5	6.4501E-01	1.2920E 00	1.2736F 00	1.2435E 00
6	5.4731E-01	1.5386E 00	1.5120F 00	1.4725E 00
7	4.7542E-01	1.7795E 00	1.7409F 00	1.6889E 00
8	4.2192E-01	2.0129E 00	1.9589F 00	1.8918E 00
9	3.8170E-01	2.2350E 00	2.1627F 00	2.0783E 00
10	3.5119E-01	2.4484E 00	2.3535F 00	2.2483E 00
11	3.2786E-01	2.7049E 00	2.5854F 00	2.4576E 00
12	3.0990E-01	2.8902E 00	2.7485F 00	2.6007E 00
13	2.9244E-01	3.0592E 00	2.9000F 00	2.7369E 00
14	2.7549E-01	3.3304E 00	3.1533F 00	2.9739E 00
15	2.5905E-01	3.6990E 00	3.5054F 00	3.3103E 00
16	2.4311E-01	4.1049E 00	3.8960F 00	3.6864E 00
17	2.2768E-01	4.6265E 00	4.3957F 00	4.1556E 00
18	2.1275E-01	5.3603E 00	5.0914F 00	4.8264E 00
19	1.9833E-01	6.3721E 00	6.0438F 00	5.7252E 00
20	1.8442E-01	7.7365E 00	7.3254F 00	6.9331E 00
21	1.7101E-01	9.5931E 00	9.0621F 00	8.5648E 00
22	1.5811E-01	1.2154E 01	1.1451F 01	1.0805E 01
23	1.4571E-01	1.5685E 01	1.4728F 01	1.3870E 01
24	1.3382E-01	2.0456E 01	1.9141F 01	1.7986E 01
25	1.2244E-01	2.6706E 01	2.4867F 01	2.3299E 01
26	1.1156E-01	3.4641E 01	3.2077F 01	2.9953E 01
27	1.0119E-01	4.4483E 01	4.0918F 01	3.8049E 01
28	9.1325E-02	5.6475E 01	5.1585F 01	4.7761E 01
29	8.1965E-02	7.0749E 01	6.4047F 01	5.8995E 01
30	7.3110E-02	8.7178E 01	7.8221F 01	7.1567E 01
31	6.4762E-02	1.0516E 02	9.3344F 01	8.4947E 01
32	5.6920E-02	1.2364E 02	1.0836F 02	9.7907E 01
33	4.9583E-02	1.4122E 02	1.2192F 02	1.0922E 02
34	4.2753E-02	1.5658E 02	1.3273F 02	1.1746E 02
35	3.6429E-02	1.6844E 02	1.3926F 02	1.2181E 02
36	3.0610E-02	1.7557E 02	1.4068F 02	1.2136E 02
37	2.5298E-02	1.7687E 02	1.3636F 02	1.1571E 02
38	2.0491E-02	1.7157E 02	1.2623F 02	1.0501E 02
39	1.6191E-02	1.5947E 02	1.1117F 02	9.0218E 01
40	1.2306E-02	1.4104E 02	9.2196F 01	7.2483E 01
41	9.1072E-03	1.1753E 02	7.1498F 01	5.3889E 01
42	6.3244E-03	9.0891E 01	5.0468F 01	3.5862E 01
43	4.0476E-03	6.3611E 01	3.1432F 01	2.0459E 01
44	2.2768E-03	3.8430E 01	1.6328F 01	9.2237E 00
45	1.0119E-03	1.8025E 01	6.2363F 00	2.7183E 00

TABLE B.11

CORNELL UNIVERSITY ZERO POWER REACTOR INTEGRAL PROPERTIES

Integral Properties	Water/Oxide Volume Ratio				
	1:1	1.5:1	2:1	3:1	4:1
f	.92185	.88785	.85480	.79331	.73687
η	1.72300	1.72867	1.73165	1.73461	1.73605
ηf	1.58835	1.53480	1.48021	1.37607	1.27925
δ_n^m	1.25149	1.30644	1.35120	1.42173	1.47787
δ_n^c	1.14087	1.14917	1.15325	1.15677	1.15807
D, cm.	.3699	.3110	.2770	.2402	.2206
L, cm.	2.0086	1.9356	1.9253	1.9659	2.0298
ℓ_t , μ sec.	28.69	35.17	41.53	53.43	64.37
\bar{v}_m , m/sec.	3667.	3318.	3134.	2945.	2849.
\bar{v}_c , m/sec.	3802.	3478.	3310.	3146.	3067.
\bar{v}_f , m/sec.	3971.	3626.	3446.	3265.	3177.
\bar{v}_h , m/sec.	3802.	3426.	3223.	3012.	2902.

while Table B.12 gives their temperature coefficients as defined by Eq. (7.5).

The effective cross sections, Eqs. (6.23) and (6.31), are given at 20°C for the five cores in Table B.13, the temperature coefficients being given in Table B.14.

Table B.15 lists the 20°C values of the mean cross sections, Eqs. (6.24) and (6.32), while Table B.16 lists the temperature coefficients of these cross sections.

TABLE B.12

CORNELL UNIVERSITY ZERO POWER REACTOR INTEGRAL PROPERTY
TEMPERATURE COEFFICIENTS

Temperature Coefficients ($10^{-4}^{\circ}\text{C}^{-1}$)	Water/Oxide Volume Ratio				
	1:1	1.5:1	2:1	3:1	4:1
\dot{f}/f	+.266	.546	.813	+1.37	+1.95
$\dot{\eta}/\eta$	-.310	-.386	-.411	-.429	-.440
$\dot{\eta}_f/\eta_f$	-.044	.160	.402	.941	+1.51
$\dot{\delta_n^m}/\delta_n^m$	-2.76	-3.71	-4.46	-5.56	-6.35
$\dot{\delta_n^c}/\delta_n^c$	-1.53	-1.78	-1.94	-2.08	-2.16
\dot{D}/D	+3.23	+4.49	+5.76	+7.27	+8.38
\dot{L}/L	+5.51	+6.89	+7.82	+9.10	+9.90
$\dot{\ell_t}/\ell_t$	+.048	-.411	-.807	-1.34	-1.63
$\dot{\bar{v}_m}/\bar{v}_m$	+8.32	+10.1	+11.2	+12.6	+13.3
$\dot{\bar{v}_c}/\bar{v}_c$	+7.76	+9.34	+10.3	+11.4	+12.1
$\dot{\bar{v}_f}/\bar{v}_f$	+6.92	+8.55	+9.58	+10.7	+11.5
$\dot{\bar{v}_h}/\bar{v}_h$	+7.76	+9.63	+10.9	+12.3	+13.0

TABLE B.13

CORNELL UNIVERSITY ZERO POWER REACTOR EFFECTIVE CROSS SECTIONS

Effective Cross Sections (cm ⁻¹)	Water/Oxide Volume Ratio				
	1:1	1.5:1	2:1	3:1	4:1
Σ_a^m	.0219	.0219	.0219	.0219	.0219
Σ_a^c	.0139	.0139	.0139	.0139	.0139
Σ_a^f	.3641	.3680	.3700	.3719	.3728
Σ_s^m	4.1967	4.0195	3.9254	3.8295	3.7806
Σ_s^c	.1470	.1346	.1283	.1220	.1190
Σ_s^f	.6685	.6112	.5811	.5510	.5364
Σ_{tr}^m	2.9376	2.8927	2.8688	2.8445	2.8322
Σ_{tr}^c	.1572	.1451	.1389	.1328	.1298
Σ_{tr}^f	1.0182	.9660	.9385	.9110	.8976
Σ_t^m	4.2186	4.0414	3.9473	3.8513	3.8025
Σ_t^c	.1609	.1485	.1421	.1358	.1328
Σ_t^f	1.0327	.9792	.9511	.9230	.9092
Σ_f^f	.2852	.2618	.2637	.2655	.2664
Σ_a^h	.1584	.1292	.1095	.0851	.0706
Σ_s^h	2.4138	2.6804	2.8600	3.0800	3.2103
Σ_{tr}^h	1.9152	2.0965	2.2227	2.3807	2.4755
Σ_t^h	2.5722	2.8097	2.9694	3.1651	3.2809
Σ_f^h	.1036	.0816	.0667	.0482	.0372

TABLE B.14

CORNELL UNIVERSITY ZERO POWER REACTOR EFFECTIVE CROSS SECTION
TEMPERATURE COEFFICIENTS

Temperature Coefficients $(10^{-4} \text{ }^{\circ}\text{C}^{-1})$	Water/Oxide Volume Ratio				
	1:1	1.5:1	2:1	3:1	4:1
$\dot{\Sigma}_a^m / \dot{\Sigma}_a^m$	-2.97	-2.97	-2.97	-2.97	-2.97
$\dot{\Sigma}_a^c / \dot{\Sigma}_a^c$	0.0	0.0	0.0	0.0	0.0
$\dot{\Sigma}_a^f / \dot{\Sigma}_a^f$	0.0	0.0	0.0	0.0	0.0
$\dot{\Sigma}_s^m / \dot{\Sigma}_s^m$	+2.09	+2.88	+3.34	+3.84	+4.11
$\dot{\Sigma}_s^c / \dot{\Sigma}_s^c$	+8.92	+9.43	+10.4	+11.6	+12.2
$\dot{\Sigma}_s^f / \dot{\Sigma}_s^f$	+7.06	+8.60	+9.62	+10.8	+11.5
$\dot{\Sigma}_{tr}^m / \dot{\Sigma}_{tr}^m$	+1.29	+1.60	+1.78	+1.97	+2.07
$\dot{\Sigma}_{tr}^c / \dot{\Sigma}_{tr}^c$	+7.19	+8.54	+9.39	+10.4	+10.9
$\dot{\Sigma}_{tr}^f / \dot{\Sigma}_{tr}^f$	+4.07	+4.76	+5.19	+5.69	+5.97
$\dot{\Sigma}_t^m / \dot{\Sigma}_t^m$	+2.07	+2.85	+3.31	+3.80	+4.06
$\dot{\Sigma}_t^c / \dot{\Sigma}_t^c$	+7.21	+8.59	+9.43	+10.4	+10.9
$\dot{\Sigma}_t^f / \dot{\Sigma}_t^f$	+4.12	+4.81	+5.26	+5.76	+6.04
$\dot{\Sigma}_f^f / \dot{\Sigma}_f^f$	-1.63	-1.85	-1.99	-2.13	-2.21
$\dot{\Sigma}_a^h / \dot{\Sigma}_a^h$	-.06	+.43	+.78	+1.35	+1.63
$\dot{\Sigma}_s^h / \dot{\Sigma}_s^h$	+1.77	+2.28	+2.63	+3.10	+3.40
$\dot{\Sigma}_{tr}^h / \dot{\Sigma}_{tr}^h$	+1.30	+1.34	+1.38	+1.48	+1.58

Table B.14 (continued)

Temperature Coefficients $(10^{-4}^{\circ}\text{C}^{-1})$	Water/Oxide Volume Ratio				
	1:1	1.5:1	2:1	3:1	4:1
$\dot{\Sigma}_t^h / \hat{\Sigma}_t^h$	+1.66	+2.19	+2.56	+3.05	+3.37
$\dot{\Sigma}_f^h / \hat{\Sigma}_f^h$	-.10	+.55	+1.20	+2.28	+3.23

TABLE B.15

CORNELL UNIVERSITY ZERO POWER REACTOR MEAN CROSS SECTIONS

Mean Cross Sections (cm ⁻¹)	Water/Oxide Volume Ratio				
	1:1	1.5:1	2:1	3:1	4:1
$\bar{\Sigma}_a^m$.0131	.0145	.0154	.0164	.0169
$\bar{\Sigma}_a^c$.0080	.0088	.0092	.0097	.0099
$\bar{\Sigma}_a^f$.2017	.2233	.2363	.2506	.2582
$\bar{\Sigma}_s^m$	2.5177	2.6648	2.7560	2.8605	2.9190
$\bar{\Sigma}_s^c$.0851	.0852	.0852	.0853	.0853
$\bar{\Sigma}_s^f$.3704	.3708	.3710	.3713	.3714
$\bar{\Sigma}_{tr}^m$	1.7624	1.9178	2.0141	2.1248	2.1867
$\bar{\Sigma}_{tr}^c$.0910	.0918	.0923	.0929	.0931
$\bar{\Sigma}_{tr}^f$.5641	.5860	.5992	.6138	.6215
$\bar{\Sigma}_t^m$	2.5309	2.6794	2.7713	2.8768	2.9359
$\bar{\Sigma}_t^c$.0931	.0939	.0944	.0950	.0953
$\bar{\Sigma}_t^f$.5721	.5940	.6073	.6219	.6296
$\bar{\Sigma}_f^f$.1430	.1588	.1684	.1789	.1844
$\bar{\Sigma}_a^h$.0917	.0830	.0747	.0622	.0535
$\bar{\Sigma}_s^h$	1.3970	1.7214	1.9524	2.2499	2.4337
$\bar{\Sigma}_{tr}^h$	1.1084	1.3463	1.5174	1.7391	1.8766
$\bar{\Sigma}_t^h$	1.4887	1.8044	2.0271	2.3120	2.4872
$\bar{\Sigma}_f^h$.0599	.0524	.0455	.0352	.0282

TABLE B.16

CORNELL UNIVERSITY ZERO POWER REACTOR MEAN CROSS SECTION
TEMPERATURE COEFFICIENTS

Temperature Coefficients $(10^{-4} \text{ }^{\circ}\text{C}^{-1})$	Water/Oxide Volume Ratio				
	1:1	1.5:1	2:1	3:1	4:1
$\dot{\Sigma}_a^m / \bar{\Sigma}_a^m$	-11.0	-12.7	-14.0	-15.0	-15.7
$\dot{\Sigma}_a^c / \bar{\Sigma}_a^c$	-7.49	-9.13	-9.78	-10.8	-11.6
$\dot{\Sigma}_a^f / \bar{\Sigma}_a^f$	-8.13	-9.78	-10.9	-12.2	-12.9
$\dot{\Sigma}_s^m / \bar{\Sigma}_s^m$	-6.16	-7.11	-7.75	-8.51	-8.94
$\dot{\Sigma}_s^c / \bar{\Sigma}_s^c$	+.16	+.14	+.12	+.11	+.10
$\dot{\Sigma}_s^f / \bar{\Sigma}_s^f$	+.11	+.11	+.10	+.09	+.08
$\dot{\Sigma}_{tr}^m / \bar{\Sigma}_{tr}^m$	-6.96	-8.36	-9.28	-10.3	-10.9
$\dot{\Sigma}_{tr}^c / \bar{\Sigma}_{tr}^c$	-.60	-.76	-.92	-1.08	-1.18
$\dot{\Sigma}_{tr}^f / \bar{\Sigma}_{tr}^f$	-2.83	-3.67	-4.23	-4.92	-5.31
$\dot{\Sigma}_t^m / \bar{\Sigma}_t^m$	-6.19	-7.15	-7.78	-8.55	-8.98
$\dot{\Sigma}_t^c / \bar{\Sigma}_t^c$	-.54	-.75	-.90	-1.05	-1.15
$\dot{\Sigma}_t^f / \bar{\Sigma}_t^f$	-2.79	-3.61	-4.18	-4.85	-5.24
$\dot{\Sigma}_f^f / \bar{\Sigma}_f^f$	-8.46	-10.2	-11.3	-12.6	-13.3
$\dot{\Sigma}_a^h / \bar{\Sigma}_a^h$	-7.69	-8.97	-9.83	-10.6	-11.1
$\dot{\Sigma}_s^h / \bar{\Sigma}_s^h$	-5.91	-7.19	-8.01	-8.93	-9.40
$\dot{\Sigma}_{tr}^h / \bar{\Sigma}_{tr}^h$	-6.36	-8.11	-9.23	-10.5	-11.2

Table B.16 (continued)

Temperature Coefficients $(10^{-4} \text{ }^{\circ}\text{C}^{-1})$	Water/Oxide Volume Ratio				
	1:1	1.5:1	2:1	3:1	4:1
$\dot{\Sigma}^h_t / \bar{\Sigma}^h_t$	-6.01	-7.28	-8.08	-8.97	-9.44
$\dot{\Sigma}^h_f / \bar{\Sigma}^h_f$	-7.76	-8.87	-9.44	-9.66	-9.70

APPENDIX C

NUMERICAL METHODS IN COUTH

This appendix describes the computational methods employed by the COUTH code in solving Eq. (6.1) for the spatially averaged moderator flux $\bar{\phi}^m(E)$, as well as the subsequent calculation of all of the parameters defined in Chap. 6. A Fortran listing of COUTH appears in Appendix E utilizing the Nelkin water model for the scattering kernel. The input to COUTH is discussed in Appendix D.

COUTH, as presently instrumented begins its calculations with the computation of the energy, velocity, and lethargy mesh as described in Sec. 7.1 and listed in Appendix B. Inspection of these meshes shows that the lethargy mesh has the finest relative spacing in the region of maximum interest, $.025 \text{ eV} \leq E \leq .6 \text{ eV}$, while both the velocity and energy mesh tend to have the finest spacing at low energy end of the mesh. For this reason all calculations in COUTH are done in lethargy, u , space utilizing the relationships

$$\phi(u) = E\phi(E) , \quad (C.1)$$

$$\sigma(u' \rightarrow u) = E\sigma(E' \rightarrow E) , \quad (C.2)$$

and

$$\Sigma(u) = \Sigma(E) . \quad (C.3)$$

The heterogeneous effects of the lattice, Sec. 2.3, are incorporated into COUTH in terms of the moderator and fuel element escape probabilities. The escape probability of source neutrons, $P_s(E)$, is calculated in the subprogram FUNCTION PSLOF utilizing diffusion theory as expressed by Eq. (3.4). $P_m(E)$, the moderator escape probability of neutrons incident from the fuel element is calculated utilizing the reciprocity relationship, Eq. (3.6), by the subprogram FUNCTION PMODF. The linear extrapolation length into a black hole, d_o , necessary for these calculations is approximated by^{83/}

$$d_o(E) \Sigma_{tr}^m(E) = \lambda = \frac{0.6229}{1 + 2.48 \Sigma_{tr}^m(E) r_o} + 0.7104 , \quad (C.4)$$

where r_o is radius of the black hole. This expression equals $4/3$ at $\Sigma_{tr}^m r_o = 0$, Zaretsky's^{84/} value of 0.889 at $\Sigma_{tr}^m r_o = 1$, and 0.7104 for $\Sigma_{tr}^m r_o$ approaching infinity. Leslie's SPECTROX method^{85/} corresponds to the special case of $\lambda = 2/3$.

The fuel rod escape probability, $P_r(E)$, is calculated from the parabolic flux approximation, Eq. (4.8). This computation is carried out by the subprogram FUNCTION PRODF. The subprogram SUBROUTINE PESCF calculates the fuel element escape probability, $P_e(E)$, utilizing the thin region transport theory embodied in Eq. (4.21).

In the explicit calculation of escape probabilities, the modified Bessel functions of the first and second kind and of order 0, 1, and 2 are required. Calculation of the functions

$I_0(z)$, $I_1(z)$, $I_2(z)$, $K_0(z)$, $K_1(z)$, and $K_2(z)$ is accomplished by the subprogram SUBROUTINE BESS.

The modified Bessel functions of the first kind, $I_n(z)$, are computed in the following manner.^{86/} Noting that for any given z , $I_n(z)$ approaches zero as n gets very large, we set $I_n(z)$ equal to zero and $I_{n-1}(z)$ equal to 1×10^{-40} where for any z , n is determined as follows. For $z \leq 45$, $n = [2z+10]$, where $[x]$ is the largest integer contained in x . For $z > 45$, n is taken equal to 100. Lower order I 's are then calculated utilizing the recurrence relationship^{87/}

$$I_{m-1}(z) = \frac{2m}{z} I_m(z) + I_{m+1}(z) . \quad (C.5)$$

Recognizing that the I 's calculated in this manner bear the correct relationship to each other, but lack normalization, the results are normalized through the expression

$$e^z = \sum_{m=-\infty}^{\infty} I_m(z) \approx I_0(z) + 2 \sum_{m=1}^n I_m(z) . \quad (C.6)$$

This same technique is utilized in the calculation of the I_m 's utilized in the computation of the Nelkin water kernel, Eq. (5.15).

The zero order modified Bessel function of the second kind, $K_0(z)$, is computed using the following approximations.^{88/}

^{83/} A. M. Weinberg and E. P. Wigner, The Physical Theory of Neutron Chain Reactors, p. 765, The University of Chicago Press, Chicago, 1958.

^{84/} D. F. Zaretsky, PICG 5, 529 (1955).

For $z \geq 5$:

$$K_0(z) \approx \left(\frac{\pi}{2z}\right)^{1/2} e^{-z} \left[1 - \frac{1^2}{1 \cdot 8x} + \frac{1^2 \cdot 3^2}{2!(8x)^2} - \frac{1^2 \cdot 3^2 \cdot 5^2}{3!(8x)^3} + \dots \right], \quad (C.7)$$

the number of terms used in this expansion being set equal to $2[z]$. For $z < 5$,

$$K_0(z) \approx \sum_{m=0}^{50} \delta_m I_{2m}(z), \quad (C.8)$$

where

$$\delta_0 = -(\gamma + \log z/2), \quad (C.9)$$

$$\gamma = \text{Euler's Constant} = 0.577215, \dots, \quad (C.10)$$

$$\delta_1 = 2, \quad (C.11)$$

and,

$$\delta_m = \frac{m-1}{m} \delta_{m-1}. \quad m \geq 2 \quad (C.12)$$

The first and second order modified Bessel functions of the second kind are calculated using the Wronskian relationship,^{89/}

$$K_m(z)I_{m+1}(z) + K_{m+1}(z)I_m(z) = \frac{1}{z}. \quad (C.13)$$

^{85/} D. C. Leslie, "The SPECTROX Method for Thermal Spectra in Lattice Cells," AEEW-M211, United Kingdom Atomic Energy Authority (1962).

^{86/} F. D. Federighi and D. T. Goldman, "KERNEL and PAM-Programs for Use in the Calculation of the Thermal Scattering Matrix for Chemically Bound Systems," KAPL-2225, Knolls Atomic Power Laboratory (1962).

The calculation of the slowing down source, $S(E)$, as given in Eq. (7.1), and of the monatomic gas model for the scattering kernel, Eq. (5.9), requires the evaluation of the error function for various arguments. The error function, $ERF(z)$, is defined by

$$ERF(z) = \frac{2}{\sqrt{\pi}} \int_0^z e^{-t^2} dt . \quad (C.14)$$

In the COUTH code, $ERF(z)$ is calculated by FUNCTION ERF in the following manner.^{90/} For $|z| \geq 4$,

$$ERF(z) \approx \frac{|z|}{z} , \quad (C.15)$$

while for $2 \leq |z| < 4$,

$$ERF(z) \approx \frac{|z|}{z} \left[1 - \frac{e^{-z^2}}{|z|\sqrt{\pi}} \left(1 - \frac{1}{2z^2} + \frac{1 \cdot 3}{2^2 z^4} - \frac{1 \cdot 3 \cdot 5}{2^3 z^6} \right. \right. \\ \left. \left. + \frac{1 \cdot 3 \cdot 5 \cdot 7}{2 \cdot 2^4 z^8} \right) \right] . \quad (C.16)$$

For $|z| < 2$,

$$ERF(z) \approx \frac{2z}{\sqrt{\pi}} \left[\sum_{n=1}^{20} \frac{(-1)^{n-1}}{(n-1)!} \frac{z^{2(n-1)}}{(2n-1)} + \frac{z^{40}}{2(20!)(41)} \right] . \quad (C.17)$$

^{87/} H. B. Dwight, Tables of Integrals and Other Mathematical Data, p. 189, The Macmillan Company, New York, 1961.

^{88/} M. Goldstein and R. M. Thaler, "Recurrence Techniques for Calculation of Bessel Functions," Mathematical Tables and Other Aids to Computation, 13, 102 (1959).

Numerical integration in the lethargy space used in COUTH is carried out by the subprogram FUNCTION TRAP. The trapezoidal rule is utilized to simplify the calculations with the uneven lethargy spacing encountered. Integration of an arbitrary function of lethargy, $f(u)$, which has been evaluated at the discrete points $f(u_i)$, $i = 1, 2, 3, \dots, n$, is approximated by

$$\int_{u_1}^{u_n} f(u) du \approx \sum_{i=1}^{n-1} \frac{1}{2} [f(u_i) + f(u_{i+1})] \Delta u_i . \quad (C.17)$$

The lethargy intervals, Δu_i , are defined by

$$\Delta u_i = u_{i+1} - u_i, \quad i = 1, 2, 3, \dots, n-1 . \quad (C.18)$$

Calculation of the scattering kernel using the monatomic gas model, Eq. (5.4), is performed by the subprogram SUBROUTINE FKERN. Only the down scattering in energy (or up-scattering in lethargy) portion of the kernel is calculated in FKERN, the upscattering portion being calculated by detailed balance, Eq. (2.5), in the main program of COUTH. Calculation of the monatomic gas kernel in the form of a 45 by 45 matrix as needed with the lethargy mesh used takes about $2\frac{1}{2}$ minutes of computer time. If the Nelkin water kernel is used, then the scattering kernel, Eq. (5.15), is calculated with the subprogram SUBROUTINE WATER. Again, only the downscattering portion of the matrix is computed,

89/ M. Goldstein and R. M. Thaler, see Footnote 88.

the upscattering portion being calculated by detailed balance in the main body of COUTH. The actual methods used in the calculation of the Nelkin water kernel are discussed in Sec. 5.2. Since the calculation of 45 by 45 matrix representing the Nelkin water kernel takes approximately 15 minutes at a given temperature, the down-scattering portion of the matrix for a physical temperature of 20°C has been reproduced on cards so that numerous lattice studies may be made at this temperature without necessitating the recomputation of the water kernel. Control cards read into COUTH (see Appendix D), determine whether the downscattering portion of scattering kernel shall be calculated using the Nelkin model, or whether the Nelkin results for 20°C shall be read directly in.

For calculations at temperatures above 20°C, the average cosine of the scattering angle for water, $\bar{\mu}(E)$, is decreased by 1×10^{-4} for every centigrade degree increase in temperature above 20°C at all energies. The slowing down source of neutrons, $S(E)$, is calculated according to Eq. (7.1), while the moderator scattering cross section, $\Sigma_s^m(E)$, is calculated using Eq. (2.2) and as discussed in Sec. 7.1. The neutron balance equation, Eq. (6.1), rewritten below in terms of the lethargy mesh is then solved using an iterative process.^{91/}

^{90/} H. B. Dwight, p. 136, see Footnote 87.

^{91/} M. J. Poole, M. S. Nelkin, and R. S. Stone, "The Measurement and Theory of Reactor Spectra," Progress in Nuclear Energy, Series I, Vol. 2, p. 99, Pergamon Press, New York, London, Paris, and Los Angeles, 1958.

$$\bar{\varphi}^m(u_i) = \frac{\bar{s}(u_i) + \int_0^{u_c} \Sigma(u_j \rightarrow u_i) \bar{\varphi}^m(u_j) du_j}{\Sigma_s^m(u_i) + \Sigma_a^m(u_i) \left[1 + \frac{f(u_i)}{1-f(u_i)} \right]} . \quad (C.19)$$

The cutoff lethargy, u_c , is 7.372 corresponding to a low energy of .00101 eV with the thermal cutoff energy, E_c , of 1.609 eV being the zero lethargy point. The relative fuel absorption $f/[1-f]$ is calculated from the escape probabilities in accordance with Eq. (2.29).

An initial guess is made that the moderator spectrum is a constant in lethargy:

$$\bar{\varphi}^m(u_i) = 1 , \quad i = 1, 2, 3, \dots, n = 45 . \quad (C.20)$$

This guess is then normalized to satisfy neutron conservation as expressed in Eq. (2.4).

$$\hat{\varphi}_1^m(u_i) = \frac{\bar{\varphi}_1^m(u_i)}{\int_0^{u_c} \Sigma_a^m(u_i) \left[1 + \frac{f(u_i)}{1-f(u_i)} \right] \bar{\varphi}_1^m(u_i) du_i} , \quad i=1, 2, \dots, n . \quad (C.21)$$

The normalized flux, $\hat{\varphi}_1^m(u_i)$ is then substituted into the right hand side of Eq. (C.19) and the next generation approximation

to the moderator flux, $\bar{\phi}_2^m(u_i)$, is calculated. This process is repeated utilizing the general expressions

$$\bar{\phi}_{k+1}^m(u_i) = \frac{\bar{S}(u_i) + \int_0^{u_c} \Sigma(u_j \rightarrow u_i) \hat{\phi}_k^m(u_j) d(u_j)}{\Sigma_s^m(u_i) + \Sigma_a^m(u_i) \left[1 + \frac{f(u_i)}{1-f(u_i)} \right]}, \quad i = 1, 2, \dots, n,$$
(C.22)

and,

$$\hat{\phi}_k^m(u_i) = \frac{\bar{\phi}_k^m(u_i)}{\int_0^{u_c} \Sigma_a^m(u_i) \left[1 + \frac{f(u_i)}{1-f(u_i)} \right] \bar{\phi}_k^m(u_i) du_i} \quad i = 1, 2, \dots, n.$$
(C.23)

The equation is considered solved when the successive iterations satisfy the following convergence criterion at every other lethargy point:

$$\left| \frac{\hat{\phi}_{k+1}^m(u_i)}{\hat{\phi}_k^m(u_i)} - 1 \right| \leq \epsilon \quad i = 1, 3, 5, 7, \dots, n.$$
(C.24)

The convergence criterion, ϵ , utilized in the COUTH calculations is 1×10^{-4} . In general solution of the integral equation, Eq. (C.19), has taken about 13 iterations with use

of the monatomic gas model, while the use of the Nelkin water kernel with its more complicated fine structure usually requires about 27 iterations for solution.

The fuel and cladding spectra, the mean velocities, the disadvantage factors, the lifetime, the thermal utilization, η_f , L, D, and the averaged cross sections are calculated in a straightforward manner as defined in Chap. 6.

An entire lattice calculation, including the computation of the escape probabilities, the spatially averaged thermal spectra, and all of the parameters defined in Chap. 6 takes about 40 seconds of computer time with use of the Nelkin water kernel, and about 30 seconds with the monatomic gas model. Calculational times for the kernel are not included in these figures. Compiling time for the Fortran source program of COUTH runs about two and one half minutes.

APPENDIX D

INPUT-OUTPUT FORMAT FOR COUTH

A Fortran statement of the COUTH code for use with the Nelkin water kernel as a scattering model is listed in Appendix E. This section describes the input required and the output received for a typical lattice calculation. The input data is listed below, the first column being the item or data card number, the second column is the Fortran FORMAT as it appears in COUTH, the third column is the Fortran list of the input variable, and the fourth column is a description of each variable.

1. (I4)	IND	Identification number. If IND = 1, the previously cal- culated down scattering portion of the Nelkin water kernel at 20°C will be used in the cal- culation. If IND \geq 2, the Nelkin water kernel will be cal- culated at the tempera- ture specified in Item 2.
---------	-----	---

2.	(2F10.6, I5, E12.4)	T	The moderator temperature in degrees absolute.
		RHΦ	The moderator density at T in gm/cc.
		N	The number of lethargy intervals. N = 44 gives mesh in Table B.1. N must be \leq 54.
		EPSI	Convergence criterion, ϵ , Eq. (C.24).
3.	(13F6.1)	XA(I)	U^{235} absorption cross section in barns.
4.	(13F6.1)	XF(I)	U^{235} fission cross section in barns.
5.	(7E11.3)	SK(J, I)	Downscattering portion of Nelkin model scattering matrix for 20°C.
6.	(20F4.3)	AMUBAR(I)	Average cosine of the scattering angle in water, $\bar{\mu}(E_i)$.

7.	(11F7.4)	CF(I)	Correction factors to the SK(J,I) diagonals see Sec. 7.1.
8.	(8F8.4,E16.4)	DEN	Fuel rod density in gm/cc.
		ENR	Fuel enrichment in weight per cent.
		RO	Fuel element diameter in inches.
		RCI	Fuel cladding inner diameter in inches.
		RF	Fuel rod diameter in inches.
		AMC	Cladding scatterer mass in amu.
		SSC	Cladding free atom cross section in barns.
		SAC	Cladding 2200 m/sec absorption cross section in barns.
		FNC	Cladding number density in atoms/barn-cm.
9.	(10A8)	TITLE	80 character title.

10. (2F10.5)	WΦ	The nominal water to oxide volume ratio for the lattice under consideration.
	AP	The lattice pitch or rod to rod spacing (in.) in a hexagonal lattice.

COUTH is instrumented to reread a series of items 10 until a negative value of WΦ is encountered. If this occurs, items 8 and 9 will be reread with the subsequent read in of a series of items 10. Calculation will stop when the computer encounters a negative value of WΦ, item 10, followed directly by a negative value for DEN, item 8. This allows one to calculate the scattering kernel at a given temperature, then consider a fuel element of certain specifications and calculate parameters for all of the lattices utilizing this fuel element. New fuel element specifications are then read in and the lattices utilizing this fuel element are analyzed. There is no limit on the number of fuel elements or the number of lattices for each fuel element type which may be considered.

The output for a typical 1 lattice calculation using a 45 point energy mesh is outlined below. The first column represents the page number after the execution of the source program, the second column gives the Fortran list of the output

variable, and the third column gives a description of the output variable.

1. I Index identifying lethargy mesh points.

E(I) Energy mesh point, E_i .

DE(I) Energy interval, $\Delta E_i = E_{i+1} - E_i$.

V(I) Velocity mesh point, v_i

DV(I) Velocity interval, Δv_i .

U(I) Lethargy mesh point, u_i .

DU(I) Lethargy interval, Δu_i .

2. BLANK

3. SK(J,I) Scattering matrix, $\sigma(U(J) \rightarrow U(I))$,

4. 5. J running horizontally and I running
6. 7. vertically.

8. E(I) Energy mesh point, E_i .

SX(I) Moderator scattering cross section in barns.

ST(I) Moderator transport cross section in barns.

SS25(I) U^{235} scattering cross section in barns.

SS28(I) U^{238} scattering cross section in barns.

SS16(I) O^{16} scattering cross section in barns.

AMUBAR(I) Average cosine of the scattering angle,
 $\bar{\mu}(E_i)$, for water.

9.	E(I)	Energy mesh point, E_i .
	XA(I)	U^{235} absorption cross section in barns.
	SF(I)	U^{235} fission cross section in barns.
	SIGMAF(I)	Fuel absorption cross section in cm^{-1} , $\Sigma_f^a(E_i)$.
	FSIGMAF(I)	Fuel absorption cross section in cm^{-1} , $\Sigma_a^f(E_i)$.
	AA(I)	$1 + \alpha(E_i)$, $\alpha(E_i)$ = fuel capture to fission ratio.
	SN(I)	Slowing down source of neutrons, $S(E)$, Eq. (7.1).
10.	E(37)	$E(37) = .0253 \text{ eV}$. This page shows $E = kT$ values for the variables used in the cladding calculations.
	PR	P_{rv} , Eqs. (4.8), (4.19).
	FJΦ	J_o , Eq. (4.22).
	TT	Cladding thickness in cm.
	FO	Solid angle factor, Eq. (4.26).
	FIN	Fraction of neutrons scattered in, Eq. (4.48).
	SIGS	Cladding scattering cross section in cm^{-1} .
	SIGT	Cladding total cross section in cm^{-1} .
	G	g , Eq. (4.45).
	S	T , Eq. (4.35).
	PU	P_u , Eq. (4.43).
	PUNIF	P_{unif} , Eq. (4.44).

RSUM	$r_{in} + r_{out}$, Eq. (4.46).
TAU	τ , Eq. (4.40).
RHΦSUM	$\rho_{in} + \rho_{out}$, Eq. (4.47).
CTE	Cladding absorption rate to fuel element absorption rate ratio, Eq. (4.55).

11. BLANK

12. BLANK

13.	WΦ	Input item 10.
	T	Input item 2.
	TITLE	Input item 9.
	E(I)	Energy, E_i .
	FLUX (I)	$\bar{\phi}^m(E_i)$, Eq. (6.1).
	FC(I)	$\bar{\phi}_c(E_i)$, Eq. (6.4).
	FS(I)	$\bar{\phi}^f(E_i)$, Eq. (6.3).
	AB(I)	$\Sigma_a^m(E) \left[1 + \frac{f(E)}{1-f(E)} \right]$.
14.	WΦ	Input item 10.
	T	Input item 2.
	TITLE	Input item 9.
	E(I)	Energy, E_i .
	PS(I)	$P_s(E_i)$, Eq. (3.4).
	PM(I)	$P_m(E_i)$, Eq. (3.6).
	PR(I)	$P_{rr}(E_i)$, Eq. (4.8), (4.19).

PE(I)	$P_e(E_i)$, Eq. (4.21).
TU(I)	$f(E_i)$, Eq. (3.8).
RFA(I)	$f/(1-f)$, Eq. (3.8).
RTE(I)	Rod abs. rate/element abs. rate, Eq. (4.53).
FJ ϕ	$J_o(E_i)$, Eq. (4.22).
15. W ϕ	Input item 10.
T	Input item 2.
TITLE	Input item 9.
F	f , Eq. (6.15).
ETA	η .
ETAF	ηf , Eq. (6.16).
DIS	δ_n^m , Eq. (6.8).
DISC	δ_n^c , Eq. (6.9).
DIFFC	D, Eq. (6.38).
DIFFL	L, Eq. (6.39).
AL	ℓ_t , Eq. (6.17).
ALL	$\ell_m = \ell_t / \eta f$.
VM	\bar{v}_m , Eq. (6.6).
VF	\bar{v}_f , Eq. (6.6).
VC	\bar{v}_c , Eq. (6.6).
HV	\bar{v}_h , Eq. (6.33).
FN25	U^{235} number density.
FN28	U^{238} number density.
FN16	Oxygen in UO_2 number density.

FNC	Cladding number density, input item 8.
FNM	Moderator number density.
N	Input item 2.
K	Number of iterations required to solve Eq. (6.1).
EPSI	Input item 2.
RHΦ	Input item 2.
ENR	Fuel enrichment in atom per cent.
AP	Input item 10.
R1	Equivalent cell radius, cm.
R0	Fuel element radius, cm.
VOLM	Moderator area, cm^2 .
VOLC	Cladding area, cm^2 .
VOLF	Fuel rod area, cm^2 .
R	Actual water to oxide volume ratio.
TITLE	Input item 10.

16. Page 16 lists the effective cross sections for each region of the cell, Eq. (6.23), and for the homogenized cell, Eq. (6.31); and the mean cross sections for each region, Eq. (6.24), and for the homogenized cell, Eq. (6.32).

Pages 12 through 16 are repeated for each lattice considered, while consideration of a fuel element with new specifications will cause pages 10 and 11 to be printed with the subsequent printing of pages 12 through 16 for each lattice considered.

APPENDIX E

FORTRAN LISTING OF COUTH

This appendix lists the Fortran statement of the COUTH source program as instrumented for calculation with the Nelkin water kernel as the scattering model. SUBROUTINE FKERN, which calculates the monatomic gas model for the scattering kernel, is also listed. For calculations with the monatomic gas model, SUBROUTINE WATER, FUNCTION ONE and FUNCTION TWO are replaced by SUBROUTINE FKERN. In addition the main program of COUTH must be modified to read in the values of the transport cross section of water as calculated with the Nelkin model for use in the calculation of the moderator escape probabilities.

PROGRAM COUTH

```
DIMENSION U(55),E(55),PS(55),PM(55),PF(55),RFA(55),TU(55),AB(55),
1SN(55),SK(55,55),SX(55),ALPHA(55),PHIN(55),DU(55),AA(55),FEA(55),
2GAMMA(55),DELTA(55),SALPHA(55),SPHIN(55),FLUX(55),ZZ(55),SXA(55),
3XA(55),XF(55),FS(55),ST(55),AMURAR(55),KN(5),IM(5),CF(55),
4SIGMAF(55),FSIGMAF(55),DE(55),DV(55),V(55),SS25(55),SS28(55),
5SS16(55),D(55),DD(55),TITLE(10),PR(55),FJO(55),RTE(55),FC(55),
6CTE(55),FB(55),TRB(55)
```

C ORDER OF DATA INPUT IS AS FOLLOWS.

IND -----	14
T,RHO,N,EPsi -----	2(F10.6),I5,2X,E10.2
XA -----	13(F6.1)
XF -----	13(F6.1)
SK -----	7(E11.3)
AMUBAR -----	20(F4.3)
CF -----	11(F7.4)
DEN,ENR,RO,RCI,RF,AMC,SSC,SAC,FNC	8(F8.4),4X,E12.4
TITLE -----	10(A8)
WO,AP -----	2(F10.5)

C IND = 1, NELKIN WATER KERNEL FOR 20 DEG. C READ IN.

C IND = 2, NELKIN WATER KERNEL CALCULATED AT T.

C T = MODERATOR TEMPERATURE IN DEGREES KELVIN.

C RHO IS THE MODERATOR DENSITY IN GM/CC.

C N = NUMBER OF LETHARGY INTERVALS.

C EPSI = CONVERGENCE CRITERION FOR THE ITERATION.

C XA IS HONECKS U235 ABSORPTION CROSS SECTION IN BARNS.

C XF IS HONECKS U235 FISSION CROSS SECTION IN BARNS.

C SK IS THE SCATTERING MATRIX.

C SK IS SIGMA(U(J) TO U(I))/UNIT LETHARGY OR E(I)*SIGMA(E(J) TO E(I))/UNIT EV. SIGMA IS IN BARNS.

C AMUBAR IS THE AVERAGE COSINE OF THE SCATTERING ANGLE.

C CF IS THE CORRECTION FACTOR TO THE SK DIAGONALS.

C DEN IS THE FUEL DENSITY IN GM/CC.

C ENR IS THE FUEL ENRICHMENT EXPRESSED AS WEIGHT PER CENT.

C RO IS THE FUEL ELEMENT DIAMETER IN INCHES.

C RCI IS THE FUEL CLADDING INNER DIAMETER IN INCHES.

C RF IS THE FUEL ROD DIAMETER IN INCHES.

C AMC IS THE CLADDING SCATTERING MASS IN AMU.

C SSC IS THE CLADDING FREE ATOM SCATTERING CROSS SECTION IN BARNS.

C SAC IS THE CLADDING 2200 M/SEC ABSORPTION CROSS SECTION IN BARNS.

C FNC IS THE CLADDING CONCENTRATION IN ATOMS/BARN-CM.

C WO IS THE NOMINAL WATER TO URANIUM OXIDE VOLUME RATIO.

C AP IS THE LATTICE PITCH IN INCHES.

19 FORMAT (1H1)

199 FORMAT (60H1SCATTERING KERNEL, SIGMA(U(J) TO U(I))/UNIT LETHARGY,
1KT = F7.5,6H, J = 12,4H TO 12, /)

200 FORMAT (14,2X,10(E11.3))

203 FORMAT (37H1WATER TO URANIUM OXIDE VOLUME RATIO,F5.1,7H TO 1.0,/,2
14H ABSOLUTE TEMPERATURE = F8.2,/,27H THERMAL UTILIZATION (F) = F8.
25,/,7H ETA = F8.5,/,9H ETA*F = F8.5,/,33H MODERATOR DISADVANTAGE F
3ACTOR = F8.5,/,32H CLADDING DISADVANTAGE FACTOR = F8.5,/,30H DIFFU
4SION COEFFICIENT (CM) = F8.4,/,25H DIFFUSION LENGTH (CM) = F8.4,/
525H LIFETIMES (MICROSECONDS),/,10X,11H THERMAL = F8.5,/,10X,8H MEA
6N = F8.5,/,27H AVERAGE VELOCITIES (M/SFC),/,10X,13H MODERATOR = F8

7.2,/,10X,8H FUFL = F8.2,/,10X,12H CLADDING = F8.2,/,10X,20H HOMOGE
NIZED CELL = F8.2)

204 FORMAT (//,30H NUMBER OF ENERGY INTERVALS = 14,/,24H NUMBER OF ITE
RATIONS = 14,/,25H CONVERGENCE CRITERION = E11.3,/,29H MODERATOR D
ENSITY (GM/CC) = F8.5,/,24H FUEL DENSITY (GM/CC) = F8.5,/,34H FUEL
ENRICHMENT (ATOM PERCENT) = F8.5,/,26H LATTICE PITCH (INCHES) = F
48.5,/,11H RADII (CM),/,10X,19H EQUIVALENT CELL = F8.5,/,10X,16H F
UEL ELEMENT = F8.5,/,10X,12H FUEL ROD = F8.5,/,14H AREAS (CM**2),
6/,10X,13H MODERATOR = F8.5,/,10X,12H CLADDING = F8.5,/,10X,12H FUE
L ROD = F8.5,/,46H ACTUAL WATER TO URANIUM OXIDE VOLUME RATIO = F
88.5,/))

206 FORMAT (4X,31HEFFECTIVE CROSS SECTIONS (1/CM),29X,26HMEAN CROSS SE
CTIONS (1/CM),/,4X,31(1H-),29X,26(1H-),/,2(8X,10HABSORPTION,42X),/
2(12X,9HMODERATOR,F10.5,29X),/,2(12X,4HFUEL,F15.5,29X),/,2(12X,8H
3CLADDING,F11.5,29X),/,2(8X,10HSCATTERING,42X),/,2(12X,9HMODERATOR,
4F10.5,29X),/,2(12X,4HFUEL,F15.5,29X),/,2(12X,8HCLADDING,F11.5,29X)
5,/,2(8X,9HTRANSPORT,43X),/,2(12X,9HMODERATOR,F10.5,29X),/,2(12X,4H
6FUFL,F15.5,29X),/,2(12X,8HCLADDING,F11.5,29X),/,2(8X,5HTOTAL,47X),
7/,2(12X,9HMODERATOR,F10.5,29X),/,2(12X,4HFUEL,F15.5,29X),/,2(12X,8
8HCLADDING,F11.5,29X),/,2(8X,7HFISSION,45X),/,2(12X,4HFUEL,F15.5,29
9X)))

207 FORMAT (//,2(8X,31HHOMOGENIZED CELL CROSS SECTIONS,21X),/,2(12X,10
1HABSORPTION,F9.5,29X),/,2(12X,10HSCATTERING,F9.5,29X),/,2(12X,9HTR
2ANSPORT,F10.5,29X),/,2(12X,5HTOTAL,F14.5,29X),/,2(12X,7HFISSION,F1
32.5,29X)))

208 FORMAT (/,34H NUMBER DENSITIES (NUMBER/BARN-CM),/,10X,8H U235 = E1
12.4,/,10X,8H U238 = E12.4,/,10X,10H OXYGEN = E12.4,/,10X,12H CLADD
2ING = E12.4,/,10X,13H MODERATOR = E12.4.))

334 FORMAT (11(F7.4)))

815 FORMAT (6H 1,3X,6HENERGY,7X,7HDELTA E,6X,8HVELOCITY,2X,7HDELTA
1 V,3X,8HLETHERGY,8H DELTA U,///,(2X,14,2X,2(E11.3,2X),2(F8.1,2X),2
2(F7.4,2X)))

1000 FORMAT (/, (1X,14,7(E15.4))))

1001 FORMAT (13(F6.1)))

1004 FORMAT (37H1WATER TO URANIUM OXIDE VOLUME RATIO,F5.1,8H TO 1.0,,
124H ABSOLUTE TEMPERATURE = F6.1))

1005 FORMAT (2(F10.5)))

1006 FORMAT (2(F10.6),15,2X,E10.2))

1007 FORMAT (8(F8.4),4X,E12.4))

1008 FORMAT (10(A8)))

1009 FORMAT (/,10(A8)))

1100 FORMAT (5H1 I ,4X,6HENERGY,7X,15HU235 ABSORPTION,2X,12HU235 FISSI
ON,1X,15HFUEL ABSORPTION,1X,12HFUEL FISSION,5X,9H1 + ALPHA,4X,12HS
2LOWING DOWN,/,23X,4(13HCROSS SECTION,2X),19X,6HSOURCE,/,26X,2(7H(B
3ARNS),8X),2(6H(1/CM),9X),/,39(3H-)))

1101 FORMAT (5H1 I ,4X,6HENERGY,7X,14HH20 SCATTERING,2X,13HH20 TRANSPO
1RT,2X,12HU235 SCATTER,3X,12HU238 SCATTER,4X,11H016 SCATTER,7X,6HMU
2 BAR,/,23X,5(13HCROSS SECTION,2X),/,26X,5(7H(BARNS),8X),/,39(3H-
3)))

1102 FORMAT (3HO I ,8X,6HENERGY,9X,9HMODERATOR,6X,8HCLADDING,7X,4HFUEL,
113X,16HABSORPTION CROSS,/,27X,3(8HSPECTRUM,7X),2X,18HSECTION (1/CM
2H2O),/,32(3H-),/, (14,6X,4(E12.4,3X),F10.4)))

1103 FORMAT (3HO I ,8X,6HENERGY,20X,2HPS,8X,2HPM,8X,2HPR,8X,2HPE,8X,2HTU
1,7X,3HRFA,7X,3HRTF,6X,5HJ OUT,/,38(3H-),/, (14,6X,F12.4,8X,8(F10

Tr. 2000 x 2000

Scanning
X-ray

Microscopy

```
2•4)))
1212 FORMAT (I4)
4000 FORMAT (7(E11•3))
4444 FORMAT (20(F4•3))
9198 FORMAT (5X,4HJ = ,10(I2,9X),/,3H I )
9199 FORMAT (I4,2X,5(E11•3))
9298 FORMAT (5X,4HJ = ,5(I2,9X),/,3H I )
READ 1212,IND
READ 1006,T,RHO,N,EPSI
NM=N+1
READ 1001,(XA(I),I=1,NM)
READ 1001,(XF(I),I=1,NM)
READ 4000,((SK(J,I),J=1,I),I=1,NM)
READ 4444,(AMUBAR(I),I=1,NM)
READ 334,(CF(I),I=1,NM)
T=8•6167E-5*T
OM1=0•205
OM2=0•481
OMR=0•06
EM=18•
EMR=2•32
EMV =3•/(1•-1•/18•-1•/2•32)
FA25=10•0
FA28=8•3
FA16=3•76
AM25=235•117/1•00896
AM28=238•125/1•00896
AM16=16•0/1•00896
RM=238•125/235•117
ANU=2•43
C      START CALCULATION OF ENERGY, VELOCITY, LETHARGY MESH.  CALCULATION
C      ENDS WITH STATEMENT 94.
B=0•1*LOGF(10•)
U(1)=0•0
DV(1)=0•1*2200•
V(1)=440•
V(2)=V(1)+DV(1)
DV(NM)=0•0
DU(NM)=0•0
DE(NM)=0•0
DO 90 I=2,34
DV(I)=DV(1)
90 V(I+1)=V(I)+DV(I)
DO 91 I=35,N
DV(I)=DV(1)*EXP(B*FLOATF(I-34))
91 V(I+1)=V(I)+DV(I)
DO 711 I=1,NM
D(I)=V(I)
711 DD(I)=DV(I)
DO 92 I=1,NM
V(I)=D(NM+1-I)
92 E(I)=(V(I)**2)*.0252977/(2200•**2)
DO 93 I=1,N
93 DV(I)=DD(NM-I)
```



```

DO 94 I=2,NM
U(I)=LOGF(E(1)/E(I))
DU(I-1)=U(I)-U(I-1)
94 DE(I-1)=E(I-1)-E(I)
PRINT 19
PRINT 815,(I,E(I),DE(I),V(I),DV(I),U(I),DU(I),I=1,NM)
PRINT 19
DO 712 I=1,5
KJ=10.*FLOATF(I)
IM(I)=KJ
712 KN(I)=KJ-9
IF(IND-2) 222,223,223
223 CALL WATER(E,T,N,SK)
DO 224 I=1,NM
224 AMUBAR(I)=AMUBAR(I)-(10.*T-.2526)/8.61637
222 DO 110 J=2,NM
JK=J-1
DO 110 I=1,JK
BB=((E(I)/E(J))**2)*EXP((E(J)-E(I))/T)
110 SK(J,I)=SK(I,J)*BB
DO 951 L=1,4
NI=KN(L)
MI=IM(L)
PRINT 199,T,NI,MI
PRINT 9198,(I,I=NI,MI)
951 PRINT 200,(I,(SK(J,I),J=NI,MI),I=1,NM)
NI=41
MI=45
PRINT 199,T,NI,MI
PRINT 9298,(I,I=NI,MI)
PRINT 9199,(I,(SK(J,I),J=NI,MI),I=1,NM)
DO 445 I=1,NM
445 SK(I,I)=SK(I,I)*CF(I)
DO 119 J=1,NM
DO 116 I=1,NM
116 SXA(I)=SK(J,I)
119 SX(J)=TRAP(SXA,DU,N)
C SX IS THE SCATTERING CROSS SECTION OF H2O IN BARNS.
DO 447 I=1,NM
SS25(I)=FA25*SCROSS(E(I),T,AM25)
SS28(I)=FA28*SCROSS(E(I),T,AM28)
SS16(I)=FA16*SCROSS(E(I),T,AM16)
C SS25,28,16 ARE THE SCATTERING CROSS SECTIONS OF U235,U238,016
C IN BARNS.
447 ST(I)=.656*SQRTF(.0253/E(I))+SX(I)*(1.-AMUBAR(I))
C ST IS THE TRANSPORT CROSS SECTION OF H2O IN BARNS.
DO 448 I=1,NM
DO 448 J=1,NM
448 SK(J,I)=SK(J,I)*RHO*.60247/18.02
PRINT 1101
PRINT 1000,(I,F(I),SX(I),ST(I),SS25(I),SS28(I),SS16(I),AMUBAR(I),
I=1,NM)
TE=T/EM+OM1/(2.*EMV)+OM2/EMV+OMR*(1./*(EXP(OMR/T)-1.0)+.5)/EMR
C TE IS THE EFFECTIVE TEMPERATURE.

```



```

DO 8 I=1,NM
ST(I)=ST(I)*RHO*.60247/18.02
SX(I)=SX(I)*RHO*.60247/18.02
C SK,ST,AND SX ARE NOW IN (1/CM).
A1=SQRTF(E(I)/TE)
8 SN(I)=E(I)*ERF(A1)
BETA=TRAP(SN,DU,N)
DO 9 I=1,NM
9 SN(I)=SN(I)/BETA
C SN IS THE NORMALIZED SOURCE
T=T/8.6167E-5
714 READ 1007,DEN,FNR,R0,RCI,RF,AMC,SSC,SAC,FNC
IF(DEN) 41,41,715
715 READ 1008,TITLE
AMC=AMC/1.00896
R0=R0*2.54/2.
RF=RF*2.54/2.
RCI=RCI*2.54/2.
ENR=100.*ENR*RM/(ENR*RM+(100.-ENR))
FN25=ENR*.60247*DEN*1.0E-2/270.26
FN28=FN25*(100.-ENR)/ENR
FN16=2.01*.60247*DEN/270.26
FNM=.60247*RHO/18.02
DO 713 I=1,NM
SIGMAF(I)=FN25*XA(I)+FN28*2.71*SQRTF(.0253/E(I))
FSIGMAF(I)=FN25*XF(I)
PR(I)=PRODF(FN25,FN28,SIGMAF(I),FSIGMAF(I),DEN,RF,RCI,R0,
1SS25(I),SS28(I),SS16(I))
713 AA(I)=SIGMAF(I)/FSIGMAF(I)
PRINT 1100
PRINT 1000,(I,E(I),XA(I),XF(I),SIGMAF(I),FSIGMAF(I),AA(I),SN(I),
1I=1,NM)
CALL PESCF(E,FNC,SSC,SAC,AMC,RCI,R0,NM,T,PR,FJO,PE,CTE)
DO 47 I=1,NM
47 RTE(I)=FJO(I)*(1.-PR(I))/(PR(I)*(1.-PE(I)))
C RTE IS THE RATIO OF THE NUMBER OF NEUTRONS ABSORBED IN THE FUEL
C ROD TO THE NUMBER ABSORBED IN THE FUEL ELEMENT.
301 READ 1005,W0,AP
IF(W0) 714,714,141
141 PRINT 19
PRINT 1004,W0,T
PRINT 1009,TITLE
R1=SQRTF(((AP*2.54)**2)*1.73205/(2.*3.14159))
Y=R1/R0
VOLM=3.14159*((R1**2)-(R0**2))
VOLF=3.14159*(RF**2)
VOLC=3.14159*((R0**2)-(RCI**2))
VOLCELL=3.14159*(R1**2)
R=VOLM/VOLF
RC=VOLM/VOLC
2 DO 7 I=1,NM
PS(I)=PSLOF(E(I),R0,Y,RHO,ST(I))
PM(I)=PMODF(E(I),R0,Y,RHO,ST(I))
TU(I)=((1.-PE(I))*PS(I))/(1.-PM(I)*PE(I))

```



```

C      TU IS THE RATIO OF THE NUMBER OF NEUTRONS ABSORBED IN THE FUEL
C      ELEMENT TO THE NUMBER ABSORBED IN THE CELL.
C      RFA(I)=TU(I)/(1.-TU(I))
C      RFA IS THE RATIO OF THE NUMBER OF NEUTRONS ABSORBED IN THE FUEL
C      ELEMENT TO THE NUMBER ABSORBED IN THE MODERATOR.
C      FEA(I)=RFA(I)*.656*RHO*.60247*SQRTF(.0253/E(I))/18.02
C      FEA IS THE FUEL ELEMENT ABSORPTION CROSS SECTION IN 1/CM.
C      AB(I)=(1.+RFA(I))*.656*RHO*.60247*SQRTF(.0253/E(I))/18.02
C      AB IS THE TOTAL ABSORPTION CROSS SECTION IN THE CELL PER CM H2O.
C      BEGIN ITERATIVE SOLUTION OF INTEGRAL EQUATION. SOLUTION ENDS ON 36
DO 112 I=1,NM
112 PHIN(I)=1.000
C      INITIAL GUESS AT SPECTRUM IS A CONSTANT
K=1
DO 13 I=1,NM
13 ALPHA(I)=PHIN(I)*AB(I)
B=TRAP(ALPHA,DU,N)
DO 23 I=1,NM
23 PHIN(I)=PHIN(I)/B
14 DO 15 I=1,NM
DO 16 J=1,NM
16 GAMMA(J)=PHIN(J)*SK(J,I)
15 DELTA(I)=TRAP(GAMMA,DU,N)
DO 27 I=1,NM
27 SPHIN(I)=(SN(I)+DELTA(I))/(AP(I)+SX(I))
DO 28 I=1,NM
28 SALPHA(I)=SPHIN(I)*AB(I)
C=TRAP(SALPHA,DU,N)
DO 29 I=1,NM
29 SPHIN(I)=SPHIN(I)/C
DO 32 I=1,NM,2
RA=SPHIN(I)/PHIN(I)
ABSDIF=ABSF(RA-1.)
IF (ABSDIF-EPSI) 32,32,38
32 CONTINUE
GO TO 36
38 K=K+1
IF (K-100) 39,39,36
39 DO 60 J=1,NM
60 PHIN(J)=SPHIN(J)
GO TO 14
36 DO 37 I=1,NM
37 FLUX(I)=SPHIN(I)/E(I)
DO 70 I=1,NM
70 ZZ(I)=FEA(I)*RTE(I)*SPHIN(I)
C1=TRAP(ZZ,DU,N)
DO 71 I=1,NM
71 ZZ(I)=AB(I)*SPHIN(I)
C2=TRAP(ZZ,DU,N)
F=C1/C2
DO 72 I=1,NM
FS(I)=SPHIN(I)*R*FEA(I)*RTE(I)/SIGMAF(I)
FC(I)=FEA(I)*CTF(I)*SPHIN(I)*RC*SQRTF(F(I))/(SQRTF(.0253)*FNC*SAC)
72 ZZ(I)=FEA(I)*RTE(I)*SPHIN(I)/AA(I)

```



```

C3=TRAP(ZZ,DU,N)
ETAF=ANU*C3/C2
ETA=ETAF/F
DO 73 I=1,NM
73 ZZ(I)=SPHIN(I)/V(I)
C4=TRAP(ZZ,DU,N)
DO 74 I=1,NM
74 ZZ(I)=FS(I)/V(I)
C5=TRAP(ZZ,DU,N)
DO 75 I=1,NM
75 ZZ(I)=FC(I)/V(I)
C6=TRAP(ZZ,DU,N)
DIS=C4/C5
DISC=C6/C5
C7=TRAP(SPHIN,DU,N)
C8=TRAP(FS,DU,N)
C9=TRAP(FC,DU,N)
VM=C7/C4
VF=C8/C5
VC=C9/C6
DO 77 I=1,NM
77 ZZ(I)=SPHIN(I)*.656*RHO*.60247*SQRTF(.0253/E(I))/18.02
C10=TRAP(ZZ,DU,N)
DO 78 I=1,NM
78 ZZ(I)=FS(I)*SIGMAF(I)
C11=TRAP(ZZ,DU,N)
DO 79 I=1,NM
79 ZZ(I)=FC(I)*SAC*FNC*SQRTF(.0253/E(I))
C12=TRAP(ZZ,DU,N)
DO 80 I=1,NM
80 ZZ(I)=SPHIN(I)*ST(I)
C13=TRAP(ZZ,DU,N)
DO 81 I=1,NM
81 ZZ(I)=SPHIN(I)*SX(I)
C14=TRAP(ZZ,DU,N)
DO 82 I=1,NM
82 ZZ(I)=FS(I)*(SS25(I)*FN25+SS28(I)*FN28+SS16(I)*FN16)
C15=TRAP(ZZ,DU,N)
DO 83 I=1,NM
83 ZZ(I)=FS(I)*(SS25(I)*FN25*(1.0-2.0/(3.0*AM25))+SS28(I)*FN28*(1.0-2.0/
1.0/(3.0*AM28))+SS16(I)*FN16*(1.0-2.0/(3.0*AM16)))
C16=TRAP(ZZ,DU,N)
T=T*8.6167E-5
DO 86 I=1,NM
FB(I)=(SPHIN(I)*VOLM+FS(I)*VOLF+FC(I)*VOLC)/VOLCELL
TRB(I)=(ST(I)*SPHIN(I)*VOLM+(FS(I)*SIGMAF(I)+ZZ(I))*VOLF+(FC(I)*(
1.0*SAC*FNC*SQRTF(.0253/E(I)))+(FNC*SSC*SCROSS(F(I),T,AMC)*(1.0-2.0/(3.0*
2AMC)))))/(VOLCELL*FB(I))
86 ZZ(I)=FB(I)/TRB(I)
C20=TRAP(ZZ,DU,N)
C21=TRAP(FB,DU,N)
DIFFC=C20/(3.0*C21)
DO 84 I=1,NM
84 ZZ(I)=FC(I)*FNC*SSC*SCROSS(E(I),T,AMC)

```



```

C17=TRAP(ZZ,DU,N)
T=T/8.6167E-5
C18=C17*(1.-2./*(3.*AMC))
DO 85 I=1,NM
85 ZZ(I)=FS(I)*FSIGMAF(I)
C19=TRAP(ZZ,DU,N)
SBAM=C10/C7
SBAF=C11/C8
SBAC=C12/C9
SBSM=C14/C7
SBSF=C15/C8
SBSC=C17/C9
SBTRM=C13/C7
SBTRF=(C11+C16)/C8
SBTRC=(C12+C18)/C9
SBTM=SBAM+SBSM
SBTF=SBAF+SBSF
SBTC=SBAC+SBSC
SBFF=C19/C8
VO=2200.0
SHAM=SBAM*VM/VO
SHAF=SBAF*VF/VO
SHAC=SBAC*VC/VO
SHSM=SBSM*VM/VO
SHSF=SBSF*VF/VO
SHSC=SBSC*VC/VO
SHTRM=SBTRM*VM/VO
SHTRF=SBTRF*VF/VO
SHTRC=SBTRC*VC/VO
SHTM=SBTM*VM/VO
SHTF=SBTF*VF/VO
SHTC=SBTC*VC/VO
SHFF=SBFF*VF/VO
DZ=C7*VOLM+C8*VOLF+C9*VOLC
SBA=(C10*VOLM+C11*VOLF+C12*VOLC)/DZ
SBS=(C14*VOLM+C15*VOLF+C17*VOLC)/DZ
SBTR=(C13*VOLM+(C11+C16)*VOLF+(C12+C18)*VOLC)/DZ
SBT=SBA+SBS
SBF=C19*VOLF/DZ
HV=DZ/(C4*VOLM+C5*VOLF+C6*VOLC)
SHA=SBA*HV/VO
SHS=SBS*HV/VO
SHTR=SBTR*HV/VO
SHT=SBT*HV/VO
SHF=SBF*HV/VO
DIFFL=SQRTF(DIFFC/SBA)
AL=((C4*VOLM+C5*VOLF+C6*VOLC)*1.0E+4)/(C2*VOLM)
AL1=AL/ETAF
DO 76 I=1,NM
FC(I)=FC(I)/E(I)
76 FS(I)=FS(I)/E(I)
40 PRINT 1102,(I,E(I),FLUX(I),FC(I),FS(I),AR(I),I=1,NM)
PRINT 1004,WO,T
PRINT 1009,TITLE

```



```

PRINT 1103,(I,E(I),PS(I),PM(I),PR(I),PE(I),TU(I),RFA(I),RTE(I),
1FJO(I),I=1,NM)
PRINT 203,W0,T,F,ETA,ETAF,DIS,DISC,DIFFC,DIFFL,AL,AL1,VM,VF,VC,HV
PRINT 208,FN25,FN28,FN16,FNC,FNM
PRINT 204,N,K,EPSI,RHO,DEN,ENR,AP,R1,R0,RF,VOLM,VOLC,VOLF,R
PRINT 1009,TITLE
PRINT 1004,W0,T
PRINT 206,SHAM,SBAM,SHAF,SBAF,SHAC,SRAC,SHSM,SBSM,SHSF,SBSF,SHSC,
1SBSC,SHTRM,SBTRM,SHTRF,SBTRF,SHTRC,SHTRC,SHTM,SBTM,SHTF,SBTF,SHTC,
2SBTC,SHFF,SBFF
PRINT 207,SHA,SRA,SHS,SRS,SHTR,SBTR,SHT,SBT,SHF,SBF
PRINT 1009,TITLE
PRINT 19
GO TO 301
41 CONTINUE
END

```

```

FUNCTION PRODF(FN25,FN28,SIGMAA,SIGMAF,DEN,RF,RCI,R0,SS25,SS28,
1SS16)
C THIS CALCULATES THE ESCAPE PROBABILITY FROM THE FUEL ROD USING
C THE PARABOLIC FLUX APPROXIMATION. SEE K.B. CADY THESIS, PG 118.
FN16=2.01*.60247*DEN/270.26
SS=SS25*FN25+SS28*FN28+SS16*FN16
SA=SIGMAA
ST=SS+SA
SF=SIGMAF
C=SS/ST
A=ST*RF
B=1.0-C
IF(A-.5) 1,1,2
1 CALL BESS(A,FI0,FI1,FI2,FK0,FK1,FK2)
FI0=A*(FI1*FK0+1.0-A*(FI1*FK1+FI0*FK0))
FI1=(FI1*FK1+1.0-2.0*FI0)/3.
FM00=1.0-2.0*FI1
PR=1.0-2.0*A*B*(1.0-FM00)/(1.0-C*FM00)
GO TO 3
2 CALL BESS(A,FI0,FI1,FI2,FK0,FK1,FK2)
FI0=A*(FI1*FK0+1.0-A*(FI1*FK1+FI0*FK0))
FI1=(FI1*FK1+1.0-2.0*FI0)/3.
F20=(FI2*FK0-1.0+2.0*FI0+2.0*FI1)/3.
F21=((FI2*FK1/A)+FI1-F20)/5.
F22=((FI2*FK2/(A**2))+(1.0/(3.0*(A**2)))-2.0*F21)/7.
FM00=1.0-2.0*FI1
FM02=1.0-4.0*FI1+8.0*F21
FM22=1.0-6.0*FI1+24.0*F21+24.0*F22-2.0/(A**2)
FM0=2.0*A*(1.0-FM00)
FM2=A*(1.0-FM02)
G=1.0-C*(4.0*FM00+4.0*FM22-6.0*FM02)+(C**2)*(4.0*FM00*FM22-3.0*
1(FM02**2))
PR=1.0-B*(FM0-C*(FM0*(4.0*FM22-3.0*FM02)+6.0*FM2*(FM00-FM02)))/G
3 PRODF=(1.0-RF/RCI)+RF*PR/RCI
END

```


SURROUTINE PESCF(E,FNC,SSC,SAC,AMC,RF,R0,NM,T,PR,FJO,PE,CTE)
 DIMENSION E(55),PR(55),FJO(55),PE(55),CTE(55)
 THIS CALCULATES THE ESCAPE PROBABILITY FROM THE FUEL ELEMENT GIVEN
 THE ESCAPE PROBABILITY FROM THE FUEL ROD. THIN REGION THEORY
 IS USED AS DEVELOPED IN K.B. CADY THESIS, APPENDIX J.

19 FORMAT (1H1)
 50 FORMAT (10H ENERGY = E12.4,/,31H FUEL ROD ESCAPE PROBABILITY = F8.
 15,/,19H ROD CURRENT OUT = F8.5,/,35H FUEL ELEMENT ESCAPE PROBABILI
 2TY = F8.5,/,27H CLADDING THICKNESS (CM) = F8.5,/,5H F0 = F8.5,/,25H
 3 FRACTION SCATTERED IN = F8.5,/,20H SIGMA SCATTERING = F8.5,/,15H
 4SIGMA TOTAL = F8.5,/,5H G = F8.5,/,5H T = F8.5,/,6H PU = F8.5,/,9H
 5 PUNIF = F8.5,/,14H RIN + ROUT = F8.5,/,7H TAU = F8.5,/,18H RHOIN
 6+ RHOOUT = F8.5,/,7H CTE = F8.5)

PI=3.14159
 GAM=.5772157
 T=T*8.6167E-5
 ZE=RF/R0
 TT=R0-RF
 FK=1.-(ZE**2)
 F0=2.*ASINF(ZE)/PI
 F1=ZE
 F2=F0+2.*ZE*SQRTF(FK)/PI
 F3=3.*ZE*(1.-(ZE**2)/3.)/2.
 D1=PI*(ZE**2)/4.
 FLAM=LOGF(4./SQRTF(FK))
 D2=(2./3.)*(1.-.75*FK-3.*((FLAM-.25)*(FK**2)/16.-3.*((FLAM-.11.)/
 112.))*(FK**3)/64.)
 FL1=(F2-4.*D1/PI)/F1
 FL2=(8.*F3/3.-2.*FK*F1-4.*D2)/F1
 C1=(PI*F0/2.+ZE*SQRTF(FK))/(2.*ZE)
 C2=D2/(ZE**2)
 FLL1=4.*C1/PI-ZE
 FLL2=2.*FK+8.*((ZE**2)/3.-4.*ZE*C2)
 FIN=ASINF((2.*ZE/(1.+ZE))/PI)
 DO 10 I=1,NM
 SIGS=SSC*FNC*SCROSS(E(I),T,AMC)
 SIGT=SIGS+FNC*SAC*SQRTF(.0253/E(I))
 SIGA=SIGT-SIGS
 S=F1-SIGT*R0*F1*FL1+.5*((SIGT*R0)**2)*F1*FL2
 X=SIGT*TT
 PU=.5*X*(GAM+LOGF(X)-1.5)+1.-(X**2)/6.+(X**3)/48.-(X**4)/360.+
 1.(X**5)/2880.
 PUNIF=PU/(1.-(SIGS*(1.-PU)/SIGT))
 IF(X-.05) 31,31,32
 31 G=(1.-F1)-2.*((1.-F2)*SIGT*R0+8.*((1.-F3)*((SIGT*R0)**2)/3.
 GO TO 33
 32 G=-.0212-.0266*LOGF(X)/(ZE**2.2)
 33 CONTINUE
 RSUM=SIGS*(1.-G-S)*PUNIF/SIGT
 TAU=1.-(SIGT*R0*FLL1+.5*((SIGT*R0)**2)*FLL2
 RHOSUM=SIGS*(1.-TAU)*PUNIF/SIGT
 RIN=FIN*RSUM
 ROUT=RSUM-RIN
 RHOIN=FIN*RHOIN


```

RHOOUT=RHOSUM-RHOIN
FJO(I)=PR(I)*(S+RIN)/(1.-RHOIN*PR(I))
PE(I)=G+ROUT+FJO(I)*(TAU+RHOOUT)
CTE(I)=SIGA*((1.-G-S)+FJO(I)*(1.-TAU))/((1.-PE(I))*(SIGA+(SIGS*
1PU)))
IF(I=37) 10,40,10
40 PRINT 19
PRINT 50,E(I),PR(I),FJO(I),PE(I),TT,FO,FIN,SIGS,SIGT,G,S,Pu,PUNIF,
1RSUM,TAU,RHOSUM,CTE(I)
PRINT 19
10 CONTINUE
T=T/8.6167E-5
END

C
FUNCTION ERF(Z)
ERF(Z) CALCULATES THE ERROR FUNCTION.
AZ=ABSF(Z)
IF (AZ=4.) 85,86,86
86 ERF=AZ/Z
RETURN
85 IF (AZ=2.) 87,88,88
87 T1=1.
T2=T1*(Z**2)/3.
T3=T2*(Z**2)*3./2.*5.
T4=T3*(Z**2)*5./21.
T5=T4*(Z**2)*7./36.
T6=T5*(Z**2)*9./55.
T7=T6*(Z**2)*11./78.
T8=T7*(Z**2)*13./105.
T9=T8*(Z**2)*15./136.
T10=T9*(Z**2)*17./171.
T11=T10*(Z**2)*19./210.
T12=T11*(Z**2)*21./253.
T13=T12*(Z**2)*23./300.
T14=T13*(Z**2)*25./351.
T15=T14*(Z**2)*27./406.
T16=T15*(Z**2)*29./465.
T17=T16*(Z**2)*31./528.
T18=T17*(Z**2)*33./595.
T19=T18*(Z**2)*35./666.
T20=T19*(Z**2)*37./741.
T21=T20*(Z**2)*39./820.
ERF=2.*.5641896*Z*(T1-T2+T3-T4+T5-T6+T7-T8+T9-T10+T11-T12+T13
1-T14+T15-T16+T17-T18+T19-T20+T21)
RETURN
88 ZA=2.*(Z**2)
S1=1.
S2=1./ZA
S3=3./(ZA**2)
S4=15./(ZA**3)
S5=52.5/(ZA**4)
ERF=(1.-.5641896*(S1-S2+S3-S4+S5))/(AZ*EXP(Z**2))* (AZ/Z)
END

```



```

SUBROUTINE BESS(Z,C,D,E,F,G,H)
C BESS CALCULATES MODIFIED BESSEL FUNCTIONS OF THE FIRST AND
C SECOND KIND.
C C=I0(Z),D=I1(Z),F=I2(Z),F=K0(Z),G=K1(Z),H=K2(Z)
C DIMENSION B(100),BK(3)
C IF(Z<45.) 1,1,2
1 N=XFIXF(2.*Z+10.)
  GO TO 3
2 N=100
3 B(N-1)=1.0E-40
  DO 8 I=N,100
8 B(I)=0.0
  SUM=2.0E-40
  NJ=N-1
  DO 4 L=2,NJ
    NL=N-L
    B(NL)=FLOATF(NL)*2.*B(NL+1)/Z+B(NL+2)
4 SUM=SUM+2.*B(NL)
  SUM=SUM-B(1)
  FACTOR=(EXPF(Z))/SUM
  DO 5 L=1,N
    B(L)=FACTOR*B(L)
    IF(B(L)<-1.0E-307) 6,6,5
6 B(L)=0.0
5 CONTINUE
  C=B(1)
  D=B(2)
  E=B(3)
  IF(Z<5.) 81,82,82
82 IF(Z<6.) 110,111,111
110 KL=10
  GO TO 140
111 IF(Z<7.) 112,113,113
112 KL=12
  GO TO 140
113 IF(Z<8.) 114,115,115
114 KL=14
  GO TO 140
115 IF(Z<9.) 116,117,117
116 KL=16
  GO TO 140
117 IF(Z<10.) 118,119,119
118 KL=18
  GO TO 140
119 KL=10
  GO TO 140
140 W=1.0
  SUM2=1.0
  DO 83 I=1,KL
    W=-W*((2.*FLOATF(I)-1.)*2)/((Z*8.)*FLOATF(I))
83 SUM2=SUM2+W
  SUM2=SUM2-W/2.
  BK(1)=(SUM2*SQRTF(3.141592654/(2.*Z)))/EXPF(Z)
  GO TO 9

```



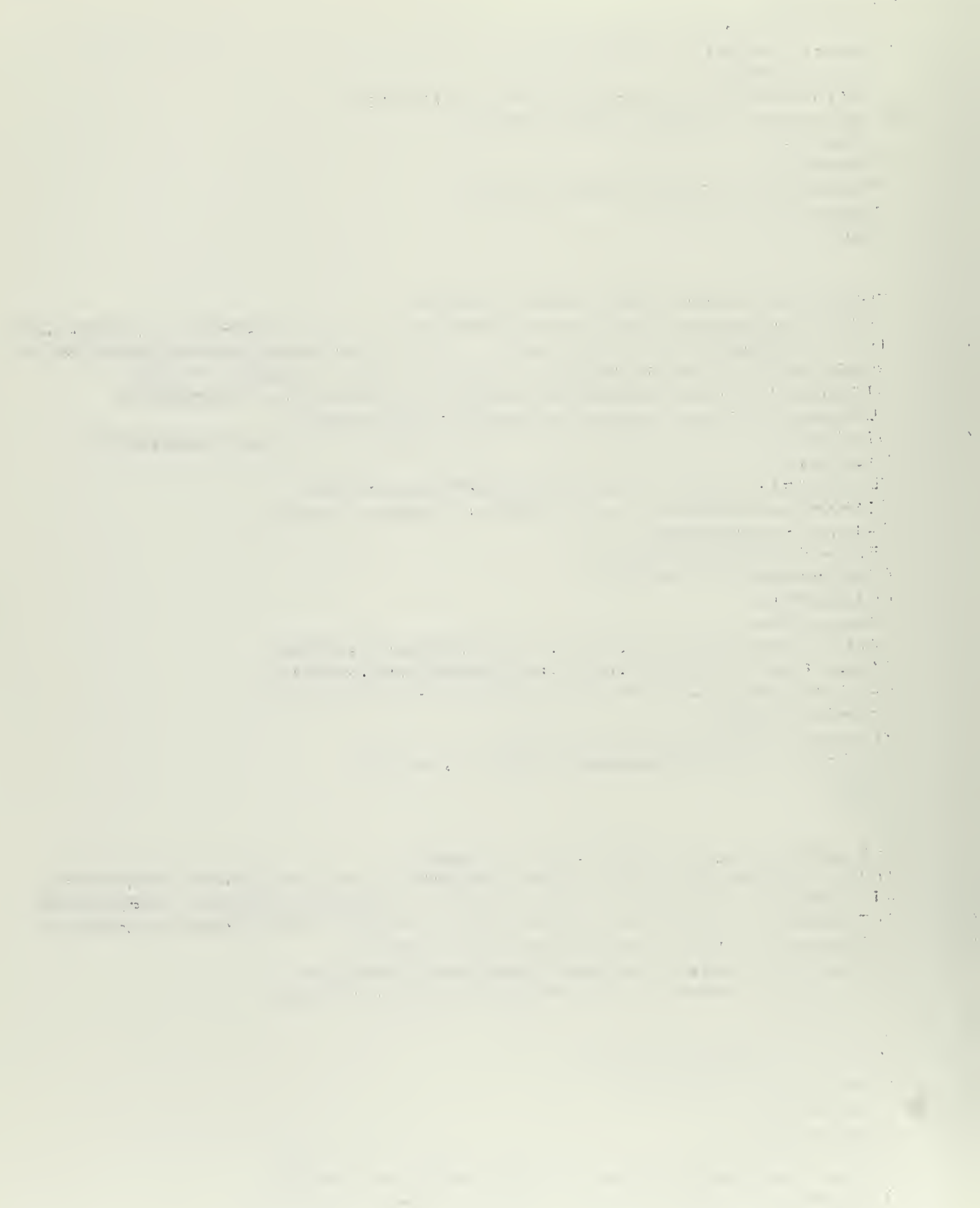
```

81 SUM1=0.0
DO 7 I=3,99,2
7 SUM1=SUM1+B(I)/FLOATF(I-1)
SUM1=4.*SUM1
BK(1)=SUM1-(.577215665+LOGF(Z/2.))*B(1)
9 BK(2)=((1./Z)-BK(1)*B(2))/B(1)
F=BK(1)
G=BK(2)
BK(3)=((1./Z)-BK(2)*B(3))/B(2)
H=BK(3)
END

FUNCTION PMODF(E,R0,Y,RHO,SIGMAGR)
C THIS CALCULATES THE ESCAPE PROBABILITY OF NEUTRONS INCIDENT ON
C THE MODERATOR FROM THE FUEL. IT IS CALCULATED FROM PSLOF BY A
C RECIPROCITY RELATIONSHIP, SEE K.B. CADY THESIS, PG 88.
C SIGMAGR IS THE TRANSPORT CROSS SECTION OF THE MODERATOR
C FLAMBDA IS THE LINEAR EXTRAPOLATION LENGTH
C SIGMAMA IS THE ABSORPTION CROSS SECTION IN THE MODERATOR
R1=R0*Y
FLAMBDA=(.623/(1.+2.48*SIGMAGR*R0))+.7104
SIGMAMA=.656*RHO*.60247*SQRTF(.0253/E)/18.02
D=1./(3.*SIGMAGR)
DELTA=FLAMBDA/SIGMAGR
FK=SQRTF(SIGMAMA/D)
RK1=FK*R1
RKO=FK*R0
CALL BESS(RKO,FI00,FI10,FI20,FK00,FK10,FK20)
CALL BESS(RK1,FI01,FI11,FI21,FK01,FK11,FK21)
B=(FK11*FI00+FI11*FK00)/(FK10*FI11-FK11*FI10)
C=B+FK*DELTA
XE=2./(C*R0*((Y**2)-1.)*FK)
PMODF=1.-2.*SIGMAMA*R0*((Y**2)-1.)*XE
END

FUNCTION PSLOF(E,R0,Y,RHO,SIGMAGR)
C THIS CALCULATES THE ESCAPE PROBABILITY OF NEUTRONS APPEARING
C AT ENERGY (E) DUE TO COLLISIONS AT OTHER ENERGIES. DIFFUSION
C THEORY IS USED WITH A SPATIALLY UNIFORM SOURCE AND AN ENERGY
C DEPENDENT LINEAR EXTRAPOLATION LENGTH.
FLAMBDA=(.623/(1.+2.48*SIGMAGR*R0))+.7104
SIGMAMA=.656*RHO*.60247*SQRTF(.0253/E)/18.02
R1=R0*Y
D=1./(3.*SIGMAGR)
DELTA=FLAMBDA/SIGMAGR
FK=SQRTF(SIGMAMA/D)
RK1=FK*R1
RKO=FK*R0
CALL BESS(RKO,FI00,FI10,FI20,FK00,FK10,FK20)
CALL BESS(RK1,FI01,FI11,FI21,FK01,FK11,FK21)
B=(FK11*FI00+FI11*FK00)/(FK10*FI11-FK11*FI10)
C=B+FK*DELTA

```



```
PSLOF=2./((C*R0*((Y**2)-1.)*FK)
END
```

```
C
C      FUNCTION TRAP(S,DU,N)
C      DIMENSION S(56),DU(56)
C      USES THE TRAPEZOIDAL RULE TO INTEGRATE THE N+1 DIMENSIONAL
C      VECTOR S. DU IS THE LETHARGY INCREMENT.
C      C=0.0
C      DO 2 I=1,N
2     C=C+.5*(S(I)+S(I+1))*DU(I)
      TRAP=C
      END
```

```
C
C      FUNCTION SCROSS(E,T,A)
C      CALCULATES SCATTERING CROSS SECTION/FREE ATOM CROSS SECTION FROM
C      THE MONATOMIC GAS MODEL. E AND T ARE IN EV, A IS IN NEUTRON
C      MASSES.
C      Y=E*A/T
C      IF(Y>700.) 1,1,2
1     X=SQRTF(Y)
      SCROSS=(1.+.5/Y)*FRF(X)+1./(X*EXPF(Y)*SQRTF(3.14159))
      RETURN
2     SCROSS=(1.+.5/Y)
      END
```

```
C
C      SUBROUTINE WATER(E,T,N,SK)
C      WATER CALCULATES THE NELKIN WATER KERNEL. FUNCTIONS ONE AND TWO
C      ARE NECESSARY.
C      DIMENSION E(55),SK(55,55),WGT(12),SKA(55),KN(5),IM(5),AMU(12)
C      OM1=0.205
C      OM2=0.481
C      OMR=0.06
C      EM=18.
C      EMR=2.32
C      EMV =3./(1.-1./18.-1./2.32)
19    FORMAT (1H1)
      NM=N+1
      KN(1)=1
      KN(2)=11
      KN(3)=21
      KN(4)=31
      IM(1)=10
      IM(2)=20
      IM(3)=30
      IM(4)=40
      AMU(1)=.9602899
      AMU(2)=.7966665
      AMU(3)=.5255324
      AMU(4)=.1834346
      AMU(5)=.98940093
      AMU(6)=.94457502
```

τις;

```
AMU(7)=.86563120
AMU(8)=.75540441
AMU(9)=.61787624
AMU(10)=.45801678
AMU(11)=.28160355
AMU(12)=.09501251
WGT(1)=.1012285
WGT(2)=.2223810
WGT(3)=.3137066
WGT(4)=.3626838
WGT(5)=.02715246
WGT(6)=.06225352
WGT(7)=.09515851
WGT(8)=.12462897
WGT(9)=.14959599
WGT(10)=.16915652
WGT(11)=.18260342
WGT(12)=.18945061
DO 102 I=1,NM
DO 101 J=1,I
BEE=E(I)+E(J)
C=SQRTF(E(I)*E(J))
D=0.
H=0.
NJ=NJ+J
NA=.5*FLOATF(NJ)
IF(I-NA) 150,150,80
150 KM=5
KL=12
GO TO 306
80 KM=1
KL=4
306 IF(E(J)-.33) 300,300,301
301 IF(E(J)-.34) 302,302,303
300 MJ=1
GO TO 304
302 MJ=3
304 OM=OMR
AM=EMR
LJ=3
CM=1./EM
GX=T/EM
B=EXPF(OM/(2.*T))
AI=((B**2)+1.)/(((B**2)-1.)*EMR*OMR)+1./(EMV*OM1)+2./(EMV*OM2)
GO TO 305
303 OM=OM1
AM=EMV
MJ=3
LJ=1
CM=1./EM+1./EMR
GX=T/EM+OMR*(1.//(EXPF(OMR/T)-1.+.5)/EMR
B=EXPF(OM/(2.*T))
AI=1.//(EMV*OM1)+2.//(EMV*OM2)
305 IF(I-J) 901,902,901
```



```

902 ALPHA=E(J)/SQRTF(3.14159*GX)
    BETA=E(J)*SQRTF(16.0/(3.14159*T))
    GO TO 903
901 ALPHA=0.
    BETA=0.
903 ZOX=2.0*B/(AM*OM*(B**2-1.0))
    DO 151 K=KM,KL
        X=BEE+2.0*C*AMU(K)
        XX=SQRTF(X)
        Z=X*ZOX
        F=ONE(E(J),E(I),X,GX,OM,CM,MJ,LJ,AI,B,Z,EMV)
        F=(2.*81.5/4.0)*(F-ALPHA/XX)+(4.24/4.0)*
        1(TWO(E(J),E(I),X,T)-BETA/XX)
        X=BEE-2.0*C*AMU(K)
        XX=SQRTF(X)
        Z=X*ZOX
        G=ONE(E(J),E(I),X,GX,OM,CM,MJ,LJ,AI,B,Z,EMV)
        G=(2.*81.5/4.0)*(G-ALPHA/XX)+(4.24/4.0)*
        1(TWO(E(J),E(I),X,T)-BETA/XX)
        D=D+WGT(K)*(F+G)
151 H=H+WGT(K)*AMU(K)*(G-F)
    IF(I-J) 70,802,70
802 FA=((2.*81.5/4.0)*ALPHA+(4.24/4.0)*BETA)*2.0/SQRTF(E(J))
    D=D+FA
    H=H+FA/3.
70 SK(J,I)=D
101 SKA(J)=SK(J,I)
    PRINT 1004,I
1004 FORMAT (4HI = I3)
1005 FORMAT (19H SCATTERING KERNEL /(7(I3,E13.4)/))
    PRINT 1005,(J,SKA(J),J=1,I)
102 CONTINUE
    DO 110 J=2,NM
        JK=J-1
        DO 110 I=1,JK
            BB=((E(I)/E(J))**2)*EXP((E(J)-E(I))/T)
110 SK(J,I)=SK(I,J)*BB
    DO 951 L=1,4
        NI=KN(L)
        MI=IM(L)
        PRINT 199,T
199 FORMAT (25H1SCATTERING KERNEL, KT = F7.4)
    PRINT 9199,(I,I=NI,MI)
9199 FORMAT (7X,10(I2,9X))
951 PRINT 200,(I,(SK(J,I),J=NI,MI),I=1,NM)
200 FORMAT (I4,2X,10(E11.3))
    NI=41
    MI=45
    PRINT 199,T
    PRINT 9199,(I,I=NI,MI)
    PRINT 220,(I,(SK(J,I),J=NI,MI),I=1,NM)
220 FORMAT (I4,2X,5(E11.3))
9876 CONTINUE
END

```

the same time, the number of species per genus was greater than the number of genera per species. This was true for all three groups of species. The mean number of species per genus for the *Gramineae* was 1.54, while the mean number of genera per species was 1.26. For the *Asteraceae*, the mean number of species per genus was 1.67, while the mean number of genera per species was 1.33. For the *Compositae*, the mean number of species per genus was 1.55, while the mean number of genera per species was 1.33.

The mean number of species per genus was greater than the mean number of genera per species for all three groups of species. This was true for all three groups of species. The mean number of species per genus for the *Gramineae* was 1.54, while the mean number of genera per species was 1.26. For the *Asteraceae*, the mean number of species per genus was 1.67, while the mean number of genera per species was 1.33. For the *Compositae*, the mean number of species per genus was 1.55, while the mean number of genera per species was 1.33.

It is evident from the data presented that the *Gramineae* and *Asteraceae* are more closely related to each other than either is to the *Compositae*. The *Gramineae* and *Asteraceae* have a higher percentage of common species than does the *Compositae*. The *Gramineae* and *Asteraceae* also have a higher percentage of common genera than does the *Compositae*.

The mean number of species per genus was greater than the mean number of genera per species for all three groups of species. This was true for all three groups of species. The mean number of species per genus for the *Gramineae* was 1.54, while the mean number of genera per species was 1.26. For the *Asteraceae*, the mean number of species per genus was 1.67, while the mean number of genera per species was 1.33. For the *Compositae*, the mean number of species per genus was 1.55, while the mean number of genera per species was 1.33.

It is evident from the data presented that the *Gramineae* and *Asteraceae* are more closely related to each other than either is to the *Compositae*. The *Gramineae* and *Asteraceae* have a higher percentage of common species than does the *Compositae*. The *Gramineae* and *Asteraceae* also have a higher percentage of common genera than does the *Compositae*.

The mean number of species per genus was greater than the mean number of genera per species for all three groups of species. This was true for all three groups of species. The mean number of species per genus for the *Gramineae* was 1.54, while the mean number of genera per species was 1.26. For the *Asteraceae*, the mean number of species per genus was 1.67, while the mean number of genera per species was 1.33. For the *Compositae*, the mean number of species per genus was 1.55, while the mean number of genera per species was 1.33.

It is evident from the data presented that the *Gramineae* and *Asteraceae* are more closely related to each other than either is to the *Compositae*. The *Gramineae* and *Asteraceae* have a higher percentage of common species than does the *Compositae*. The *Gramineae* and *Asteraceae* also have a higher percentage of common genera than does the *Compositae*.

The mean number of species per genus was greater than the mean number of genera per species for all three groups of species. This was true for all three groups of species. The mean number of species per genus for the *Gramineae* was 1.54, while the mean number of genera per species was 1.26. For the *Asteraceae*, the mean number of species per genus was 1.67, while the mean number of genera per species was 1.33. For the *Compositae*, the mean number of species per genus was 1.55, while the mean number of genera per species was 1.33.

Appendix E

```

FUNCTION ONE(EP,E,X,GX,OM,CM,MJ,LJ,AI,B,Z,EMV)
C THIS CALCULATES (SIGMA(UP TO U,MU)/(SIGMA BOUND ATOM/4)) FOR
C NELKIN PROTON. EP,E,X, AND T ARE IN EV.
DIMENSION BI(200),AA(3),CC(3)
OM1=0.205
OM2=0.481
AA(1)=1.
AA(2)=X/(EMV*OM1)
AA(3)=(AA(2)**2)/2.
CC(1)=1.
CC(2)=2.*X/(EMV*OM2)
CC(3)=(CC(2)**2)/2.
PROD1=0.0
SUM=0.
D=E*SQRTF(E/(EP*X**GX*3.14159))
N=1.5*Z+10.
BI(N)=0.
SUM=1.0E-20
BI(N-1)=SUM
NN=N-1
DO 11 J=2,NN
I=N-J
BI(I)=2.*FLOATF(I)*BI(I+1)/Z+BI(I+2)
11 SUM=SUM+BI(I)
SUM=2.*SUM-BI(1)
C=EXPF(Z)/SUM
DO 12 J=1,NN
12 BI(J)=C*BI(J)
DO 1050 M=1,MJ
FM=M-1
PROD=0.
DO 17 L=1,LJ
EL=L-1
SUM=0.
DO 13 N=1,NN
EN=N-1
BB=E-EP+X*CM+EN*OM+EL*OM1+FM*OM2
AZ=(BB**2)/(4.*X*GX)
IF(AZ-705.) 112,112,113
112 P=((B**EN)*BI(N))/EXPF(AZ)
GO TO 114
113 P=0.0
114 SUM=SUM+P
W=P/SUM
IF(W-1.0E-4) 14,14,13
13 CONTINUE
PRINT 500,N
500 FORMAT (5H N = 13)
14 DO 15 N=2,NN
EN=N-1
BB=E-EP+X*CM-EN*OM+EL*OM1+FM*OM2
AZ=(BB**2)/(4.*X*GX)
IF(AZ-705.) 115,115,116
115 P=(BI(N)/(B**EN))/EXPF(AZ)

```



```

      GO TO 117
116 P=0.0
117 SUM=SUM+P
      W=P/SUM
      IF(W-1.0E-4) 16,16,15
15 CONTINUE
      PRINT 500,N
16 PROD=AA(L)*SUM+PROD
17 CONTINUE
      PROD1=CC(M)*PROD+PROD1
1050 CONTINUE
      ONE=D*PROD1/EXPF(X*A1)
      END

FUNCTION TWO(EP,E,X,T)
C THIS CALCULATES (SIGMA UP TO U,MU)/(SIGMA BOUND ATOM/4))
C FOR A FREE GAS OF MASS 16. EP,E,X,AND T ARE IN EV.
B=E-EP+X/16.
D=E*SQRTF(E*16./(X*T*3.14159*EP))
TWO=D/EXPF((B**2)*16./(4.*X*T))
END
      END          COUTH

SUBROUTINE FKERN(NM,SFA,T,A,E,SK)
C SUBROUTINE FKERN CALCULATES THE SCATTERING MATRIX USING THE
C MONATOMIC GAS MODEL.
C
DIMENSION E(55),SK(55,55),W(55),RX(55),EX(55)
ETA=(A+1.)/(2.*SQRTF(A))
RIO=(A-1.)/(2.*SQRTF(A))
DO 43 I=1,NM
W(I)=SQRTF(E(I)/T)
RX(I)=RIO*W(I)
43 EX(I)=ETA*W(I)
DO 10 I=1,NM
DO 10 J=1,I
10 SK(J,I)=.5*SFA*(ETA**2)*(E(I)/E(J))*((ERF(EX(I)-RX(J))+ERF(EX(I)+
1RX(J))+(EXP((W(J)**2)-(W(I)**2))))*(ERF(EX(J)-RX(I))-ERF(RX(I)+
2EX(J)))))
      END

```


APPENDIX F

NOTATION

Roman Letters

a	Fuel rod radius in mean free path, $a = \sum_t^f r_f$
A	Fuel element area, Eq. (2.12)
A	Ratio of scatterer mass to neutron mass, Eq. (5.1)
A	Parameter for substitution into the Nelkin Water Kernel, Eqs. (5.17) and (5.18)
A	Mass number, Eq. (7.3)
c	Ratio of the scattering to the total cross section, p. 27
C(E)	Correction factors to the diagonal terms in the Nelkin Water Matrix, p. 59
C ₁	Eq. (4.36)
C ₂	Eq. (4.37)
d(E)	Linear extrapolation length into the fuel element, Eq. (2.18)
d _o (E)	Linear extrapolation length into a black hole, Eq. (C.4)
D	Diffusion coefficient for the homogenized cell, Eq. (6.38)
D ₁	Eq. (4.30)
D ₂	Eq. (4.32)

$D_m(E)$	Diffusion coefficient for the moderator, Eq. (2.13)
$D_f(E)$	Diffusion coefficient for the fuel, p. 27
E	Neutron energy in eV
E_c	Thermal cutoff energy
f	Thermal utilization, Eqs. (6.13) and (6.15)
$f(\mu)$	Eq. (5.21)
$f(E)$	Eqs. (2.7), (2.28), and (3.8)
F_o	Eq. (4.26)
F_1	Eq. (4.27)
F_2	Eq. (4.28)
F_3	Eq. (4.29)
g	Sec. 4.3, Eq. (4.45)
G(E)	Eq. (2.17)
h	Planck's Constant
$I_n(z)$	Modified Bessel function of the first kind
$J_-(E)$	Current into the fuel element, Eq. (2.24)
$J_o(E)$	Net current entering the cladding from the fuel rod, Eq. (4.22)
$J_n(E)$	Net current entering the fuel element, Eq. (2.12)
$K_n(z)$	Modified Bessel function of the second kind
ℓ_t	Thermal lifetime, Eq. (6.17)
L	Diffusion length for the homogenized cell, Eq. (6.39)
L_1^{-1}	Eq. (4.33)

\bar{L}_1^2	Eq. (4.34)
$\bar{\mathcal{L}}_1^1$	Eq. (4.38)
$\bar{\mathcal{L}}_1^2$	Eq. (4.39)
M	p. 47
$M(E)$	Maxwellian distribution, Eq. (2.6)
M_{ij}	Cylindrical moments, Sec. 4.1
M_r	p. 47
M_v	p. 47
$N(E)$	Spatially averaged source, Eq. (2.11)
$N(\vec{r}, E)$	Neutron source, Eq. (2.11)
$\bar{N}^i(E)$	Spatially averaged energy dependent neutron density in region i, Eq. (6.5)
\bar{N}^i	Total neutron density in region i, Eq. (6.7)
$P_e(E)$	Fuel element escape probability, Chap. 4
$P_m(E)$	Moderator escape probability, Sec. 3.2
$P_r(E)$	Fuel rod escape probability, Sec. 4.1
$P_{rv}(E)$	Escape probability for the fuel rod and void region, Sec. 4.2
$P_s(E)$	Moderator escape probability, Sec. 3.1
P_u	Eq. (4.43)
P_{unif}	Eq. (4.44)
r_o	Fuel element radius
r_1	Equivalent cell radius
r_c	Inner radius of the cladding
r_f	Fuel rod radius

r_{in}	Sec. 4.3, Eq. (4.49)
r_{out}	Sec. 4.3, Eq. (4.50)
RR_j^i	Reaction rate of type j in region i, Eqs. (6.18) and (6.19)
$S(E)$	Neutron slowing down source, Eq. (2.3)
$\bar{S}(E)$	Spatially averaged slowing down source of neutrons, Eqs. (2.10), (5.27), and (7.1)
$S(\vec{r}, E)$	Spatially dependent slowing down source of neutrons, Eq. (2.10)
t	Eq. (4.24)
T	Moderator temperature in electron volts
T	Sec. 4.3, Eq. (4.35)
u	Lethargy
$v(E)$	Neutron velocity
\bar{v}_i	Average neutron velocity in region i, Eq. (6.6)
V^i	The volume of region i
w_k	Weighting coefficients for the Gaussian quadrature integration formula, p. 50
x	Eq. (4.42)
X	Eq. (5.2)
y	p. 15, $y = r_1/r_o$
y	Eq. (5.14)
z	Eqs. (5.17) and (5.18)
z	Eq. (5.5)

Greek Letters

$\alpha(E)$	Fuel capture to fission ratio
$\beta(E)$	Eq. (4.2)
γ	Euler's Constant
δ_n^m	Moderator neutron density disadvantage factor, Eq. (6.8)
δ_n^c	Cladding neutron density disadvantage factor, Eq. (6.9)
δ_ϕ^m	Moderator flux disadvantage factor, Eq. (6.10)
δ_ϕ^c	Cladding flux disadvantage factor, Eq. (6.11)
ϵ	Convergence criterion, Eq. (C.24)
ζ	Eq. (4.20)
η	Number of fission neutrons produced per thermal absorption in the fuel, Eq. (6.16)
η	Eq. (5.7)
θ	Eq. (4.25)
κ	p. 15
κ_f	p. 28
λ	Eq. (C.4)
Λ	Eq. (4.31)
μ	Cosine of the scattering angle
$\bar{\mu}(E)$	Average cosine of the scattering angle, Eq. (5.24)
μ_k	A zero of the Legendre polynomials, p. 50
ν	Number of fission neutrons produced per thermal fission
ξ	Eq. (4.23)
ξ	Eqs. (5.17) and (5.18)

π	=	3.14159
ρ		Eq. (5.8)
ρ_{in}		Sec. 4.3, Eq. (4.51)
ρ_{out}		Sec. 4.3, Eq. (4.52)
σ_b		Bound atom microscopic cross section
σ_f		Free atom microscopic cross section
$\sigma_j^i(E)$		Microscopic cross section expressed in barns for interaction type j in material i
$\sigma(E' \rightarrow E, \mu)$		Differential scattering kernel, Eqs. (5.1) and (5.15)
$\sigma(E' \rightarrow E)$		Scattering kernel, Eqs. (5.4) and (5.19)
$\sigma^*(E \rightarrow E)$		Modified diagonals for the Nelkin water kernel, Eq. (5.26)
$\sigma_1(E' \rightarrow E)$		First moment of the scattering kernel, Eq. (5.23)
$\Sigma_j^i(E)$		Macroscopic cross section expressed in cm^{-1} for interaction type j in material i
$\hat{\Sigma}_j^i$		Macroscopic effective cross section for inter- action type j in material i, Eqs. (6.23) and (6.31)
$\bar{\Sigma}_j^i$		Macroscopic mean cross section for interaction type j in material i, Eqs. (6.24) and (6.32)
$\Sigma(E' \rightarrow E)$		Macroscopic scattering kernel, Eq. (2.1)
τ		Sec. 4.3, Eq. (4.40)
$\phi^m(E)$		Energy dependent flux in an infinite homogeneous moderator, Eq. (2.1)

$\bar{\phi}^i(E)$	Spatially averaged energy dependent flux in region i
$\bar{\phi}_o^i$	Spatially averaged 2200 m/sec flux in region i
$\bar{\phi}_T^i$	Spatially averaged thermal flux in region i
$\bar{\phi}_k^m(u_i)$	k^{th} iteration for the moderator flux at lethargy u_i , Eq. (C.22)
$\hat{\phi}_k^m(u_i)$	$\bar{\phi}_k^m(u_i)$ normalized, Eq. (C.23)
$\phi_u(\vec{r})$	Eq. (4.5)
χ	Eqs. (5.17) and (5.18)
$\chi(E)$	Eq. (2.21)
ω_r	p. 47
ω_1	p. 47
ω_2	p. 47

Subscripts and Superscripts

a	absorption
c	cladding
f	fuel
f	fission
h	homogenized cell
m	moderator
s	scattering
t	total
tr	transport

WORKS CITED

BOOKS

K. M. Case, F. de Hoffmann, and G. Placzek, Introduction to the Theory of Neutron Diffusion, Vol. I, United States Government Printing Office, 1953. (See Footnotes 28 and 35.)

H. B. Dwight, Tables of Integrals and Other Mathematical Data, The Macmillan Company, New York, 1961. (See Footnotes 87 and 90.)

S. Glasstone and M. C. Edlund, The Elements of Nuclear Reactor Theory, D. Van Nostrand Company, Inc., Princeton, Toronto, London, and New York, 1952. (See Footnotes 20 and 25.)

A. M. Weinberg and E. P. Wigner, The Physical Theory of Neutron Chain Reactors, The University of Chicago Press, Chicago, 1958. (See Footnotes 1, 23, 26, 30, 63, 76, and 83.)

JOURNALS

A. Amouyal, P. Benoist, and J. Horowitz, "Nouvelle Méthode de Determination du Facteur d'Utilization Thermique d'une Cellule," J. Nucl. Energy 6, 79 (1957). (See Footnotes 10 and 27.)

J. R. Beyster, et al., "Measurement of Neutron Spectra in Water, Polyethylene, and Zirconium Hydride," Nucl. Sci. Eng. 9, 168 (1961). (See Footnote 54.)

- K. B. Cady and M. Clark, Jr., "Neutron Transport in Cylindrical Rods," *Nucl. Sci. Eng.* 18, 491-507 (1964). (See Footnotes 24 and 32.)
- K. B. Cady and C. R. Mac Vean, "A Simplified Formulation of Space-Energy Cell Theory," *Trans. Am. Nucl. Soc.* 6, 234-235 (1963). (See Footnote 70.)
- G. P. Calame, "Diffusion Parameters of Water for Various Scattering Kernels," *Nucl. Sci. Eng.* 19, 189 (1964). (See Footnote 55.)
- L. G. de Sobrino and M. Clark, Jr., "A Study of the Wilkins Equation," *Nucl. Sci. Eng.* 10, 388 (1961). "Comparison of the Wilkins Equation with Experiments on Water Systems," *Nucl. Sci. Eng.* 10, 377 (1961). (See Footnote 47.)
- M. Goldstein and R. M. Thaler, "Recurrence Techniques for Calculation of Bessel Functions," *Mathematical Tables and Other Aids to Computation*, 13, 102 (1959). (See Footnotes 88 and 89.)
- A. Hassitt, "Methods of Calculation for Heterogeneous Reactors," Progress in Nuclear Energy, Series I, Vol. 2, Pergamon Press, New York, London, Paris, and Los Angeles, 1958. (See Footnote 4.)
- R. L. Hellens and H. C. Honeck, "Summary and Preliminary Analysis of the BNL Slight Enriched Uranium, Water Moderated Lattice Measurements," Light Water Lattices, International Atomic Energy Agency, Vienna, 1962. (See Footnote 75.)

- H. C. Honeck, "The Calculation of the Thermal Utilization and Disadvantage Factor in Uranium/Water Lattices," *Nucl. Sci. Eng.* 18, 49-68 (1964). (See Footnotes 7, 15, 38, 73, 74, 77, 78, 79, and 81; Table A.3; and Figs. 8.1, 8.2, and 8.3.)
- A. N. Lowan, N. Davis, and A. Levinson, "Tables of the Zeros of the Legendre Polynomials of Order 1-16 and the Weight Coefficients for Gauss's Mechanical Quadrature Formula," *Bull. Am. Math. Soc.* 48, 739 (1942). (See Footnote 57.)
- M. S. Nelkin, "Scattering of Slow Neutrons by Water," *Phys. Rev.* 119, 741-746 (1961). (See Footnotes 13, 41, 46, 48, and 53.)
- C. D. Petrie, M. L. Storm, and P. F. Zweifel, "Calculation of Thermal Group Constants for Mixtures Containing Hydrogen," *Nucl. Sci. Eng.* 2, 728-744 (1957). (See Footnote 64.)
- G. C. Pomraning, "On the Energy Averaging of the Diffusion Coefficient," *Nucl. Sci. Eng.* 19, 250 (1964). (See Footnote 67.)
- G. C. Pomraning, "On the Validity of the Constant Source Assumption for the Cell Problem," *Nucl. Sci. Eng.* 18, 400-403 (1964). (See Footnote 21.)
- M. J. Poole, M. S. Nelkin, and R. S. Stone, "The Measurement and Theory of Reactor Spectra," Progress in Nuclear Energy, Series I, Vol. 2, Pergamon Press, New York, London, Paris, and Los Angeles, 1958. (See Footnotes 2, 18, 51, and 91.)

- K. S. Singwi and L. S. Kothari, "Transport Cross Section of Thermal Neutrons in Solid Moderators," Second Geneva Conference Proceedings 16, 325 (1958). (See Footnote 65.)
- N. G. Sjöstrand, "Definition of the Diffusion Constant in One-Group Theory," J. Nucl. Energy, Part A, Reactor Science 12, 151 (1964). (See Footnote 66.)
- E. Starr and J. Koppel, "Determination of Diffusion Hardening in Water," Nucl. Sci. Eng. 14, 244 (1962). (See Footnote 56.)
- G. W. Stuart and R. W. Woodruff, "Method of Successive Generations," Nucl. Sci. Eng. 10, 388 (1961). (See Footnote 33.)
- R. S. Varga, "Numerical Methods for Solving Multi-Dimensional Multigroup Diffusion Equations," Proceedings of Symposia in Applied Mathematics, Vol. XI, Nuclear Reactor Theory, American Mathematical Society, Providence, 1961. (See Footnote 16.)
- D. F. Zaretsky, "Effective Boundary Conditions for Grey Bodies," First Geneva Conference Proceedings 5, 525-530 (1955). (See Footnote 84.)

REPORTS

- D. D. Clark, "The Cornell University Nuclear Reactor Laboratory," CURL-1, Cornell University (1961). (See Footnote 14 and 68 and Table A.2.)

- F. D. Federighi and D. T. Goldman, "KERNEL and PAM-Programs for Use in the Calculation of the Thermal Scattering Matrix for Chemically Bound Systems," KAPL-2225, Knolls Atomic Power Laboratory (1962). (See Footnotes 49, 58, and 86.)
- D. Hughes and B. Schwartz, "Neutron Cross Sections," BNL-325, 2nd Ed., Brookhaven National Laboratory (1958). (See Footnotes 60 and 72.)
- H. C. Honeck, "THERMOS-A Thermalization Transport Theory Code for Reactor Lattice Calculations," BNL-5826, Brookhaven National Laboratory (1961). (See Footnotes 6, 17, and 59.)
- D. C. Leslie, "The Calculation of Thermal Spectra," Proceedings of the Brookhaven Conference on Neutron Thermalization, BNL-719, Vol. II, pp. 592-609, Brookhaven National Laboratory (1962). (See Footnote 9.)
- D. C. Leslie, "The SPECTROX Method for Thermal Spectra in Lattice Cells," AEEW-M211, United Kingdom Atomic Energy Authority (1962). (See Footnotes 8, 19, 22, and 85.)
- Neutron Spectra in Lattices and Infinite Media, Proceedings of the Brookhaven Conference on Neutron Thermalization, BNL-719, Vol. II, Brookhaven National Laboratory (1962). (See Footnotes 3 and 5.)
- A. Radkowsky, "Temperature Dependence of the Thermal Transport Mean Free Path," Physics Quarterly Report (April, May, June, 1950), ANL-4476, p. 89, Argonne National Laboratory (July, 1950). (See Footnote 42.)

- The Scattering Law, Proceedings of the Brookhaven Conference on Neutron Thermalization, BNL-719, Vol. I. Brookhaven National Laboratory (1962). (See Footnote 44.)
- E. P. Wigner and J. E. Wilkins, Jr., "Effect of the Temperature of the Moderator on the Velocity Distribution of Neutrons with Numerical Calculations for H as the Moderator," AECD-2275 (1944). (See Footnotes 11, 39, 45, and 52.)
- J. E. Wilkins, Jr., "Effect of the Temperature of the Moderator on the Velocity Distribution of Neutrons for a Heavy Moderator, CP-2481 (1944). (See Footnotes 12, 40, 45, and 50.)
- C. H. Wescott, "The Specification of Neutron Flux and Effective Cross Sections," AECL-352 (1956). (See Footnote 61.)
- THESES
- S. S. Berg, "Initial Experiments on the Cornell University Zero Power Reactor Cores," Cornell University Thesis (1964). (See Footnotes 69 and 80 and Table A.1.)
- K. B. Cady, "Neutron Transport in Cylindrical Rods," Massachusetts Institute of Technology Thesis (1962). (See Footnotes 29, 31, 34, 36, and 37.)
- J. A. Larrimore, "Temperature Coefficients of Reactivity in Homogenized Thermal Nuclear Reactors," Massachusetts Institute of Technology Thesis (1962). (See Footnote 62.)
- J. Suich, "Temperature Coefficients in Heterogeneous Reactor Lattices," Massachusetts Institute of Technology Thesis (1963). (See Footnotes 71 and 82.)

thesM27

A simplified cell theory applied to the



3 2768 002 03371 4

DUDLEY KNOX LIBRARY